Molecular Cell

Cas9 deactivation with photocleavable guide RNAs

Graphical Abstract

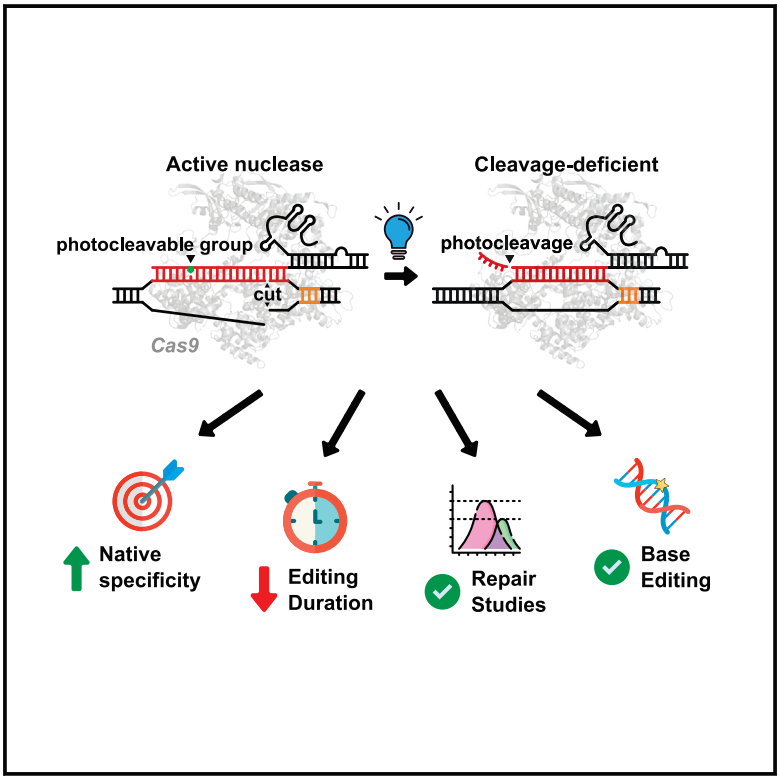

Authors

Roger S. Zou, Yang Liu, Bin Wu, Taekjip Ha

Correspondence

tjha@jhu.edu

In brief

Zou et al. developed light-mediated control over Cas9 and base editor deactivation by introducing a photocleavable moiety into guide RNA. Deactivation occurs within seconds and approaches completeness. This modification natively enhanced specificity. Timed deactivation facilitated studies of DNA repair by synchronizing the termination of DNA damage within a cell population.

Highlights

- Light-mediated deactivation of Cas9 and base editors with a modified guide RNA
- Deactivation occurs within seconds and approaches completeness
- The modified guide RNA natively results in enhanced specificity
- Facilitates DNA repair studies through synchronized termination of DNA damage

Zou et al., 2021, Molecular Cell *81*, 1–13
April 1, 2021
https://doi.org/10.1016/j.molcel.2021.02.007

Please cite this article in press as: Zou et al., Cas9 deactivation with photocleavable guide RNAs, Molecular Cell (2021), https://doi.org/10.1016/j.molcel.2021.02.007

Molecular Cell

CellPress

Technology

Cas9 deactivation with photocleavable guide RNAs

Roger S. Zou,[1,5] Yang Liu,[2,5] Bin Wu,[2] and Taekjip Ha[1,2,3,4,6,*]
[1]Department of Biomedical Engineering, Johns Hopkins University, Baltimore, MD 21205, USA
[2]Department of Biophysics and Biophysical Chemistry, Johns Hopkins University, Baltimore, MD 21205, USA
[3]Department of Biophysics, Johns Hopkins University, Baltimore, MD 21205, USA
[4]Howard Hughes Medical Institute, Baltimore, MD 21205, USA
[5]These authors contributed equally
[6]Lead contact
*Correspondence: tjha@jhu.edu
https://doi.org/10.1016/j.molcel.2021.02.007

SUMMARY

Precise control of CRISPR-Cas9 would improve its safety and applicability. Controlled CRISPR inhibition is a promising approach but is complicated by separate inhibitor delivery, incomplete deactivation, and slow kinetics. To overcome these obstacles, we engineered photocleavable guide RNAs (pcRNAs) that endow Cas9 nucleases and base editors with a built-in mechanism for light-based deactivation. pcRNA enabled the fastest (<1 min) and most complete (<1% residual indels) approach for Cas9 deactivation. It also exhibited significantly enhanced specificity with wild-type Cas9. Time-resolved deactivation revealed that 12–36 h of Cas9 activity or 2–4 h of base editor activity was sufficient to achieve high editing efficiency. pcRNA is useful for studies of the cellular response to DNA damage by abolishing sustained cycles of damage and repair that would otherwise desynchronize response trajectories. Together, pcRNA expands the CRISPR toolbox for precision genome editing and studies of DNA damage and repair.

INTRODUCTION

Since the initial characterization of SpCas9 (Cas9 for short) as a CRISPR-associated RNA-guided endonuclease from *S. pyogenes*, engineering efforts have transformed the enzyme into a highly versatile genome editing platform for research, industrial, and therapeutic applications (Doudna, 2020; Hsu et al., 2014; Jinek et al., 2012; Knott and Doudna, 2018). However, its fundamental mechanism of action involves targeted induction of mutagenic DNA lesions (Cong et al., 2013; Komor et al., 2016; Mali et al., 2013), leading to the possibility of off-target editing, genotoxicity, translocations, and malignancy (Ferrarelli, 2018; Fu et al., 2013; Haapaniemi et al., 2018; Kosicki et al., 2018). Therefore, limiting genome editing action only to the desired target sequence, time duration, and spatial location is desirable (Gangopadhyay et al., 2019). Controlled inactivation has promise to be an effective approach for this purpose by stopping the activity of genome editing agents on demand, such that cellular exposure to a genome editor is limited only to its minimally required ''dose'' (Dolgin, 2020). Anti-CRISPR proteins, initially discovered as a natural phage defense mechanism against CRISPR-mediated adaptive immunity in bacteria, have been repurposed to inhibit genome editing in mammalian cells (Harrington et al., 2017; Pawluk et al., 2016, 2018; Shin et al., 2017). Other inhibition strategies, such as with small molecules (Kundert et al., 2019; Maji et al., 2019) or oligonucleotides (Barkau et al., 2019; Li et al., 2018), have also been demonstrated. However, they require a separate delivery strategy, suffer from incomplete inactivation, necessitate careful dose titration to exert the desired inhibitory effect, exhibit complex inhibition kinetics, and/or require constant presence to avoid reversal of inhibition. To address these obstacles, a CRISPR-Cas9 system with a built-in kill-switch mechanism that is both rapid and complete would be a powerful addition to the genome editing toolbox.

Targeted DNA damage by Cas9 is only the first step of genome editing; the final editing outcome is rather the product of the complex and incompletely understood DNA damage response (DDR) (Chakrabarti et al., 2019; Brinkman et al., 2018; Leenay et al., 2019; Liu et al., 2020; Richardson et al., 2018; van Overbeek et al., 2016; Wienert et al., 2019; Yeh et al., 2019). Indeed, DDR is an essential collection of processes in living organisms that maintains genomic integrity, with implications in cancer, genetic diseases, and aging (Chang et al., 2017; Scully et al., 2019). Understanding the cellular response to DNA damage is therefore necessary in order to identify the possible risks of genome editing, to improve its effectiveness through modulation of DDR pathways, to treat diseases that involve dysfunctional DDR, and to fundamentally appreciate how living organisms maintain genomic integrity in a naturally genotoxic environment.

However, studies of DDR have been hampered by suboptimal strategies for DNA damage induction. Chemical or

Please cite this article in press as: Zou et al., Cas9 deactivation with photocleavable guide RNAs, Molecular Cell (2021), https://doi.org/10.1016/j.molcel.2021.02.007

physical agents such as DNA crosslinkers or irradiation, respectively (Aleksandrov et al., 2018; Lieberman et al., 1971), allow a fast and short pulse of activity to facilitate downstream kinetic studies but are complicated by mixed DNA lesions and lack of sequence specificity. In contrast, endonuclease-driven methods such as meganucleases, TALENS, and Cas9 enable induction of pure, sequence-specific DNA lesions but struggle to accurately track repair resolution because of sustained cycles of damage and repair that desynchronize repair trajectories, leading to a mixed cell population at different stages of repair (Aymard et al., 2014; Caron et al., 2015; Clouaire et al., 2018; Clouaire and Legube, 2019; Vítor et al., 2020). A fast and complete deactivation mechanism for Cas9 would combine the advantages of both approaches: a means of inducing pure, sequence-specific DNA lesions compatible with time-resolved profiling of cellular recovery after DNA damage.

Here, we developed a new mechanism for Cas9 deactivation, achieved through structure-function-guided engineering of a photocleavable group in guide RNA (gRNA). We showed that this modified photocleavable gRNA, or pcRNA for short, achieves almost complete Cas9 deactivation within 1 min of light exposure. To our knowledge, this is the fastest and most complete strategy for Cas9 deactivation, improving on prior arts by at least an order of magnitude in both speed and residual activity. We found that pcRNA also endows Cas9 with greatly reduced off-target genome editing. We further demonstrated the ability of pcRNA to reveal the minimum temporal "dose" of CRISPR activity necessary for the desired editing outcome. Finally, we showed that pcRNA-based Cas9 systems enable systematic investigation of the cellular response to DNA damage. This study lays the foundation for exquisitely controlled Cas9 deactivation to synergistically advance both precision genome editing and studies of DNA repair.

Design

We developed an approach to endow Cas9 with a built-in deactivation mechanism through function-guided modification of a single nucleotide in the CRISPR RNA (crRNA). Because truncated crRNA with 15 or fewer nucleotides of target complementarity (counting from protospacer adjacent motif [PAM]) abolishes cleavage activity (Dahlman et al., 2015; Kiani et al., 2015), we hypothesized that replacement of a single nucleotide with a photocleavable 2-nitrobenzyl linker (PC-linker) (Ordoukhanian and Taylor, 1995) at or before the 15th nucleotide of a full-length crRNA would enable its rapid light-mediated conversion from a cleavage-competent full-length form to a cleavage-deficient truncated form. Despite the photocleavable group's small profile (Figure 1A), the 15th nucleotide was chosen for replacement to minimize potential disruption of Cas9 activity, as base-pairing mismatch tolerance is maximized furthest from PAM (Fu et al., 2016; Hsu et al., 2013; Zheng et al., 2017). Therefore, we hypothesized that this pcRNA would minimally perturb the Cas9-gRNA complex and retain Cas9 cleavage competency, but brief illumination with a low dose of 365-nm-wavelength light would cleave the PC-linker, truncating the region of target complementarity to below 15 nt and rendering Cas9 cleavage deficient (Figure 1B; Figure S1A).

RESULTS

A rapid, built-in Cas9 deactivation mechanism using pcRNAs

We first validated that Cas9 deactivation with light approaches completeness and occurs within seconds using *in vitro* cleavage of three different synthetic DNA sequences. Cas9 protein in complex with pcRNA was illuminated with a 365 nm light-emitting diode (LED) source for 30 s, then target DNA was added within 45 s from the start of light illumination. After incubation at 37°C for 1 h, there was almost no detectable cleavage of target DNA for samples exposed to light but high cleavage efficiency for samples without light, comparable with that of Cas9 with wild-type gRNA (Figure 1C; Figure S1B). Thirty seconds of illumination was sufficient for complete truncation of the pcRNA (Figure 1D; Figure S1C). We next tested the activity of Cas9/pcRNA ribonucleoproteins (RNPs) delivered by electroporation into HEK293T cells with or without 1 min exposure to the deactivation light. This dose of light did not lead to any growth inhibition or cell death (Figure S1D). The percentage of insertions and deletions (indels) 3 days after RNP delivery was computed from a combination of Sanger sequencing/TIDE analysis (Brinkman et al., 2014) and targeted deep sequencing. Cells without light exposure had high indel efficiencies, whereas light-induced deactivation of Cas9/pcRNA within 2 min after delivery reduced indels to almost undetectable levels (Figure 1E). Deactivation completeness inside cells was comparable with deactivation *in vitro* prior to cellular delivery, whereas indel efficiencies without deactivation approached levels obtained using wild-type gRNA (Figure S1E). Both completeness (<1% of normalized residual indels) and speed of deactivation (<1 min) using the pcRNA system were at least an order of magnitude better than other reported strategies of Cas9 inhibition (Figures 1F and 1G) (Barkau et al., 2019; Carlson-Stevermer et al., 2020; Dolgin, 2020; Kleinjan et al., 2017; Maji et al., 2019; Shin et al., 2017).

pcRNA should also be compatible with other platforms that use the Cas9 component such as single-nucleotide base editors, which only function effectively upon full DNA unwinding and target-strand nicking; truncated guides retain binding but inhibit base editing, presumably because of the lack of full unwinding and nickase activity (Rees and Liu, 2018). Thus, we investigated whether our system enables light-mediated deactivation of Cas9-dependent DNA editing by base editors. AncBE4max protein (Koblan et al., 2018) in complex with pcRNA was delivered to HEK293T cells, and the percentage of base editing from targeted deep sequencing was determined 3 days later. We observed almost complete suppression of base editing with light exposure 2 min after RNP delivery and high-efficiency base editing without light (Figure 1H). Base editing efficiencies without deactivation also approached levels obtained using wild-type gRNA, and the completeness of base editor deactivation inside cells was comparable with *in vitro* deactivation prior to cellular delivery (Figure S1F). Therefore, pcRNA provides natively high activity and near complete deactivation also to cytosine base editors.

We hypothesized that the use of light would facilitate spatial control of Cas9 deactivation. We delivered Cas9/pcRNA to HEK293T cells, deactivated Cas9 only in a subset of cells

Please cite this article in press as: Zou et al., Cas9 deactivation with photocleavable guide RNAs, Molecular Cell (2021), https://doi.org/10.1016/j.molcel.2021.02.007

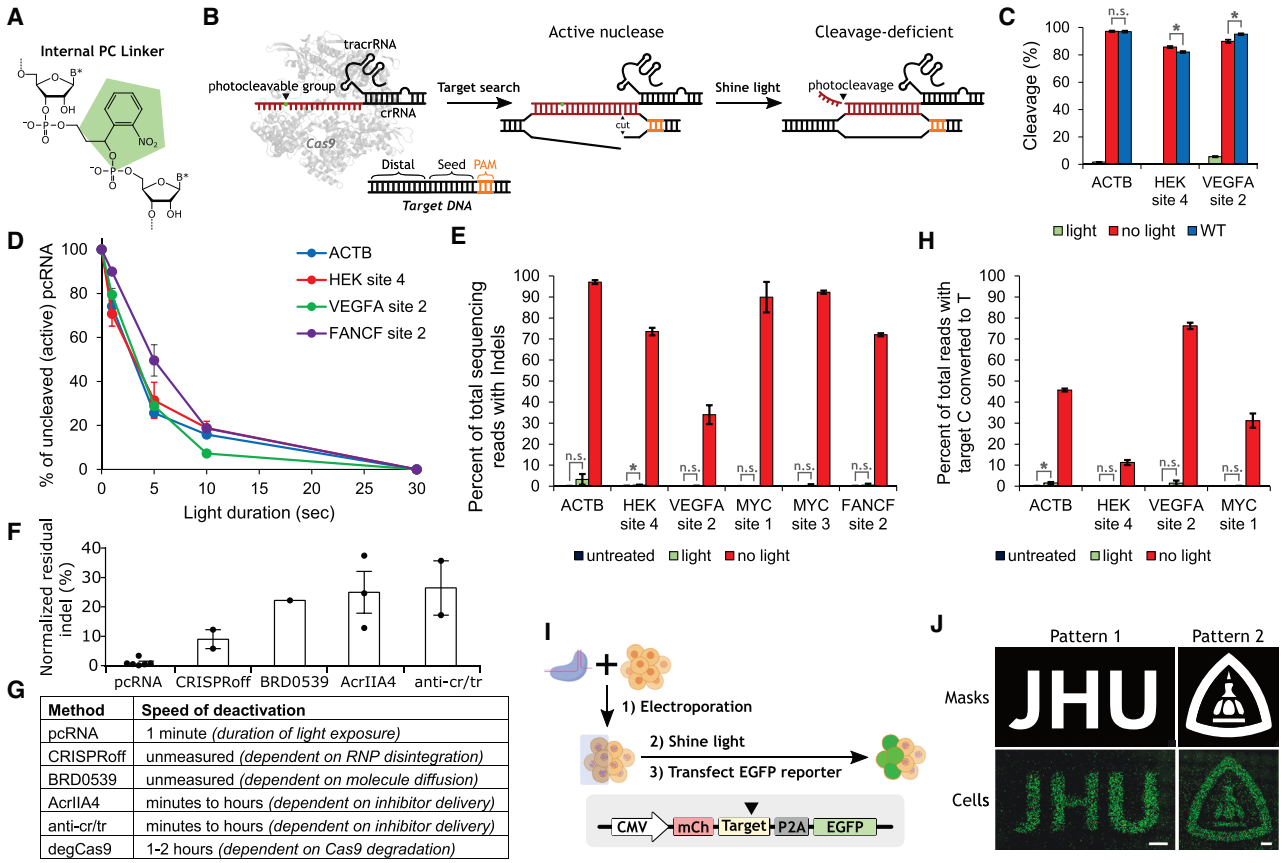

G

Method	Speed of deactivation
pcRNA	1 minute *(duration of light exposure)*
CRISPRoff	unmeasured *(dependent on RNP disintegration)*
BRD0539	unmeasured *(dependent on molecule diffusion)*
AcrIIA4	minutes to hours *(dependent on inhibitor delivery)*
anti-cr/tr	minutes to hours *(dependent on inhibitor delivery)*
degCas9	1-2 hours *(dependent on Cas9 degradation)*

Figure 1. Rapid Cas9 deactivation using pcRNAs

(A) Structure of photocleavable (PC) 2-nitrobenzyl linker.

(B) Schematic of Cas9 deactivation mechanism.

(C) *In vitro* cleavage, 1 h after Cas9/pcRNA RNP delivery. light, deactivation with light for 30 s, followed by addition of target DNA within an additional 15 s; no light, no deactivation; WT, use of control (unmodified) gRNA.

(D) Measurement of direct pcRNA photocleavage leading to a truncated crRNA, as summarized from gel shift assays (Figure S1C).

(E) Indel measurements in cells 72 h after Cas9/pcRNA RNP delivery. untreated, HEK293T cells without Cas9; light, deactivation within 2 min after electroporation; no light, no deactivation.

(F) Comparison of deactivation completeness between pcRNA and other methods in literature, as measured by the percentage of residual genome editing even with the highest inhibitor dose. Normalized residual indel percentage = percentage of residual indels/percentage of indels without inhibition. CRISPRoff is from Carlson-Stevermer et al. (2020). BRD0539 is from Maji et al. (2019). AcrIIA4 is from Shin et al. (2017). Anti-cr/tr is from Barkau et al. (2019). Results for pcRNA were derived from (E). Error bars represent ± SEM across different experiments.

(G) Comparison of the effective deactivation speed between pcRNA and other methods in literature, same as (F). degCas9 is from Kleinjan et al. (2017).

(H) Base editing in cells 72 h after AncBE4max/pcRNA RNP delivery, with the same conditions as (E).

(I) Schematic of spatial control assay. The grayed rectangle shows the plasmid with the Cas9 cleavage site marked with a black triangle.

(J) Illustration of the patterned optical masks used when illuminating cells (top row) and the corresponding fluorescence cell imaging for GFP expression (bottom row). White areas allow illumination through the mask. Scale bars indicate 1 mm.

In (C), (D), (E), and (H), error bars represent ±SD across biological replicates (n = 3). n.s., not significant; *p < 0.05, **p < 0.01, and ***p < 0.001.

See also Figure S1.

through an optical mask of a complex pattern at sub-millimeter spatial resolution, then transfected all cells with an EGFP reporter plasmid containing the Cas9 cleavage site (Figure 1I). Only cells exposed to light exhibited EGFP expression, consistent with functional reporter plasmids, that is, uncleaved by Cas9, only in cells with deactivated Cas9 (Figure 1J).

Together, these experiments validated the effectiveness of pcRNA in conferring a fast and versatile spatiotemporal deactivation mechanism to Cas9-based genome editing systems.

pcRNAs natively improved genome editing specificity

Off-target editing is serious concern for genome editing technologies (Casini et al., 2018; Kocak et al., 2019; Vakulskas et al., 2018). Combining CRISPR deactivation with enhanced specificity would be powerful, but Cas9 mutants with enhanced genome editing specificity (Chen et al., 2017; Hu et al., 2018; Kleinstiver et al., 2016; Slaymaker et al., 2016) may not be compatible with additional perturbation of gRNA from the photocleavable group. Fortunately, gRNA perturbations have also been shown to improve

Please cite this article in press as: Zou et al., Cas9 deactivation with photocleavable guide RNAs, Molecular Cell (2021), https://doi.org/10.1016/j.molcel.2021.02.007

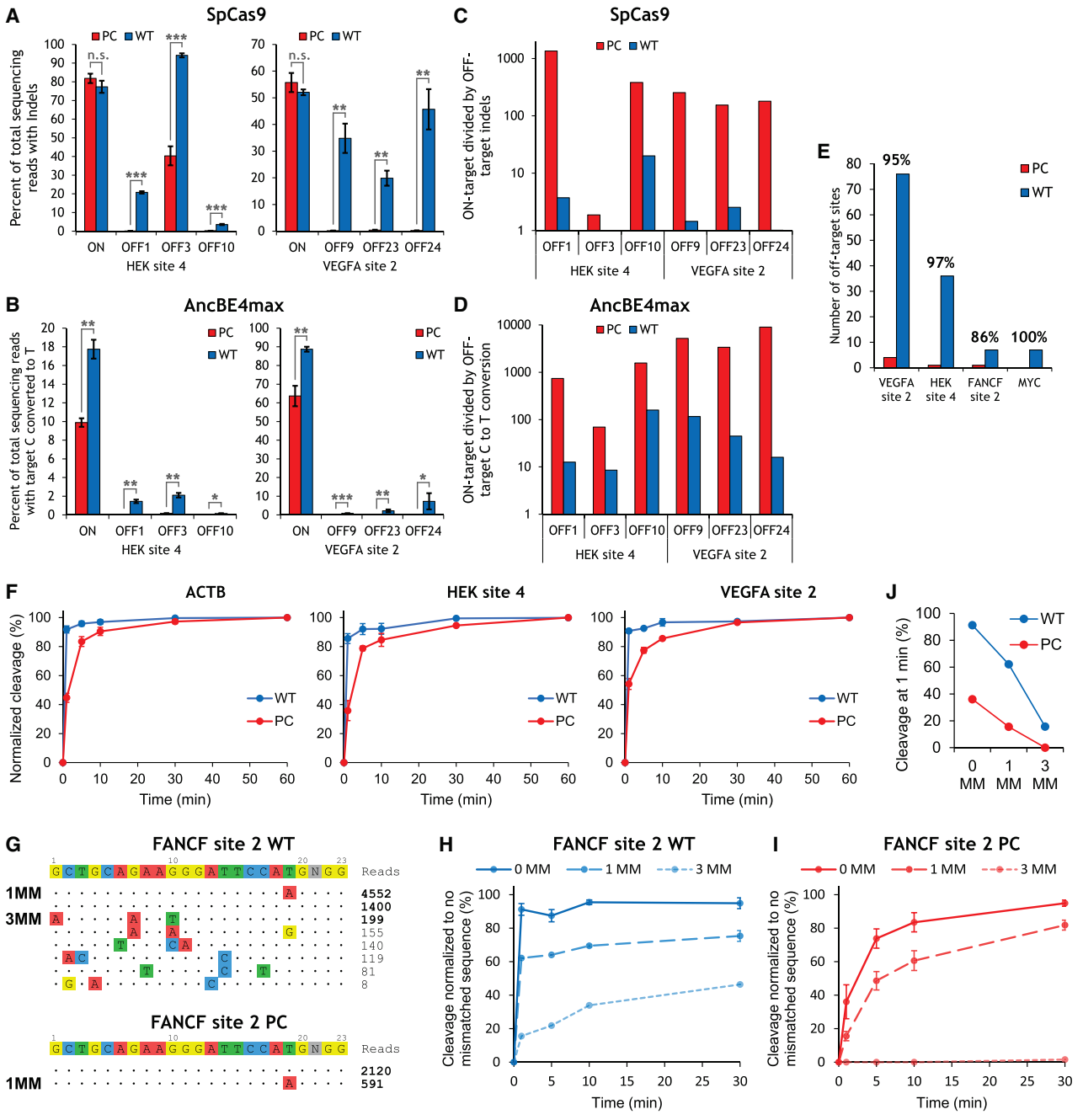

Figure 2. pcRNAs natively exhibited enhanced specificity

(A) Percentage of indels at the on-target and select off-target sites using Cas9 with either pcRNA (PC) or wild-type guide RNA (WT). Error bars represent ±SD across biological replicates (n = 3). n.s., not significant; *p < 0.05, **p < 0.01, and ***p < 0.001.

(B) Same as (A) for AncBE4max.

(C) Percentage of on-target indels divided by the percentage of off-target indels for each tested off-target site.

(D) Same as (C), for AncBE4max-mediated cytosine to thymine conversion.

(E) Quantification of off-target sites detected using GUIDE-seq for Cas9 with pcRNA (PC) or wild-type gRNA (WT). Percentage reduction in the number of off-target sites from WT to PC is labeled above the plot.

(F) Time-resolved *in vitro* cleavage efficiencies at on-target sites using Cas9 with either pcRNA (PC) or wild-type guide RNA (WT). Error bars represent ±SD across replicates (n = 2).

(G) GUIDE-seq using wild-type gRNA (WT) or pcRNA (PC) targeting *FANCF site 2*. 1MM is a target sequence with one mismatch. 3MM is a target sequence with three mismatches.

(legend continued on next page)

Please cite this article in press as: Zou et al., Cas9 deactivation with photocleavable guide RNAs, Molecular Cell (2021), https://doi.org/10.1016/j.molcel.2021.02.007

specificity, likely by altering its sensitivity to nucleotide mismatches between gRNA and genomic DNA (Cromwell et al., 2018; Fu et al., 2013; Yin et al., 2018), so we tested whether inclusion of the photocleavable group to gRNA would directly enhance Cas9 specificity. We measured indels and cytosine base editing at select off-target sites of *VEGFA site 2* and *HEK site 4* 72 h after delivery of either Cas9 or AncBE4max with pcRNA to cells. We observed dramatic suppression of Cas9-mediated indels and AncBE4max-mediated base editing at all tested off-target sites (Figures 2A and 2B; Figure S2A), improving the ratio of on-target to off-target editing by 2- to 9,000-fold compared with wild-type gRNA (Figures 2C and 2D). GUIDE-seq (Tsai et al., 2015) at 72 h after Cas9/pcRNA delivery further revealed that the significantly improved targeting specificity holds genome-wide, with 86%–100% reduction in the number of detected off-target sites using pcRNA compared with wild-type gRNA (Figure 2E; Figure S2B). Proportion of off-target GUIDE-seq reads was also greatly reduced with pcRNA compared with wild-type gRNA, comparable with or better than other enhanced specificity Cas9s for the same evaluated target sequences from published datasets (Figure S2C).

To understand the mechanism behind the enhanced specificity, we investigated the cleavage kinetics of Cas9/pcRNA using *in vitro* cleavage assays. For all target sequences tested, the initial cleavage rate was lower using pcRNA compared with wild-type gRNA, even though the eventual cleavage efficiency was comparable (Figure 2F). We further evaluated cleavage of select mismatched target sequences determined from GUIDE-seq results of *FANCF site 2* (Figure 2G). A single mismatch at the PAM-proximal position still led to more than 60% cleavage within 1 min using wild-type gRNA, compared with less than 20% cleavage using pcRNA (Figures 2H–2J). With three mismatches, wild-type gRNA still resulted in rapid cleavage, whereas pcRNA resulted in almost no activity (Figure 2J). Together, our results suggest that pcRNA provides specificity enhancement through heightened kinetic control over Cas9 cleavage and increased sensitivity to mismatches. Given that Cas9 is believed to exhibit multiple-turnover activity inside cells (Clarke et al., 2018; Wang et al., 2020) with much shorter dwell times for off-target sequences compared with on-target sequences (Knight et al., 2015; Ma et al., 2016), off-target binding sites would be much less likely to experience cleavage before Cas9/pcRNA dissociation. Decrease in the intrinsic cleavage rate and sensitivity to mismatches are also believed to be mechanisms exhibited by other enhanced-specificity Cas9s (Singh et al., 2018).

Minimum "dose" of active genome editor necessary for high editing efficiencies

As genome editing enzymes can be active for days to weeks in cells (Kim et al., 2014; Zuris et al., 2015), characterizing the minimum duration of active enzyme or "dose" necessary to achieve a desired level of final editing is crucial for balancing high on-target editing with the lowest probability of accruing adverse side effects (Haapaniemi et al., 2018; Kosicki et al., 2018). We used pcRNA to investigate this question by measuring the effect of varying the deactivation time point on endpoint editing percentage evaluated at 72 h (Figure 3A). AncBE4max required shorter durations of activity to achieve high editing at endpoint, with 2–4 h sufficient to attain 50%–80% of maximum potential, compared with 12–36 hs with Cas9 (Figures 3B and 3C).

Because deactivation is sequence independent, we hypothesized that the large variability in dose dependence of editing percentages between target sites can be attributed to heterogeneous, target-dependent genome editing kinetics (Rose et al., 2017). To quantify this difference in editing kinetics, we evaluated editing outcomes of standard Cas9/pcRNA or AncBE4max/pcRNA measured directly at an early 15 h time point (Figure 3D). Editing percentage scored at 15 h was indeed heterogeneous between target sequences, ranging from 10% to 95% indels for Cas9 and from 5% to 80% base editing for AncBE4max, suggesting that it captures the dynamic range of editing kinetics before genome editing saturation. Crucially, editing percentage at 15 h was highly correlated with editing percentage, measured at 72 h, after deactivation at 12 h (R^2 = 0.93 for Cas9 and R^2 = 0.76 for AncBe4max), confirming that the heterogeneity in dose dependence of editing percentages between target sites can be attributed to heterogeneous genome editing kinetics (Figures 3E and 3F).

We aimed to develop a mathematical model to predict the minimal temporal dose required for a desired level of final genome editing that takes into account the wide variation in editing kinetics. Editing percentage at 15 h was used to estimate editing percentage, measured at 72 h, after deactivation at 12 h, followed by model parameter estimation (STAR methods) that enabled prediction of endpoint editing efficiencies for any duration of active Cas9 activity (Figures 3G and 3H; Figure S3). This mathematical model accounts for the variability in genome editing kinetics because the input, that is, editing percentage at 15 h measured using standard Cas9/pcRNA, conveniently encodes information on intrinsic genome editing kinetics. Together, this time-resolved analysis suggests that extended activity past the first 4 h for AncBE4max or 36 h for Cas9 may be minimally productive for on-target editing.

Limiting the duration of activity has been previously demonstrated using anti-CRISPR proteins to selectively reduce off-target genome editing compared with on-target (Shin et al., 2017). To test whether our light-induced deactivation system can achieve a similar effect, we performed GUIDE-seq on cells at 72 h with Cas9/pcRNA deactivated with light after 3 h of activity. Compared with samples without light, we found that limiting Cas9 to 3 h of activity did not reduce the number of detected off-target sites for *HEK site 4*, and reduced just one detected off-target site for *VEGFA site 2* (Figure S2B). Furthermore, for the one *HEK site 4* off-target site (OFF3) that still had appreciable indel activity with pcRNA, limiting the activity window of Cas9 actually worsened the ratio of on- to off-target editing

(H and I) Time-resolved *in vitro* cleavage efficiencies of the on-target site for *FANCF site 2* (0 MM) and off-target sites 1MM and 3MM labeled in (G). Error bars represent ±SD across replicates (n = 2).
(J) Cleavage at 1 min from (H) and (I).
See also Figure S2.

Please cite this article in press as: Zou et al., Cas9 deactivation with photocleavable guide RNAs, Molecular Cell (2021), https://doi.org/10.1016/j.molcel.2021.02.007

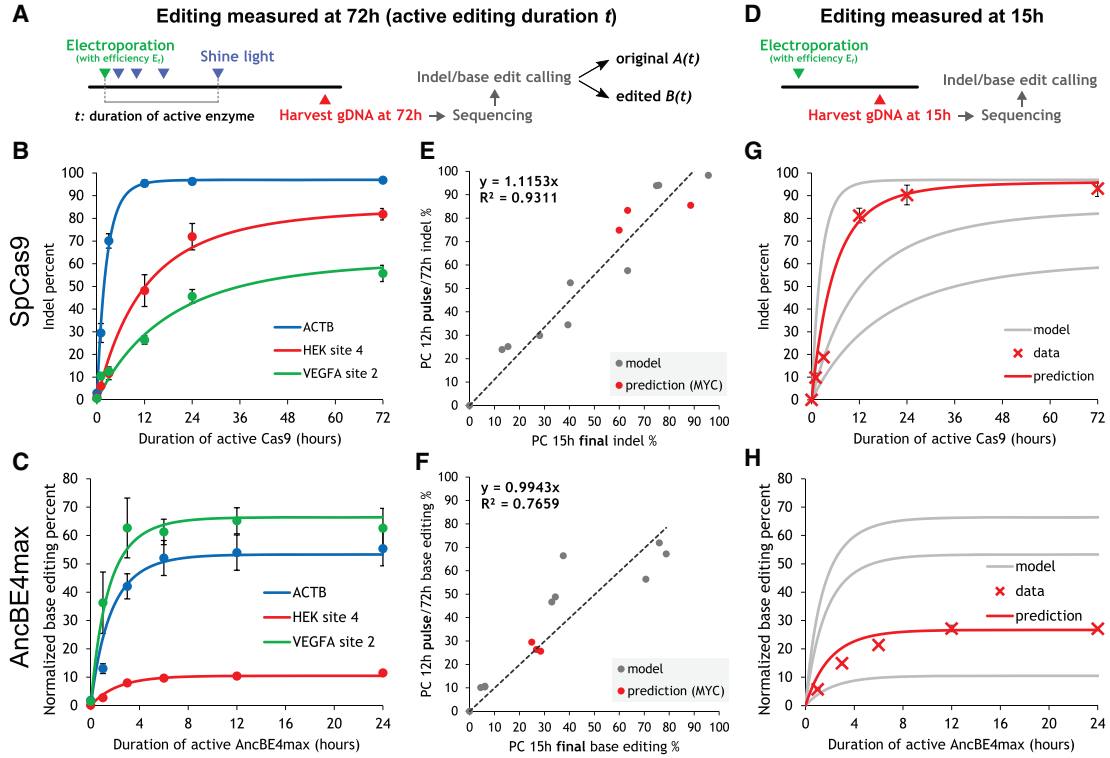

Figure 3. Hours of active Cas9 or AncBE4max are sufficient for high-efficiency genome editing

(A) Schematic of temporal control of Cas9 or AncBE4max activity with timed light-mediated deactivation

(B and C) Shining light to cells at early time points inhibits endpoint (72 h) Cas9 indels or AncBE4max base editing. The circles represent averaged experimental data. Lines represent the model predictions after fitting experimental data. Error bars represent ±SD across biological replicates (n = 3).

(D) Schematic of direct measurement of Cas9 or AncBE4max genome editing at the 15 h time point.

(E and F) Deactivation at 12 h followed by indel/base editing measurement at 72 h (y axis) is highly correlated with indel/base editing measurements directly at 15 h (x axis). Gray points ("model") correspond to triplicate measurements for *ACTB*, *HEK site 4*, and *VEGFA site 2*, which was used to determine the line of best fit (dotted line). Red points ("prediction") correspond to triplicate measurements for *MYC*, a new target sequence to validate the predictive accuracy of our model.

(G and H) The mathematical model was fit (gray lines) using *ACTB*, *HEK site 4*, and *VEGFA site 2* data from (B) and (C). For a new target sequence, *MYC*, given its indel/base editing measurements at 15 h, indel/base editing measurements at 72 h after Cas9/AncBE4max deactivation at 12 h can be predicted using (E) and (F), which can then be used to determine model parameters and predict the full kinetic curve (red line).

See also Figure S3.

(Figure S3E). It is possible that the dramatically improved specificity imparted by the use of pcRNA itself made it challenging for early deactivation to confer additional off-target reduction. Nevertheless, the specificity benefit from stopping Cas9 early may not be a general phenomenon. However, early deactivation of base editing after 3 h did lead to a modest improvement in final base editing purity (Figure S3F), defined as the fraction of final thymine, divided by the fraction of thymine, adenine, and guanine, at the targeted nucleotide (Rees and Liu, 2018).

Time-resolved characterization of repair protein departure after Cas9-mediated DSBs

Next, we used the pcRNA system to enable synchronized measurements of DNA repair pathway progression and resolution. Rapid and complete deactivation terminates the accrual of new DNA lesions such that cellular recovery from DNA damage can be precisely assayed without confounding effects from additional DNA damage. We exposed HEK293T cells to Cas9/pcRNAs targeting *ACTB* and *MYC* for 1 h, followed by Cas9 deactivation and chromatin immunoprecipitation sequencing (ChIP-seq) for MRE11 as a function of time after deactivation. MRE11 has been previously shown to localize to sites of Cas9-mediated double-strand breaks (DSBs) (Wienert et al., 2019; Liu et al., 2020). Enrichment was quantified as the number of reads in a 5 kb window centered at either the *ACTB* or *MYC* cleavage site, normalized by the total number of reads in millions. For both target sequences, we observed an initial rise/plateau in MRE11 enrichment for the first 15 min after Cas9 deactivation, consistent with additional MRE11 recruitment to previously generated, but newly exposed, DSB sites (Figures 4A and 4B; Figures S4A and S4B) (Liu et al., 2020). The rise was followed by MRE11 departure with a calculated half-life of less than 1 h for both target sequences (Figure 4C; Figure S4C).

We also performed ChIP-seq for 53BP1, which assembles higher order chromatin structures to maintain genome integrity (Ochs et al., 2019). ChIP-seq signal was quantified by dividing

Please cite this article in press as: Zou et al., Cas9 deactivation with photocleavable guide RNAs, Molecular Cell (2021), https://doi.org/10.1016/j.molcel.2021.02.007

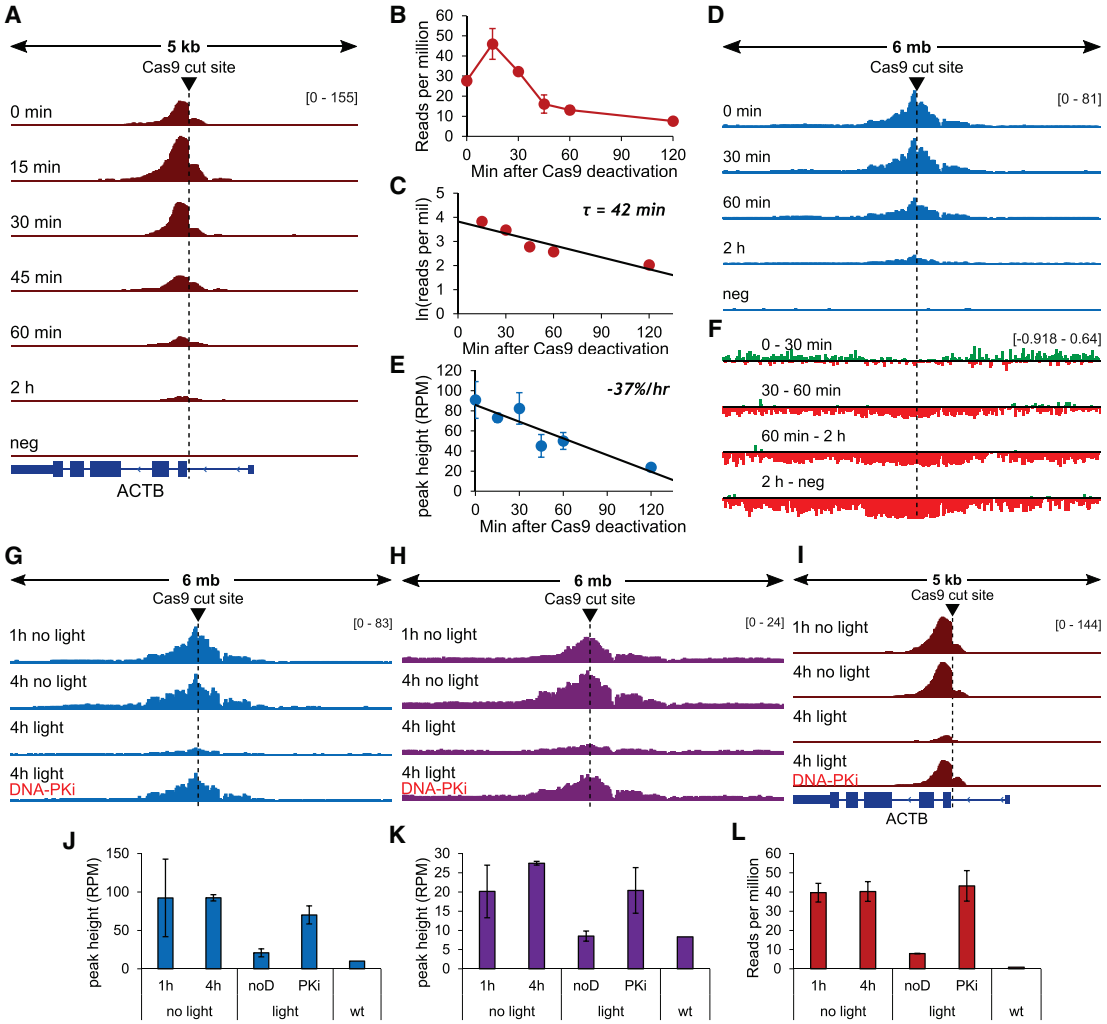

Figure 4. Dynamics of DNA repair factor departure after Cas9 deactivation at *ACTB*

(A) Cas9 was deactivated 1 h after RNP delivery. MRE11 ChIP-seq enrichment at *ACTB* was tracked as a function of time after deactivation, starting from 0 min; "neg" corresponds to no Cas9/pcRNA delivery.

(B) For the 5 kb window centered at the *ACTB* cut site, number of reads per million total sequencing reads was plotted for all time points in (A). Error bars represent ±SEM across biological replicates (n = 2).

(C) Log transform of t = 15 min to 2 h from (B), with a calculated half-life of 42 min.

(D) Same experimental conditions as (A) for 53BP1 ChIP-seq.

(E) Quantification of maximum peak height from (D), which decreased by approximately 37% per hour from 0 min. Error bars represent ±SEM across biological replicates (n = 2).

(F) For each 5 kb bin, the fractional change in RPM enrichment between two 53BP1 ChIP-seq samples was calculated and plotted. Green and red corresponds to positive and negative changes, respectively.

(G–I) 53BP1 (blue), γH2AX (purple), and MRE11 (red) enrichment centered at *ACTB* at 1 and 4 h after Cas9/pcRNA delivery but without deactivation (top two rows) or at 4 h after delivery but with deactivation at 1 h, with or without 0.5 μM DNA-PKcs inhibitor Ku-0060648 (bottom two rows).

(J–L) Quantification of (G)–(I). "wt" corresponds to wild-type HEK293T cells without Cas9/pcRNA delivery. Error bars represent ±SEM across biological replicates (n = 2).

See also Figure S4.

the genome into 5 kb bins and calculating the number of reads, normalized by the total number of reads in millions, in each bin. We confirmed that Cas9-induced DSBs led to 53BP1 signal spanning multiple megabases, consistent with previous literature (Figure 4D; Figure S4D) (Clouaire et al., 2018; Liu et al., 2020). After light-induced deactivation, 53BP1 peak signal depleted by ~33% per hour (Figure 4E; Figure S4E). The fractional decrease in signal over consecutive time points was relatively uniform over megabases surrounding the cleavage site (Figure 4F; Figure S4F), suggesting uniform 53BP1 dissociation from genomic DNA. Together, ChIP-seq for MRE11 and 53BP1 provided the first estimate, to our knowledge, of repair protein

Please cite this article in press as: Zou et al., Cas9 deactivation with photocleavable guide RNAs, Molecular Cell (2021), https://doi.org/10.1016/j.molcel.2021.02.007

departure kinetics at pure, sequence-specific DSBs, finding that the vast majority of both proteins departed within 2 h of Cas9 deactivation.

Because 53BP1 appeared to dissociate in a coordinated manner from genomic DNA, even when located megabases away from the cut site, we evaluated whether 53BP1 dissociation is responsive to disruptions in DNA repair. We tested inhibition of DNA-dependent protein kinase catalytic subunit (DNA-PKcs), an enzyme integral to DSB repair, using KU-0060648, which has been shown to inhibit repair progression (Ding et al., 2003; Graham et al., 2016; Mamo et al., 2017; Perrault et al., 2004; Uematsu et al., 2007). Whereas Cas9 deactivation led to greatly reduced 53BP1 occupancy 3 h later, combining with DNA-PKcs inhibition led to sustained occupancy of 53BP1 even megabases away, even though DNA-PKcs is only known to span kilobases from the cut site (Caron et al., 2015) (Figure 4G; Figure S4G). This phenotype was similar to what was observed without Cas9 deactivation, which also exhibited sustained 53BP1 signal due to sustained induction of new DSBs. Delay in repair factor departure upon DNA-PKcs inhibition was also present for MRE11 as well as phosphorylated H2AX (γH2AX), another DNA damage marker that spans megabases from the cut site (Figures 4G–4L; Figures S4G–S4L). These results highlight how repair protein departure, rather than being a passive process after initial recruitment, is tightly regulated and responsive to repair progression.

DISCUSSION

We have expanded the CRISPR toolbox by developing a rapid and near complete deactivation mechanism for Cas9-based nucleases and base editors. The advantages of our system stem from its simple, built-in design: given brief exposure to a low-intensity, commercially available LED that induces disruption of the photocleavable group in gRNA, Cas9 is immediately, irreversibly, and almost completely deactivated within seconds, a binary outcome akin to a kill switch. Light-based delivery facilitates exposure of every cell to an equal dose of deactivating light. Furthermore, irreversible deactivation is a feature that greatly simplifies our system, especially because CRISPR applications generally do not need reactivation after the desired genome editing has already occurred.

Such a system has many applications to genome editing. pcRNAs allow convenient calibration of genome editing efficiency as well as an intrinsic kill switch to editing activity. Given that genome editing agents are genotoxic, controlling the extent of activity may minimize the probability of accruing adverse outcomes, ranging from off-target editing to large deletions or translocations even at the desired target site (Haapaniemi et al., 2018; Kosicki et al., 2018; Shin et al., 2017). In the context of therapeutic genome editing, for example, controlled deactivation of Cas9 RNP-based primary T cell engineering (Roth et al., 2018) would minimize exposure to mutagenic genome editing agents, potentially reducing the risk for cell death or malignancy prior to injection back into human subjects. In embryo editing, deactivation of Cas9 before the embryo divides beyond the one-cell stage could be a convenient approach to eliminate mosaicism (Maji et al., 2019; Marx, 2019). For all applications, fast deactivation and minimal residual activity, which we observe using pcRNAs, is important to ensure the greatest experimental control such that there is no unintended editing after deactivation has occurred.

This study also demonstrates the utility of Cas9 deactivation for studies of DNA repair. Cas9 is a precise and efficient tool to induce targeted DSBs, but without deactivation, sustained activity leads to repetitive cycles of DNA damage and repair that abrogate effective kinetic analysis of repair resolution (Clouaire and Legube, 2019; Vítor et al., 2020). Combined with high-throughput sequencing such as ChIP-seq, we were able to quantify the dynamics of chromatin restoration after DNA repair. Extension of pcRNA to Cas9 nickases (Trevino and Zhang, 2014), base editors (Rees and Liu, 2018), and prime editors (Anzalone et al., 2019) as well as other assays such as assay for transposase-accessible chromatin using sequencing (ATAC-seq) (Buenrostro et al., 2013) and ChIP-seq for histone modifications or other repair proteins (Clouaire et al., 2018) would enable comprehensive investigation of DNA repair resolution across different lesion types.

Comparison with other methods of inhibiting CRISPR activity

Unlike pcRNA, many other strategies for Cas9 inhibition require delivery of exogenous inhibitors, which lead to complications in achieving rapid and complete control of Cas9 deactivation. For example, delivery of anti-CRISPR proteins requires electroporation of purified anti-CRISPR proteins or plasmid-based liposomal transfection, both of which can take hours to be in effect (Shin et al., 2017). Executing the correct timing of CRISPR versus anti-CRISPR delivery to achieve the desired genome editing outcome is therefore difficult and cumbersome. Furthermore, delivery efficiencies can be very heterogeneous across millions of cells and challenging to optimize, especially for hard-to-transfect cells. A significant percentage of cells may not be exposed to a sufficient dose of inhibitor, resulting in partial inactivation. Similar disadvantages apply to oligonucleotide inhibitors, which use the same delivery strategies (Barkau et al., 2019; Li et al., 2018). In contrast, small-molecule inhibitors are more convenient to administer and can achieve rapid kinetics, but suffer from incomplete inactivation, require sustained inhibitor presence (Maji et al., 2019), and/or have not been demonstrated in mammalian cells (Kundert et al., 2019). Cas9 fused to an auxin-inducible degron is another small-molecule approach for Cas9 removal that could achieve complete deactivation after degradation of all Cas9, but reliance on the cell's proteasome leads to slow kinetics (Kleinjan et al., 2017). In addition, most previous methods did not demonstrate generalization to other Cas9-based systems such as base editors, and none of them exhibited spatial control over deactivation. Therefore, to the best of our knowledge, the pcRNA system is the only way, thus far, to achieve rapid (<1 min), complete (<1% residual indels), and spatially controlled deactivation.

Recently, a new study also achieved Cas9 deactivation with alternative placement of PC-linker molecules in the stem-loop section of gRNA and demonstrated both spatial and time-resolved deactivation capability (Carlson-Stevermer et al., 2020). However, applicability to base editors was not demonstrated, deactivation completeness and speed were not

Please cite this article in press as: Zou et al., Cas9 deactivation with photocleavable guide RNAs, Molecular Cell (2021), https://doi.org/10.1016/j.molcel.2021.02.007

precisely measured, and their design likely does not confer natively enhanced specificity.

Precision genome editing with improved specificity and dose minimization

The level of enhanced specificity using pcRNA appeared to be comparable with other strategies of enhanced specificity from literature. Evaluating GUIDE-seq results for genome-wide detection of off-target sites allowed direct comparison with protein-engineered enhanced specificity Cas9s, with pcRNAs resulting in comparable or even greater reductions in off-target GUIDE-seq reads (Figure S2C). For evaluation of specificity using well-annotated off-target sites, truncated (Fu et al., 2014), DNA-incorporated (Yin et al., 2018), or bridged nucleic acid (BNA) and locked nucleic acid (LNA)-incorporated gRNAs (Cromwell et al., 2018) all reported comparable specificity enhancements ranging from tens to 10,000-fold at off-target sites of different target sequences, which is also comparable to our results.

In vitro cleavage assays revealed (1) decreases in the intrinsic cleavage rate and (2) sensitivity to mismatches as mechanisms for the natively enhanced specificity using pcRNA, which were also mechanisms observed for other enhanced specificity Cas9s (Singh et al., 2018). Just like other strategies of reducing off-target editing (e.g., protein engineering, other gRNA modifications), these findings suggest that the photocleavable group in the crRNA may modulate of the thermostability between Cas9, gRNA, and target DNA, such that only target sequences with minimal mismatches will readily experience cleavage (Casini et al., 2018; Chen et al., 2017; Fu et al., 2013; Kleinstiver et al., 2016; Kocak et al., 2019; Slaymaker et al., 2016; Vakulskas et al., 2018; Yin et al., 2018).

Limitations

Although pcRNA exhibits very high deactivation efficiency, we do observe low (less than 1%) levels of residual indels. Two mechanisms likely explain this scenario. First, there is some likelihood that the post-photocleaved truncated gRNA is able to exhibit very low levels of residual cleavage. Second, achieving full deactivation completeness would require truncation of every single pcRNA in the system. This may be challenging to accomplish in a biological sample because of stochasticity and/or experimental variation, especially as 365-nm-wavelength light exhibits low levels of penetrance into cells and tissues (Ash et al., 2017). Increasing the illumination dose may ensure more complete deactivation, but at the cost of potential cellular toxicity. As a corollary, low tissue penetrance would likely limit pcRNA from *in vivo* applications, though new photocleavable oligonucleotide chemistries that employ two-photon excitation has potential to extend the depth of deactivation activity (Weyel et al., 2017).

We showed that our strategy likely exhibits natively enhanced specificity because of perturbations to Cas9-gRNA-DNA interactions, which is similar to other strategies for enhancing Cas9 specificity. However, these perturbations often lead to a trade-off between enhanced specificity and Cas9 activity (Schmid-Burgk et al., 2020). Therefore, although the target sequences shown have comparable activity between wild-type gRNA and pcRNA with Cas9, pcRNA does appear to have weaker activity when used with base editors, and it is possible for some target sequences to exhibit lower levels of activity in cells. Target sequences previously demonstrated to work with pcRNAs and/or those validated to have high editing activity with wild-type gRNA should be chosen first, for the highest likelihood of exhibiting high pcRNA on-target activity.

Finally, because pcRNAs are chemically synthesized, its use may be limited in certain applications that require genetic encoding of gRNA. However, as demonstrated here and in previous literature, chemically synthesized gRNAs such as pcRNAs have many delivery strategies, including RNP electroporation, RNP lipofection, and gRNA electroporation/lipofection of Cas9-expressing cells (Liu et al., 2020). Indeed, Cas9 RNP delivery is prevalent and often exhibits several advantages compared with genetically encoded Cas9 and gRNAs (Chen et al., 2016; Vakulskas et al., 2018; Zuris et al., 2015).

Versatile tool for systematic studies of the cellular response to DNA damage

Studies of DDR are hampered by convenient methods for targeted and controlled DNA damage induction. Previous technologies can be categorized into (1) non-specific DNA damage agents such as chemical mutagens, ionizing radiation, and laser micro-irradiation or (2) endonucleases, such as meganucleases (I-*Sce*I, *Fok*I, *Asi*SI), TALENS, zinc-finger nucleases, and CRISPR-Cas9 (Clouaire and Legube, 2019; Vítor et al., 2020). Non-specific agents induce a pulse of DNA damage that facilitates downstream kinetic analysis but suffer from low-throughput induction, heterogeneous DNA damage, and/or no sequence specificity. Heterogeneous DNA lesions in close proximity may influence DNA repair dynamics in unpredictable ways, and lack of sequence specificity precludes the applicability of powerful assays such as ChIP. In contrast, endonuclease methods are sequence specific by design but exhibit a crucial limitation: sustained activity that leads to repetitive cycles of DNA damage and repair, which abrogate effective kinetic analysis of repair resolution (Clouaire and Legube, 2019; Vítor et al., 2020). Our pcRNA technology combines the advantages of endonuclease methods, through its sequence specificity and lesion purity, with the advantage of non-specific mutagens, through convenient deactivation of DNA damage. This combination permits systematic interrogation of endogenous repair factor dynamics at pure, sequence-specific DSBs that best recapitulate physiologic repair progression.

A recent study introduced vfCRISPR, a rapid Cas9 photoactivation strategy at seconds and sub-cellular resolutions (Liu et al., 2020). Activation of Cas9 cleavage within seconds empowered interrogation of DNA repair processes, especially of DSB recognition and initial repair protein recruitment. However, like other endonuclease-based methods, lack of deactivation capability results in multiple cycles of repair and dissolution that can confound time-resolved measurements after the initial response. Our pcRNA technology is the first demonstration of Cas9 deactivation as applied to studies of DNA repair and is thus poised to systematically address the complementary question of how Cas9-mediated DSBs resolve and how the chromatin recovers from DNA damage. However, whereas vfCRISPR could achieve sub-cellular Cas9 activation, pcRNA can only attain cellular but

Please cite this article in press as: Zou et al., Cas9 deactivation with photocleavable guide RNAs, Molecular Cell (2021), https://doi.org/10.1016/j.molcel.2021.02.007

not sub-cellular deactivation resolution. This is because after hypothetical deactivation of Cas9 in a small sub-cellular volume, the majority population of active Cas9 that surrounds this volume will diffuse in, thus reversing the deactivation.

The departure dynamics determined here can also be compared with previous methods that generate complex DNA lesions, such as laser micro-irradiation, in which a high-powered laser physically induces DNA damage (Aleksandrov et al., 2018). MRE11 and RAD50, along with NBS1, form the multi-protein MRN complex (Rupnik et al., 2008); the MRE11 departure half-life of 42–50 min determined from our study is comparable with ~33 min for RAD50 after laser micro-irradiation (Aleksandrov et al., 2018). This analysis suggests that our study recapitulates repair factor dynamics that are consistent across DSBs generated by different methods, without confounding effects arising from mixed DNA lesions.

For further systematic study of repair protein dynamics at single Cas9-induced DSBs, time-resolved ChIP-seq after Cas9/pcRNA deactivation, combining with perturbations such as cell cycle synchronization and repair pathway modulation (Yeh et al., 2019), can be easily extended to assay other factors involved in DSB repair such as Ku70/80, BRCA1, and FANCD2 (Scully et al., 2019). Furthermore, ChIP-seq for epigenetic markers, chromatin conformation capture, RNA sequencing (RNA-seq), and proteomics could systematically survey how epigenetic states, three-dimensional (3D) genome organization, transcriptomes, and proteomes, respectively, change before, during, and after DNA damage and repair (Aymard et al., 2017; Derks et al., 2014; Iannelli et al., 2017; von Stechow and Olsen, 2017).

"Plug-and-play" functionality

Finally, a significant advantage of gRNA engineering with pcRNA is its convenient "plug-and-play" functionality across multiple genome editing systems. We demonstrated its compatibility with both Cas9 nucleases and cytosine base editors, which exhibit different mechanism of actions and generate different DNA lesions, but both require a full-length gRNA for efficient activity. Therefore, pcRNA should be compatible with other Cas9-based systems in which a truncated gRNA leads to deactivation, such as nickases (Trevino and Zhang, 2014), adenine base editors (Rees and Liu, 2018), and prime editors (Anzalone et al., 2019). pcRNA would immediately endow spatiotemporal deactivation control and enhanced specificity to these genome editing platforms, as well as empower systematic study of single-strand break, base excision or mismatch, and flap repair pathways, respectively. Furthermore, structure-function-guided engineering of the photocleavable group to gRNA may be a general approach of conferring convenient, spatiotemporal deactivation functionality to non-Cas9 CRISPR systems such as Cpf1, Cas13, and CasX (Pickar-Oliver and Gersbach, 2019).

STAR★METHODS

Detailed methods are provided in the online version of this paper and include the following:

- KEY RESOURCES TABLE
- RESOURCE AVAILABILITY
  - Lead contact
  - Materials availability
  - Data and code availability
- EXPERIMENTAL MODEL AND SUBJECT DETAILS
- METHOD DETAILS
  - Molecular cloning
  - SpCas9 purification
  - AncBE4max purification
  - Electroporation of SpCas9/AncBE4max RNP
  - Deactivation light exposure for in cell and *in vitro* experiments
  - Preparing samples for kinetics measurements in cells
  - Sanger Sequencing for measuring insertions or deletions
  - High throughput sequencing of genomic DNA samples
  - *In vitro* cleavage assay
  - GUIDE-seq
  - Spatial control of Cas9 deactivation
  - Determination of electroporation efficiency from immunofluorescence microscopy
  - Chromatin immunoprecipitation
- QUANTIFICATION AND STATISTICAL ANALYSIS
  - Analysis of cytosine base editing efficiency
  - Data processing of high throughput sequencing results
  - High-throughput sequencing and data processing of ChIP samples
  - 53BP1 and γH2AX enrichment analysis
  - MRE11 enrichment and fragment analysis from paired-end ChIP-seq reads
  - Mathematical Model A for duration-resolved endpoint editing
  - Mathematical Model B for duration-resolved endpoint editing
- ADDITIONAL RESOURCES
  - Detailed protocol

SUPPLEMENTAL INFORMATION

Supplemental Information can be found online at https://doi.org/10.1016/j.molcel.2021.02.007.

ACKNOWLEDGMENTS

We thank Dr. Shiva Razavi and Shuaixin He for assistance with protein purification, Dr. Geraldine Seydoux for access to the Lonza 4D nucleofector, Dr. Winston Timp for access to a MiSeq and Bioruptor Pico sonicator, and Dr. Haiping Hao of the Transcriptomics and Deep Sequencing Core for sequencing of ChIP samples. This work was supported by grants from the NIH (R35 GM 122569 and U01 DK 127432 to T.H. and T32 GM 73009 and F30 CA 254160 to R.S.Z.), National Science Foundation (NSF) (PHY 1430124 and EFMA 1933303 to T.H., 1817447 to B.W.) and Pew Charitable Trust (00030601 to B.W.). T.H. is an investigator of the Howard Hughes Medical Institute.

AUTHOR CONTRIBUTIONS

R.S.Z. and T.H. initially conceived the project. R.S.Z. and Y.L. performed experiments and analyzed the data. R.S.Z. and B.W. developed the theoretical models. All authors contributed to the writing of the manuscript. T.H. supervised the project.

DECLARATION OF INTERESTS

T.H. is married to a member of *Molecular Cell*'s Advisory Board. The authors and Johns Hopkins University have authored patent application PCT/US20/57255 including the work described herein.

Received: September 15, 2020
Revised: December 23, 2020
Accepted: February 2, 2021
Published: March 3, 2021

REFERENCES

Aleksandrov, R., Dotchev, A., Poser, I., Krastev, D., Georgiev, G., Panova, G., Babukov, Y., Danovski, G., Dyankova, T., Hubatsch, L., et al. (2018). Protein dynamics in complex DNA lesions. Mol. Cell *69*, 1046–1061.e5.

Anzalone, A.V., Randolph, P.B., Davis, J.R., Sousa, A.A., Koblan, L.W., Levy, J.M., Chen, P.J., Wilson, C., Newby, G.A., Raguram, A., and Liu, D.R. (2019). Search-and-replace genome editing without double-strand breaks or donor DNA. Nature *576*, 149–157.

Ash, C., Dubec, M., Donne, K., and Bashford, T. (2017). Effect of wavelength and beam width on penetration in light-tissue interaction using computational methods. Lasers Med. Sci. *32*, 1909–1918.

Aymard, F., Bugler, B., Schmidt, C.K., Guillou, E., Caron, P., Briois, S., Iacovoni, J.S., Daburon, V., Miller, K.M., Jackson, S.P., and Legube, G. (2014). Transcriptionally active chromatin recruits homologous recombination at DNA double-strand breaks. Nat. Struct. Mol. Biol. *21*, 366–374.

Aymard, F., Aguirrebengoa, M., Guillou, E., Javierre, B.M., Bugler, B., Arnould, C., Rocher, V., Iacovoni, J.S., Biernacka, A., Skrzypczak, M., et al. (2017). Genome-wide mapping of long-range contacts unveils clustering of DNA double-strand breaks at damaged active genes. Nat. Struct. Mol. Biol. *24*, 353–361.

Barkau, C.L., O'Reilly, D., Rohilla, K.J., Damha, M.J., and Gagnon, K.T. (2019). Rationally designed anti-CRISPR nucleic acid inhibitors of CRISPR-Cas9. Nucleic Acid Ther. *29*, 136–147.

Brinkman, E.K., Chen, T., Amendola, M., and van Steensel, B. (2014). Easy quantitative assessment of genome editing by sequence trace decomposition. Nucleic Acids Res. *42*, e168.

Brinkman, E.K., Chen, T., de Haas, M., Holland, H.A., Akhtar, W., and van Steensel, B. (2018). Kinetics and fidelity of the repair of Cas9-induced double-strand DNA breaks. Mol. Cell *70*, 801–813.e6.

Buenrostro, J.D., Giresi, P.G., Zaba, L.C., Chang, H.Y., and Greenleaf, W.J. (2013). Transposition of native chromatin for fast and sensitive epigenomic profiling of open chromatin, DNA-binding proteins and nucleosome position. Nat. Methods *10*, 1213–1218.

Carlson-Stevermer, J., Kelso, R., Kadina, A., Joshi, S., Rossi, N., Walker, J., Stoner, R., and Maures, T. (2020). CRISPRoff enables spatio-temporal control of CRISPR editing. Nat. Commun. *11*, 5041.

Caron, P., Choudjaye, J., Clouaire, T., Bugler, B., Daburon, V., Aguirrebengoa, M., Mangeat, T., Iacovoni, J.S., Álvarez-Quilón, A., Cortés-Ledesma, F., and Legube, G. (2015). Non-redundant functions of ATM and DNA-PKcs in response to DNA double-strand breaks. Cell Rep. *13*, 1598–1609.

Casini, A., Olivieri, M., Petris, G., Montagna, C., Reginato, G., Maule, G., Lorenzin, F., Prandi, D., Romanel, A., Demichelis, F., et al. (2018). A highly specific SpCas9 variant is identified by in vivo screening in yeast. Nat. Biotechnol. *36*, 265–271.

Chakrabarti, A.M., Henser-Brownhill, T., Monserrat, J., Poetsch, A.R., Luscombe, N.M., and Scaffidi, P. (2019). Target-specific precision of CRISPR-mediated genome editing. Mol. Cell *73*, 699–713.e6.

Chang, H.H.Y., Pannunzio, N.R., Adachi, N., and Lieber, M.R. (2017). Non-homologous DNA end joining and alternative pathways to double-strand break repair. Nat. Rev. Mol. Cell Biol. *18*, 495–506.

Chen, S., Lee, B., Lee, A.Y.F., Modzelewski, A.J., and He, L. (2016). Highly efficient mouse genome editing by CRISPR ribonucleoprotein electroporation of zygotes. J. Biol. Chem. *291*, 14457–14467.

Chen, J.S., Dagdas, Y.S., Kleinstiver, B.P., Welch, M.M., Sousa, A.A., Harrington, L.B., Sternberg, S.H., Joung, J.K., Yildiz, A., and Doudna, J.A. (2017). Enhanced proofreading governs CRISPR-Cas9 targeting accuracy. Nature *550*, 407–410.

Clarke, R., Heler, R., MacDougall, M.S., Yeo, N.C., Chavez, A., Regan, M., Hanakahi, L., Church, G.M., Marraffini, L.A., and Merrill, B.J. (2018). Enhanced bacterial immunity and mammalian genome editing via RNA-polymerase-mediated dislodging of Cas9 from double-strand DNA breaks. Mol. Cell *71*, 42–55.e8.

Clouaire, T., and Legube, G. (2019). A snapshot on the cis chromatin response to DNA double-strand breaks. Trends Genet. *35*, 330–345.

Clouaire, T., Rocher, V., Lashgari, A., Arnould, C., Aguirrebengoa, M., Biernacka, A., Skrzypczak, M., Aymard, F., Fongang, B., Dojer, N., et al. (2018). Comprehensive mapping of histone modifications at DNA double-strand breaks deciphers repair pathway chromatin signatures. Mol. Cell *72*, 250–262.e6.

Cong, L., Ran, F.A., Cox, D., Lin, S., Barretto, R., Habib, N., Hsu, P.D., Wu, X., Jiang, W., Marraffini, L.A., and Zhang, F. (2013). Multiplex genome engineering using CRISPR/Cas systems. Science *339*, 819–823.

Cromwell, C.R., Sung, K., Park, J., Krysler, A.R., Jovel, J., Kim, S.K., and Hubbard, B.P. (2018). Incorporation of bridged nucleic acids into CRISPR RNAs improves Cas9 endonuclease specificity. Nat. Commun. *9*, 1–11.

Dahlman, J.E., Abudayyeh, O.O., Joung, J., Gootenberg, J.S., Zhang, F., and Konermann, S. (2015). Orthogonal gene knockout and activation with a catalytically active Cas9 nuclease. Nat. Biotechnol. *33*, 1159–1161.

Derks, K.W., Hoeijmakers, J.H., and Pothof, J. (2014). The DNA damage response: the omics era and its impact. DNA Repair (Amst.) *19*, 214–220.

Dimitrova, N., Chen, Y.C.M., Spector, D.L., and de Lange, T. (2008). 53BP1 promotes non-homologous end joining of telomeres by increasing chromatin mobility. Nature *456*, 524–528.

Ding, Q., Reddy, Y.V., Wang, W., Woods, T., Douglas, P., Ramsden, D.A., Lees-Miller, S.P., and Meek, K. (2003). Autophosphorylation of the catalytic subunit of the DNA-dependent protein kinase is required for efficient end processing during DNA double-strand break repair. Mol. Cell. Biol. *23*, 5836–5848.

Dolgin, E. (2020). The kill-switch for CRISPR that could make gene-editing safer. Nature *577*, 308–310.

Doudna, J.A. (2020). The promise and challenge of therapeutic genome editing. Nature *578*, 229–236.

Ferrarelli, L.K. (2018). CRISPR, cancer, and p53. Sci. Signal. *11*, 7344.

Fu, Y., Foden, J.A., Khayter, C., Maeder, M.L., Reyon, D., Joung, J.K., and Sander, J.D. (2013). High-frequency off-target mutagenesis induced by CRISPR-Cas nucleases in human cells. Nat. Biotechnol. *31*, 822–826.

Fu, Y., Sander, J.D., Reyon, D., Cascio, V.M., and Joung, J.K. (2014). Improving CRISPR-Cas nuclease specificity using truncated guide RNAs. Nat. Biotechnol. *32*, 279–284.

Fu, B.X., St Onge, R.P., Fire, A.Z., and Smith, J.D. (2016). Distinct patterns of Cas9 mismatch tolerance in vitro and in vivo. Nucleic Acids Res. *44*, 5365–5377.

Gangopadhyay, S.A., Cox, K.J., Manna, D., Lim, D., Maji, B., Zhou, Q., and Choudhary, A. (2019). Precision control of CRISPR-Cas9 using small molecules and light. Biochemistry *58*, 234–244.

Graham, T.G., Walter, J.C., and Loparo, J.J. (2016). Two-stage synapsis of DNA ends during non-homologous end joining. Mol. Cell *61*, 850–858.

Haapaniemi, E., Botla, S., Persson, J., Schmierer, B., and Taipale, J. (2018). CRISPR-Cas9 genome editing induces a p53-mediated DNA damage response. Nat. Med. *24*, 927–930.

Harrington, L.B., Doxzen, K.W., Ma, E., Liu, J.J., Knott, G.J., Edraki, A., Garcia, B., Amrani, N., Chen, J.S., Cofsky, J.C., et al. (2017). A broad-spectrum inhibitor of CRISPR-Cas9. Cell *170*, 1224–1233.e15.

Hsu, P.D., Scott, D.A., Weinstein, J.A., Ran, F.A., Konermann, S., Agarwala, V., Li, Y., Fine, E.J., Wu, X., Shalem, O., et al. (2013). DNA targeting specificity of RNA-guided Cas9 nucleases. Nat. Biotechnol. *31*, 827–832.

Hsu, P.D., Lander, E.S., and Zhang, F. (2014). Development and applications of CRISPR-Cas9 for genome engineering. Cell *157*, 1262–1278.

Hu, J.H., Miller, S.M., Geurts, M.H., Tang, W., Chen, L., Sun, N., Zeina, C.M., Gao, X., Rees, H.A., Lin, Z., and Liu, D.R. (2018). Evolved Cas9 variants with broad PAM compatibility and high DNA specificity. Nature *556*, 57–63.

Iannelli, F., Galbiati, A., Capozzo, I., Nguyen, Q., Magnuson, B., Michelini, F., D'Alessandro, G., Cabrini, M., Roncador, M., Francia, S., et al. (2017). A damaged genome's transcriptional landscape through multilayered expression profiling around in situ-mapped DNA double-strand breaks. Nat. Commun. *8*, 15656.

Jinek, M., Chylinski, K., Fonfara, I., Hauer, M., Doudna, J.A., and Charpentier, E. (2012). A programmable dual-RNA-guided DNA endonuclease in adaptive bacterial immunity. Science *337*, 816–821.

Kiani, S., Chavez, A., Tuttle, M., Hall, R.N., Chari, R., Ter-Ovanesyan, D., Qian, J., Pruitt, B.W., Beal, J., Vora, S., et al. (2015). Cas9 gRNA engineering for genome editing, activation and repression. Nat. Methods *12*, 1051–1054.

Kim, S., Kim, D., Cho, S.W., Kim, J., and Kim, J.S. (2014). Highly efficient RNA-guided genome editing in human cells via delivery of purified Cas9 ribonucleoproteins. Genome Res. *24*, 1012–1019.

Kleinjan, D.A., Wardrope, C., Nga Sou, S., and Rosser, S.J. (2017). Drug-tunable multidimensional synthetic gene control using inducible degron-tagged dCas9 effectors. Nat. Commun. *8*, 1191.

Kleinstiver, B.P., Pattanayak, V., Prew, M.S., Tsai, S.Q., Nguyen, N.T., Zheng, Z., and Joung, J.K. (2016). High-fidelity CRISPR-Cas9 nucleases with no detectable genome-wide off-target effects. Nature *529*, 490–495.

Knight, S.C., Xie, L., Deng, W., Guglielmi, B., Witkowsky, L.B., Bosanac, L., Zhang, E.T., El Beheiry, M., Masson, J.B., Dahan, M., et al. (2015). Dynamics of CRISPR-Cas9 genome interrogation in living cells. Science *350*, 823–826.

Knott, G.J., and Doudna, J.A. (2018). CRISPR-Cas guides the future of genetic engineering. Science *361*, 866–869.

Koblan, L.W., Doman, J.L., Wilson, C., Levy, J.M., Tay, T., Newby, G.A., Maianti, J.P., Raguram, A., and Liu, D.R. (2018). Improving cytidine and adenine base editors by expression optimization and ancestral reconstruction. Nat. Biotechnol. *36*, 843–846.

Kocak, D.D., Josephs, E.A., Bhandarkar, V., Adkar, S.S., Kwon, J.B., and Gersbach, C.A. (2019). Increasing the specificity of CRISPR systems with engineered RNA secondary structures. Nat. Biotechnol. *37*, 657–666.

Komor, A.C., Kim, Y.B., Packer, M.S., Zuris, J.A., and Liu, D.R. (2016). Programmable editing of a target base in genomic DNA without double-stranded DNA cleavage. Nature *533*, 420–424.

Kosicki, M., Tomberg, K., and Bradley, A. (2018). Repair of double-strand breaks induced by CRISPR-Cas9 leads to large deletions and complex rearrangements. Nat. Biotechnol. *36*, 765–771.

Kundert, K., Lucas, J.E., Watters, K.E., Fellmann, C., Ng, A.H., Heineike, B.M., Fitzsimmons, C.M., Oakes, B.L., Qu, J., Prasad, N., et al. (2019). Controlling CRISPR-Cas9 with ligand-activated and ligand-deactivated sgRNAs. Nat. Commun. *10*, 2127.

Langmead, B., and Salzberg, S.L. (2012). Fast gapped-read alignment with Bowtie 2. Nat. Methods *9*, 357–359.

Leenay, R.T., Aghazadeh, A., Hiatt, J., Tse, D., Roth, T.L., Apathy, R., Shifrut, E., Hultquist, J.F., Krogan, N., Wu, Z., et al. (2019). Large dataset enables prediction of repair after CRISPR-Cas9 editing in primary T cells. Nat. Biotechnol. *37*, 1034–1037.

Li, H., Handsaker, B., Wysoker, A., Fennell, T., Ruan, J., Homer, N., Marth, G., Abecasis, G., and Durbin, R.; 1000 Genome Project Data Processing Subgroup (2009). The sequence alignment/map format and SAMtools. Bioinformatics *25*, 2078–2079.

Li, B., Zeng, C., Li, W., Zhang, X., Luo, X., Zhao, W., Zhang, C., and Dong, Y. (2018). Synthetic oligonucleotides inhibit CRISPR-Cpf1-mediated genome editing. Cell Rep. *25*, 3262–3272.e3.

Lieberman, M.W., Baney, R.N., Lee, R.E., Sell, S., and Farber, E. (1971). Studies on DNA repair in human lymphocytes treated with proximate carcinogens and alkylating agents. Cancer Res. *31*, 1297–1306.

Liu, Y., Zou, R.S., He, S., Nihongaki, Y., Li, X., Razavi, S., Wu, B., and Ha, T. (2020). Very fast CRISPR on demand. Science *368*, 1265–1269.

Ma, H., Tu, L.C., Naseri, A., Huisman, M., Zhang, S., Grunwald, D., and Pederson, T. (2016). CRISPR-Cas9 nuclear dynamics and target recognition in living cells. J. Cell Biol. *214*, 529–537.

Maji, B., Gangopadhyay, S.A., Lee, M., Shi, M., Wu, P., Heler, R., Mok, B., Lim, D., Siriwardena, S.U., Paul, B., et al. (2019). A high-throughput platform to identify small-molecule inhibitors of CRISPR-Cas9. Cell *177*, 1067–1079.e19.

Mali, P., Yang, L., Esvelt, K.M., Aach, J., Guell, M., DiCarlo, J.E., Norville, J.E., and Church, G.M. (2013). RNA-guided human genome engineering via Cas9. Science *339*, 823–826.

Mamo, T., Mladek, A.C., Shogren, K.L., Gustafson, C., Gupta, S.K., Riester, S.M., Maran, A., Galindo, M., van Wijnen, A.J., Sarkaria, J.N., and Yaszemski, M.J. (2017). Inhibiting DNA-PK_{CS} radiosensitizes human osteosarcoma cells. Biochem. Biophys. Res. Commun. *486*, 307–313.

Marx, V. (2019). A rocky road for the maturation of embryo-editing methods. Nat. Methods *16*, 147–150.

Ochs, F., Karemore, G., Miron, E., Brown, J., Sedlackova, H., Rask, M.B., Lampe, M., Buckle, V., Schermelleh, L., Lukas, J., and Lukas, C. (2019). Stabilization of chromatin topology safeguards genome integrity. Nature *574*, 571–574.

Ordoukhanian, P., and Taylor, J.S. (1995). Design and synthesis of a versatile photocleavable DNA building block. Application to phototriggered hybridization. J. Am. Chem. Soc. *117*, 9570–9571.

Pawluk, A., Amrani, N., Zhang, Y., Garcia, B., Hidalgo-Reyes, Y., Lee, J., Edraki, A., Shah, M., Sontheimer, E.J., Maxwell, K.L., and Davidson, A.R. (2016). Naturally occurring off-switches for CRISPR-Cas9. Cell *167*, 1829–1838.e9.

Pawluk, A., Davidson, A.R., and Maxwell, K.L. (2018). Anti-CRISPR: discovery, mechanism and function. Nat. Rev. Microbiol. *16*, 12–17.

Perrault, R., Wang, H., Wang, M., Rosidi, B., and Iliakis, G. (2004). Backup pathways of NHEJ are suppressed by DNA-PK. J. Cell. Biochem. *92*, 781–794.

Pickar-Oliver, A., and Gersbach, C.A. (2019). The next generation of CRISPR-Cas technologies and applications. Nat. Rev. Mol. Cell Biol. *20*, 490–507.

Rees, H.A., Komor, A.C., Yeh, W.H., Caetano-Lopes, J., Warman, M., Edge, A.S., and Liu, D.R. (2017). Improving the DNA specificity and applicability of base editing through protein engineering and protein delivery. Nature Commun *8*, 1–10.

Rees, H.A., and Liu, D.R. (2018). Base editing: precision chemistry on the genome and transcriptome of living cells. Nat. Rev. Genet. *19*, 770–788.

Richardson, C.D., Kazane, K.R., Feng, S.J., Zelin, E., Bray, N.L., Schäfer, A.J., Floor, S.N., and Corn, J.E. (2018). CRISPR-Cas9 genome editing in human cells occurs via the Fanconi anemia pathway. Nat. Genet. *50*, 1132–1139.

Rose, J.C., Stephany, J.J., Valente, W.J., Trevillian, B.M., Dang, H.V., Bielas, J.H., Maly, D.J., and Fowler, D.M. (2017). Rapidly inducible Cas9 and DSB-ddPCR to probe editing kinetics. Nat. Methods *14*, 891–896.

Roth, T.L., Puig-Saus, C., Yu, R., Shifrut, E., Carnevale, J., Li, P.J., Hiatt, J., Saco, J., Krystofinski, P., Li, H., et al. (2018). Reprogramming human T cell function and specificity with non-viral genome targeting. Nature *559*, 405–409.

Rupnik, A., Grenon, M., and Lowndes, N. (2008). The MRN complex. Curr. Biol. *18*, R455–R457.

Schmid-Burgk, J.L., Gao, L., Li, D., Gardner, Z., Strecker, J., Lash, B., and Zhang, F. (2020). Highly parallel profiling of Cas9 variant specificity. Mol. Cell *78*, 794–800.e8.

Schneider, C.A., Rasband, W.S., and Eliceiri, K.W. (2012). NIH Image to ImageJ: 25 years of image analysis. Nat. Methods *9*, 671–675.

Scully, R., Panday, A., Elango, R., and Willis, N.A. (2019). DNA double-strand break repair-pathway choice in somatic mammalian cells. Nat. Rev. Mol. Cell Biol. *20*, 698–714.

Shin, J., Jiang, F., Liu, J.J., Bray, N.L., Rauch, B.J., Baik, S.H., Nogales, E., Bondy-Denomy, J., Corn, J.E., and Doudna, J.A. (2017). Disabling Cas9 by an anti-CRISPR DNA mimic. Sci. Adv. *3*, e1701620.

Singh, D., Wang, Y., Mallon, J., Yang, O., Fei, J., Poddar, A., Ceylan, D., Bailey, S., and Ha, T. (2018). Mechanisms of improved specificity of engineered Cas9s revealed by single-molecule FRET analysis. Nat. Struct. Mol. Biol. *25*, 347–354.

Slaymaker, I.M., Gao, L., Zetsche, B., Scott, D.A., Yan, W.X., and Zhang, F. (2016). Rationally engineered Cas9 nucleases with improved specificity. Science *351*, 84–88.

Trevino, A.E., and Zhang, F. (2014). Genome editing using Cas9 nickases. Methods Enzymol. *546*, 161–174.

Tsai, S.Q., Zheng, Z., Nguyen, N.T., Liebers, M., Topkar, V.V., Thapar, V., Wyvekens, N., Khayter, C., Iafrate, A.J., Le, L.P., et al. (2015). GUIDE-seq enables genome-wide profiling of off-target cleavage by CRISPR-Cas nucleases. Nat. Biotechnol. *33*, 187–197.

Uematsu, N., Weterings, E., Yano, K., Morotomi-Yano, K., Jakob, B., Taucher-Scholz, G., Mari, P.O., van Gent, D.C., Chen, B.P., and Chen, D.J. (2007). Autophosphorylation of DNA-PKCS regulates its dynamics at DNA double-strand breaks. J. Cell Biol. *177*, 219–229.

Vakulskas, C.A., Dever, D.P., Rettig, G.R., Turk, R., Jacobi, A.M., Collingwood, M.A., Bode, N.M., McNeill, M.S., Yan, S., Camarena, J., et al. (2018). A high-fidelity Cas9 mutant delivered as a ribonucleoprotein complex enables efficient gene editing in human hematopoietic stem and progenitor cells. Nat. Med. *24*, 1216–1224.

van Overbeek, M., Capurso, D., Carter, M.M., Thompson, M.S., Frias, E., Russ, C., Reece-Hoyes, J.S., Nye, C., Gradia, S., Vidal, B., et al. (2016). DNA repair profiling reveals nonrandom outcomes at Cas9-mediated breaks. Mol. Cell *63*, 633–646.

Vítor, A.C., Huertas, P., Legube, G., and de Almeida, S.F. (2020). Studying DNA double-strand break repair: an ever-growing toolbox. Front. Mol. Biosci. *7*, 24.

von Stechow, L., and Olsen, J.V. (2017). Proteomics insights into DNA damage response and translating this knowledge to clinical strategies. Proteomics *17*, 1600018.

Wang, A.S., Chen, L.C., Wu, R.A., Hao, Y., McSwiggen, D.T., Heckert, A.B., Richardson, C.D., Gowen, B.G., Kazane, K.R., Vu, J.T., et al. (2020). The histone chaperone FACT induces Cas9 multi-turnover behavior and modifies genome manipulation in human cells. Mol. Cell *79*, 221–233.e5.

Weyel, X.M.M., Fichte, M.A.H., and Heckel, A. (2017). A two-photon-photocleavable linker for triggering light-induced strand breaks in oligonucleotides. ACS Chem. Biol. *12*, 2183–2190.

Wienert, B., Wyman, S.K., Richardson, C.D., Yeh, C.D., Akcakaya, P., Porritt, M.J., Morlock, M., Vu, J.T., Kazane, K.R., Watry, H.L., et al. (2019). Unbiased detection of CRISPR off-targets in vivo using DISCOVER-Seq. Science *364*, 286–289.

Yeh, C.D., Richardson, C.D., and Corn, J.E. (2019). Advances in genome editing through control of DNA repair pathways. Nat. Cell Biol. *21*, 1468–1478.

Yin, H., Song, C.Q., Suresh, S., Kwan, S.Y., Wu, Q., Walsh, S., Ding, J., Bogorad, R.L., Zhu, L.J., Wolfe, S.A., et al. (2018). Partial DNA-guided Cas9 enables genome editing with reduced off-target activity. Nat. Chem. Biol. *14*, 311–316.

Zheng, T., Hou, Y., Zhang, P., Zhang, Z., Xu, Y., Zhang, L., Niu, L., Yang, Y., Liang, D., Yi, F., et al. (2017). Profiling single-guide RNA specificity reveals a mismatch sensitive core sequence. Sci. Rep. *7*, 40638.

Zuris, J.A., Thompson, D.B., Shu, Y., Guilinger, J.P., Bessen, J.L., Hu, J.H., Maeder, M.L., Joung, J.K., Chen, Z.Y., and Liu, D.R. (2015). Efficient delivery of genome-editing proteins in vitro and in vivo. Nat. Biotechnol. *33*, 73.

Please cite this article in press as: Zou et al., Cas9 deactivation with photocleavable guide RNAs, Molecular Cell (2021), https://doi.org/10.1016/j.molcel.2021.02.007

STAR★METHODS

KEY RESOURCES TABLE

REAGENT or RESOURCE	SOURCE	IDENTIFIER
Antibodies		
Mre11 Antibody	Novus Biologicals	Cat# NB100-142, RRID:AB_10077796
53BP1 Antibody	Novus Biologicals	Cat# NB100-305, RRID:AB_10001695
Recombinant Anti-gamma H2A.X (phospho S139) antibody [EP854(2)Y]	Abcam	Cat# ab81299, RRID:AB_1640564
Cas9 Antibody (7A9-3A3)	Cell Signaling Technology	Cat# 14697, RRID:AB_2750916
Goat anti-Mouse IgG (H+L) Cross-Adsorbed Secondary Antibody, Cyanine5	Thermo Fisher	Cat# A10524, RRID:AB_2534033
Bacterial and virus strains		
DH5alpha competent *E. coli*	New England BioLabs	C2987H
BL21 Star (DE3) competent *E. coli*	Thermo Fisher	C601003
Chemicals, peptides, and recombinant proteins		
KU-0060648	Sigma-Aldrich	SML1257
SpCas9	This paper	N/A
AncBE4max	This paper	N/A
Deposited data		
Raw and analyzed data	This paper	PRJNA622564
Gel and imaging data	This paper	https://doi.org/10.17632/p3gt8vvr5b
Experimental models: cell lines		
Human: HEK293T	ATCC	CRL-3216
Oligonucleotides		
Cas9 crRNA and tracrRNAs, see Table S1A	Integrated DNA Technologies	N/A
Primers for cloning, see Table S1B	Integrated DNA Technologies	N/A
Primers for Amplicon PCR, see Table S1C	Integrated DNA Technologies	N/A
Primers for next generation sequencing, see Tables S1D–S1E	Integrated DNA Technologies	N/A
Oligos for preparing ChIP-seq libraries, se Table S1F	Integrated DNA Technologies	N/A
Recombinant DNA		
Plasmid: pET42b-AncBE4max	This paper	Addgene #165157
Plasmid: pLPC-mCh-ACTB-P2A-EGFP	This paper	Addgene #165158
Plasmid: pHO4d-Cas9	Fu et al., 2014	Addgene #67881
Plasmid: mCherry-BP1-2 pLPC-Puro	Dimitrova et al., 2008	Addgene #19835
Plasmid: pCMV_AncBE4max_P2A_EGFP	Koblan et al., 2018	Addgene #112100
Plasmid: pET42b-HF-BE3	Rees et al., 2017	Addgene #87438
Software and algorithms		
ImageJ	Schneider et al., 2012	https://imagej.nih.gov/ij/
Bowtie2	Langmead and Salzberg, 2012	http://bowtie-bio.sourceforge.net/bowtie2/index.shtml
Samtools	Li et al., 2009	http://samtools.sourceforge.net/
Analysis code	This paper	https://github.com/rogerzou/chipseq_pcRNA
Other		
Bench Protocol	This paper	Methods S1

Please cite this article in press as: Zou et al., Cas9 deactivation with photocleavable guide RNAs, Molecular Cell (2021), https://doi.org/10.1016/j.molcel.2021.02.007

RESOURCE AVAILABILITY

Lead contact

- Further information and requests for resources and reagents should be directed to and will be fulfilled by the Lead Contact, Taekjip Ha (tjha@jhu.edu).

Materials availability

- Plasmids (pET42b-AncBE4max and pLPC-mCh-ACTB-P2A-EGFP) generated in this study have been deposited to Addgene #165157 and #165158

Data and code availability

- The accession number for the sequencing data reported in this paper is [Database]: [PRJNA622564].
- All code used to generate the conclusions of the paper can be accessed at https://github.com/rogerzou/chipseq_pcRNA.
- Original gel and imaging data have been deposited to Mendeley Data: [https://doi.org/10.17632/p3gt8vvr5b].
- The published article includes the remaining datasets generated during this study.

EXPERIMENTAL MODEL AND SUBJECT DETAILS

- HEK293T, female, were cultured at 37°C under 5% CO_2 in Dulbecco's Modified Eagle's Medium (DMEM, Corning), supplemented with 10% FBS (Clontech), 100 units/ml penicillin and 100 μg/ml streptomycin (DMEM complete). Cells were tested every month for mycoplasma.

METHOD DETAILS

Molecular cloning

Cloning pET42b-AncBE4max for protein expression and purification

The AncBE4max fragment from pCMV_AncBE4max_P2A_EGFP mammalian expression plasmid (Addgene #112100) was ligated to a pET42b vector backbone (Addgene #87438) using NEBuilder® HiFi DNA Assembly Master Mix (New England BioLabs E2621) and transformed into NEB5α cells following manufacturer's instructions. Primer sequences Gib_pET42b_F and Gib_pET42b_R were used to PCR amplify the pET42b backbone, and primer sequences Gib_BEmax_F and Gib_BEmax_R were used to amplify AncBE4max.

Cloning pLPC-mCh-ACTB-P2A-EGFP for mCh/EGFP reporter of Cas9 cleavage activity in cells

The backbone with mCherry was obtained from restriction digest of mCherry-BP1-2 pLPC-Puro (Addgene 19835) with BamHI-HF (New England BioLabs). ACTB fragment was obtained from PCR of genomic DNA from HEK293T cells using primers ACTB_150nt_fwd and ACTB_150nt_rev. P2A-EGFP fragment was obtained from PCR of pCMV_AncBE4max_P2A_EGFP (Addgene #112100) using primers P2A-EGFP_fwd and P2A-EGFP_rev. The 3 pieces were ligated together with NEBuilder® HiFi DNA Assembly Master Mix (New England BioLabs E2621) and transformed into NEB5α cells following manufacturer's instructions.

All primers sequences used for these two cloning projects are in Table S1.

SpCas9 purification

BL21-CodonPlus (DE3)-RIL competent cells (Agilent Technologies 230245) were transformed with Cas9 plasmid (Addgene #67881) and inoculated in 25 mL of LB-ampicillin media. The bacteria culture was first allowed to grow overnight (37°C, 220 rpm) and then transferred to 2 L of LB supplemented with ampicillin and 0.1% glucose until OD_{600} of ~0.5. Subsequently, the cells were induced with IPTG at a final concentration of 0.2 mM and maintained overnight at 18°C. The bacteria cells were pelleted at 4500 x g, 4°C for 15 min and resuspended in 40 mL of lysis buffer containing 20 mM Tris pH 8.0, 250 mM KCl, 20 mM imidazole, 10% glycerol, 1 mM TCEP, 1 mM PMSF, and cOmplete EDTA-free protease inhibitor tablet (Sigma-Aldrich 11836170001). This cell suspension was lysed using a microfluidizer and the supernatant containing Cas9 protein was clarified by spinning down cell debris at 16,000 x g, 4°C for 40 min and filtering with 0.2 μm syringe filters (Thermo Scientific F25006). 4ml Ni-NTA agarose bead slurry (QIAGEN 30210) was pre-equilibrated with lysis buffer. The clarified supernatant was then loaded at 4°C. The protein-bound Ni-NTA beads were washed with 40 mL wash buffer containing 20 mM Tris pH 8.0, 800 mM KCl, 20 mM imidazole, 10% glycerol, and 1 mM TCEP. Gradient elution was performed with buffer containing 20 mM HEPES pH 8.0, 500 mM KCl, 10% glycerol, and varying concentrations of imidazole (100, 150, 200, and 250 mM) at 7 mL collection volume per fraction. The eluted fractions were tested on an SDS-PAGE gel and imaged by Coomassie blue (Bio-Rad 1610400) staining. To remove any DNA contamination, 5 mL HiTrap Q HP (Cytiva 17115401) was charged with 1M KCl and then equilibrated with elution buffer containing 250 mM imidazole. The purified protein solution was then passed over the Q column at 4°C. The flow-through was collected and dialyzed in a 10 kDa SnakeSkin dialysis tubing (Thermo Fisher

Please cite this article in press as: Zou et al., Cas9 deactivation with photocleavable guide RNAs, Molecular Cell (2021), https://doi.org/10.1016/j.molcel.2021.02.007

68100) against 1 L of dialysis buffer (20 mM HEPES pH 7.5, and 500 mM KCl, 20% glycerol) at 4°C, overnight. Next day, the protein was dialyzed for an additional 3 hours in fresh 1L of dialysis buffer. The final Cas9 protein was concentrated to 10 μg/μl using Amicon Ultra-15 Centrifugal Filter Unit, Ultracel-10 (Millipore Sigma UFC901008), aliquoted, and flash-frozen and stored at −80°C.

AncBE4max purification

Protein expression and purification of AncBE4max was similar to that for SpCas9. BL21 Star (DE3) competent cells (Thermo Fisher Scientific C601003) were transformed and inoculated in 25 mL of LB-kanamycin media. The bacteria culture was first allowed to grow overnight (37°C, 220 rpm) and then transferred to 2 L of LB supplemented with kanamycin and 0.1% glucose until OD_{600} of ~0.7. Subsequently, the cells were induced with IPTG at a final concentration of 0.5 mM and maintained overnight at 18°C. The bacteria cells were pelleted at 4500 x g, 4°C for 15 min and resuspended in 20 mL of lysis buffer containing 100 mM Tris pH 8.0, 1M NaCl, 20% glycerol, 5 mM TCEP, 0.4 mM PMSF, and cOmplete EDTA-free protease inhibitor tablet (Sigma-Aldrich 11836170001). This cell suspension was lysed by sonication (10%, 1.5 s ON, 5 s OFF, 10 min ON time) and the supernatant containing AncBE4max was clarified by spinning down cell debris at 16,000 x g, 4°C for 40 min and filtering with 0.2 μm syringe filters (Thermo Scientific F25006). HisPur Ni-NTA agarose bead slurry (Thermo Fisher Scientific 88221) was pre-equilibrated with lysis buffer. The clarified supernatant was then loaded at 4°C. The protein-bound Ni-NTA beads were washed with 40 mL wash buffer containing 100 mM Tris-HCl pH 8.0, 1M NaCl, 20% glycerol, and 5 mM TCEP. Gradient elution was performed with buffer containing 100mM Tris-HCl pH 8.0, 500 mM NaCl, 20% glycerol, 5mM TCEP, and varying concentrations of imidazole (100, 150, 200, 250mM) at 7 mL collection volume per fraction. The eluted fractions were tested on an SDS-PAGE gel and imaged by Coomassie blue (Bio-Rad 1610400) staining. To remove any DNA contamination, 5 mL HiTrap Q HP (Cytiva 17115401) was charged with 1M KCl and then equilibrated with elution buffer containing 250 mM imidazole. The purified protein solution was then passed over the Q column at 4°C. The flow-through was collected and dialyzed in a 20k MWCO Slide-A-Lyzer G2 Dialysis Cassette (Thermo Fisher 87736) against 1 L of dialysis buffer (25 mM HEPES pH 7.5, and 500 mM KCl, 20% glycerol) at 4°C, overnight. Next day, the protein was dialyzed for an additional 3 hours in fresh dialysis buffer. The final protein was concentrated to 10 μg/μl using Amicon Ultra-15 Centrifugal Filter Unit, Ultracel-10 (Millipore Sigma UFC901008), aliquoted, and flash-frozen and stored at −80°C.

Electroporation of SpCas9/AncBE4max RNP

1.2 μl of 100 μM crRNA (either photocleavable or wild-type) was mixed with 1.2 μl of 100 μM tracrRNA (Integrated DNA Technologies) and heated to 95°C for 5 min in a thermocycler, then allowed to cool on benchtop for 5 min. To form the RNP complex, 1.7 μl of 10 μg/μl of purified Cas9 or AncBE4max was mixed with the annealed 2.4 μl 50 μM cr:tracrRNA, 0.9 μl of 1x PBS was mixed in, then the total 5 μL solution was incubated for an additional 20 min at room temperature to allow for RNP formation.

HEK293T cells were properly maintained to a confluency of ~90% prior to electroporation. 800,000 cells were trypsinized with 5 min incubation in the incubator, then 1:1 of DMEM complete was added to inactivate trypsin. This mixture was centrifuged (3 min, 200 g), supernatant removed, followed by resuspension of the cell pellet in 1 mL PBS, centrifugation (3 min, 200 g), and finally complete removal of supernatant. 20 μL of nucleofection solution (3.6 μl of Supplement solution mixed with 16.5 μl of SF solution from SF Cell Line 4D-Nucleofector X Kit S) (Lonza) was mixed thoroughly with the cell pellet. The 5 μL RNP solution was mixed in along with 1 μL of Cas9 Electroporation Enhancer (Integrated DNA Technologies). The entirety of the final solution was transferred to one well of a provided 16-strip cuvette. Electroporation was then performed according to the manufacturer's instructions on the 4D-Nucleofector™ Core Unit (Lonza) using code CA-189. Some white residue may appear in the cell mixture after electroporation, but that is completely normal. DMEM complete was added before plating to culture wells pre-coated with 1:100 collagen. As detailed in the following sections, 50k cells were plated to 96-wells for kinetics experiments, while 400k cells were plated to a 6-well for GUIDE-seq.

Deactivation light exposure for in cell and *in vitro* experiments

The JAXMAN 365 nm LED flashlight purchased from Amazon (https://www.amazon.com/JAXMAN-Ultraviolet-365nm-Detector-Flashlight/dp/B06XW7S1CS/) was used for light-mediated deactivation. A custom 3D-printed flashlight holder was also designed, which can hold 1, 3, or 6 flashlights in tandem, for convenient manipulation of LED flashlights during deactivation.

(https://github.com/rogerzou/chipseq_pcRNA/blob/master/Jaxman_LED_flashlight_holder_design/files/8zeFECPViSo.stl)

For *in vitro* deactivation, the RNP solution was in an open PCR tube, and the flashlight was held approximately 2 cm above the solution for 30 s. For in cell deactivation, approximately 90% of DMEM complete was removed from the well, the flashlight was held approximately 2 cm above the cells for 1 minute, then fresh DMEM was added. The flashlight delivered approximately 1.3 J/cm^2 of 365 nm wavelength light. Exposure to ambient (room) light does not appear to inactivate pcRNAs. However, as a precaution, samples with pcRNA are covered with aluminum foil whenever possible.

Preparing samples for kinetics measurements in cells

HEK293T cells were introduced with SpCas9/AncBE4max in complex with pcRNA through electroporation (800,000 cells per cuvette), following the protocol detailed in 'Electroporation of SpCas9/AncBE4max RNP'. Cells were plated to 96-wells (50,000 cells per well), and incubated in standard cell culture conditions. At various time points, cells were exposed to a flashlight for 1 minute, following the protocol detailed in 'Deactivation light exposure for in cell and *in vitro* experiments'. For pre-cleaved pcRNA, 1 minute

Please cite this article in press as: Zou et al., Cas9 deactivation with photocleavable guide RNAs, Molecular Cell (2021), https://doi.org/10.1016/j.molcel.2021.02.007

of light was delivered to the RNP complex before electroporation. 72 h after electroporation, cells were harvested with DPBS and genomic DNA was isolated using DNeasy Blood & Tissue Kit (QIAGEN 69506) according to the manufacturer's instructions, except with 1 h (instead of 10 min) incubation with lysis buffer/Proteinase K at 55°C.

Sanger Sequencing for measuring insertions or deletions

Genomic DNA samples were amplified with PCR using Q5 Hot Start High-Fidelity 2X Master Mix (New England BioLabs M0494). Primer pairs for all sequences are listed in Table S1. For example, the primer set for amplifying around the *ACTB* target site is ACTB_F and ACTB_R. After PCR, cleanup was performed using 1.5x AMPure XP (Beckman Coulter A63881) following the manufacturer's instructions. 3 ng/μl of each sample was submitted to Genewiz for Sanger sequencing. Indels were calculated using TIDE analysis at http://shinyapps.datacurators.nl/tide/.

High throughput sequencing of genomic DNA samples

Genomic DNA samples were amplified with PCR using Q5 Hot Start High-Fidelity 2X Master Mix (New England BioLabs M0494). Primer pairs for all sequences are listed in Table S1. For example, the primer set for amplifying around the *ACTB* target site is NGS_ACTB_F and NGS_ACTB_R. After amplicon PCR, cleanup was performed using 1.6x AMPure XP (Beckman Coulter A63881) following the manufacturer's instructions. Dual-indexing PCR was performed using KAPA HiFi HotStart ReadyMix (Roche 07958935001) and PCR cleanup was performed using 1x AMPure XP. Samples were quantified using QuBit (Thermo Fisher Scientific), pooled, diluted, and loaded onto a MiSeq (Illumina). Sequencing was performed with the following number of cycles "151 | 8 | 8 | 151" with the paired-end Nextera sequencing protocol.

In vitro cleavage assay

Target DNA are amplified from genomic DNA using primers designed for Sanger sequencing, and purified with QIAQuick PCR Purification Kit (QIAGEN). 10 μM cr:tracrRNA solution was prepared at equal molar ratio by heating to 95°C for 5 min and cooling on a heat block for 1 hour. Either photocleavable crRNA or wild-type crRNA were used to mix with tracrRNA to form Cas9-pcRNA or Cas9-wtRNA, respectively (all purchased from Integrated DNA Technologies). 3 pmol of Cas9 was incubated with 5 pmol of gRNA to form RNP for 30 min in 10 μl of 1x NEBuffer 3.1 (New England Biolabs). The tube was placed on a 37°C heat block for 1 min, 365 nm light was applied for 30 s (following protocol detailed in 'Deactivation light exposure for in cell and *in vitro* experiments'), then 60 fmol of target DNA was added and thoroughly mixed. A no light control omits application of light, and a positive control uses the wild-type crRNA. To demonstrate light-induced deactivation, all samples were incubated for 1 h at 37°C. After incubation, 10 μg of Proteinase K (Thermo Fisher) was added to each tube and further incubated in 55°C for 45 min. The DNA was then purified with QIAquick PCR Purification Kit (QIAGEN) before loading on an agarose gel for visualization. To calculate the cleavage efficiency, the integrated intensity of cleaved bands was divided by that of total DNA as quantified using ImageJ.

GUIDE-seq

800,000 HEK293T cells were electroporated with the protocol detailed in section 'Electroporation of SpCas9/AncBE4max RNP', with an additional 25 pmol dsODN mixed with the RNP prior to mixing with cells suspended in nucleofection solution. After electroporation, 400k cells were plated to a 6-well and placed in an incubator. 72 h after electroporation, cells were harvested with DPBS and genomic DNA was isolated using DNeasy Blood & Tissue Kit (QIAGEN 69506) according to the manufacturer's instructions, except with 1 h (instead of 10 min) incubation with lysis buffer/Proteinase K at 55°C. Library preparation was done with the corrected adaptor sequences previously described (Tsai et al., 2015). The library was quantified with qPCR using NEBNext® Library Quant Kit for Illumina® (New England BioLabs E7630), pooled, diluted, and loaded onto a MiSeq (Illumina). Sequencing was performed with the following number of cycles "150 | 8 | 16 | 150" with the paired-end Nextera sequencing protocol following the protocol described previously (Tsai et al., 2015). Data analysis was done using code adapted from https://github.com/aryeelab/guideseq, with alignment to GRCh37/hg19 and using with the original filter for sequences containing six or fewer mismatches between candidate off-target sites and the on-target sequence including the NGG PAM.

Spatial control of Cas9 deactivation

HEK293T cells were electroporated with SpCas9-pcRNA targeting ACTB using the electroporation protocol described earlier, and plated on 14 mm glass-bottom dishes at ~80% confluency (Cellvis D35-14-1.5-N). 12 h later, cells were illuminated using a LED light from the bottom of the dish with a mask between the cells and LED. Cells were transfected with GFP reporter plasmid within 30 min of light delivery. Fluorescence imaging for GFP was performed 24 h later using 10x air objective on a Nikon Ti-E fluorescence microscope equipped with an Andor EMCCD.

Determination of electroporation efficiency from immunofluorescence microscopy

HEK293T cells were electroporated with SpCas9-wtRNA targeting ACTB using the electroporation protocol described earlier, and plated on 20 mm glass-bottom dishes at ~50% confluency (Cellvis D35-20-1.5-N). 1 h later after cells are adherent to surface, cell fixation was performed with 4% of paraformaldehyde in 1x PBS for 10 min and then quenched by 1x PBS supplemented with 0.1 M glycine for 10 min. After thoroughly rinsing with 1x PBS, 0.5% Triton-X was used to permeabilize cell membrane for 10 min.

2% w/v BSA in 1x PBS was used to passivate the sample for 1 h and at room temperature. Without further rinsing, primary antibody was diluted in 1x PBS and directly added into the chamber for targeting the protein of interests. After 1 h incubation, primary antibody was removed and the sample was thoroughly washed with 1x PBS three times. Secondary antibody was typically diluted in 1:1000 and applied to the sample for 1 h. Finally, the sample was rinsed three times and mounted with Prolong Diamond mounting media (Thermo Fisher Scientific) overnight. Electroporation efficiency was estimated from manual counting of Cas9 positive-cells using a hemocytometer.

Mouse anti-SpCas9 (7A9-3A3) was purchased from Cell Signaling Technology (14697). Cy5 conjugated Goat anti-mouse antibody (A10524) was purchased from Thermo Fisher Scientific. Dilution of primary antibody was based on the recommended ratio from the manufacturers.

Chromatin immunoprecipitation

Electroporation was performed on a larger scale than in the section titled "Electroporation of SpCas9/AncBE4max RNP" with the following changes: 2 μl of 100 uM of crRNA was annealed to 2 μl of 100 uM tracrRNA; 147.6 μl SF solution + 32.4 μl supplement were used totaling 180 μl of the electroporation solution; 4 μl of electroporation enhancer was used; after mixing with 36 million HEK293T cells, the final volume was approximately 260 μl, split equally between two 100 μl cuvettes. After electroporation, the cells were split to the appropriate number of samples (at most 6 samples) and plated at ~80% confluency. To expose select samples to 0.5 μM of DNA-PKcs inhibitor Ku-0060648, cells were deposited into cell media containing 0.5 μM Ku-0060648 (diluted 1:5000 from 2.5mM stock in DMSO).

The ChIP protocol was adapted from previous literature. Briefly, cells were washed once with room temperature PBS, then washed off the plate with 10 mL DMEM and transferred to 15 mL falcon tubes. 721 μl of 16% formaldehyde (methanol free) was added for 15 min in RT. 750 μl of 2M glycine was added to quench the formaldehyde. Cells were spun down with 1200 g at 4°C for 3 min, then washed with ice-cold PBS twice, spinning down with the same centrifugation conditions. Cells were then resuspended in 4ml lysis buffer LB1 (50mM HEPES, 140mM NaCl, 1mM EDTA, 10% glycerol, 0.5% Igepal CA-630, 0.25% Triton X-100, pH to 7.5 using KOH, add 1x protease inhibitor right before use) for 10 min at 4°C, then spun down 2000 g with at 4°C for 3 min. The supernatant was decanted. Cells were then resuspended in 4ml LB2 (10mM Tris-HCl pH 8, 200mM NaCl, 1mM EDTA, 0.5mM EGTA, pH to 8.0 using HCl, add 1x protease inhibitor right before use) for 5 min at 4°C, spun down with the same protocol, and the supernatant decanted. Cells were then resuspended in 1.5 mL LB3 (10mM Tris-HCl pH 8, 100mM NaCl, 1mM EDTA, 0.5mM EGTA, 0.1% Na-Deoxycholate, 0.5% N-lauroylsarcosine, pH to 8.0 using HCl, add 1x protease inhibitor right before use) and transferred to 2 mL Eppendorf tubes for sonication with 55% amplitude, 30 s ON, 30 s OFF for 12 min total time (Q125 sonicator Q125-110). A custom-designed 3D printed tube holder was placed on a glass container filled with ice water during sonication. Samples were spun down with 20000 g at 4°C for 10 min, and supernatant was transferred to 1.5 mL LB3 + 300 μl of 10% Triton X-100 in a 15 mL falcon tube.

- https://github.com/rogerzou/chipseq_pcRNA/blob/master/2mL_tube_holder_for_sonication/files/k77AEoSKdcg.stl
- https://www.amazon.com/Whole-Housewares-Square-Candle-Centerpiece/dp/B07MT8TDJ8/

Beads pre-loaded with antibodies were prepared before cell harvesting. 75 μl Protein A beads (Thermo Fisher) were used per IP. 450 μl beads (for 6 IPs) were transferred to 2 mL Eppendorf tube on magnetic stand. Beads were washed twice with blocking buffer BB (0.5% BSA in PBS), then resuspended in 900 μl BB (150 μl per IP). 18 μl of antibody (3 μl per IP) (MRE11 – Novus NB100-142; γH2AX – Abcam ab81299; 53BP1 – Novus NB100-305) were added and placed on rotator for 1-2 h. Right before IP, the 2 mL tube was placed on a magnetic rack and washed 3x with BB, before resuspending in 600 μl BB. 100 μl of beads in BB were transferred to each IP and placed in 4°C rotator for 6+ hours.

Samples were transferred to 2 mL Eppendorf tubes on a magnetic stand, washed 6x with 1 mL RIPA buffer (50 mM HEPES, 500 mM LiCl, 1 mM EDTA, 1% Igepal CA-630, 0.7% Na-Deoxycholate, pH to 7.5 using KOH), then washed 1x with 1 mL TBE buffer (20 mM Tris-HCl pH 7.5, 150 mM NaCl), before decanting. Beads containing ChIP-ed DNA were mixed with 70 μl elution buffer EB (50mM Tris-HCl pH 8.0, 10mM EDTA, 1% SDS) and incubated 65°C for 6+ hours. 40 μl of TE buffer was mixed to dilute the SDS, followed by 2 μl of 20 mg/ml RNaseA (New England BioLabs) for 30 min at 37°C. 4 μl of 20 mg/ml Proteinase K (New England BioLabs) was added and incubated for 1 h at 55°C. The genomic DNA was column purified (QIAGEN) and eluted in 41 μl nuclease free water.

QUANTIFICATION AND STATISTICAL ANALYSIS

Analysis of cytosine base editing efficiency

Because multiple cytosines can be edited per target sequence, unless each cytosine is explicitly indicated, the cytosine with the highest editing was chosen (C5 for all ON and OFF targets of *HEK site 4*; C5 for ON, C5 for OFF9, C7 for OFF23, C3 for OFF24 of *VEGFA site 2*, where C# is the #th cytosine counting from the PAM distal side).

Data processing of high throughput sequencing results

Sequencing reads were either demultiplexed automatically using MiSeq Reporter (Illumina) or with a custom Python script to individual FASTQ files. This script also performs indel and base calling. For indel calling, sequencing reads were scanned for

exact matches to two 20-bp sequences that flank ± 20 bp from the ends of the target sequence. If no exact matches were found, the read was excluded from analysis. After additional filtering for an average quality score > 20, an indel is defined as a sequence that differs in length from the reference length. For base calling, sequencing reads were scanned for exact matches to two 20 bp sequences that flank the target sequence. If no exact matches were found, or the match led to sequences of different length compared to the reference sequence, the read was excluded from analysis. Any base with quality score > 30 was counted.

High-throughput sequencing and data processing of ChIP samples

Oligo sequences for library preparation are in Table S1. End-repair/A-tailing was performed on 17 μl of ChIPed DNA using NEBNext® Ultra II End Repair/dA-Tailing Module (New England BioLabs), followed by ligation (MNase_F/MNase_R) with T4 DNA Ligase (New England BioLabs). 10, 13, and 13 cycles of PCR using PE_i5 and PE_i7XX primer pairs were performed for γH2AX, 53BP1, and MRE11 ChIP samples, respectively to amplify libraries. Samples were pooled, quantified with QuBit (Thermo), Bioanalyzer (Agilent) and qPCR (BioRad), then sequenced on a NextSeq 500 (Illumina) using high-output paired 2x36bp reads. All ChIP-seq raw reads in FASTQ format and processed alignments in BAM format are uploaded to Sequence Read Archive (SRA) under BioProject accession PRJNA622564 (https://www.ncbi.nlm.nih.gov/bioproject/PRJNA622564).

Reads were demultiplexed after sequencing using bcl2fastq. Paired-end reads were aligned to hg38 using bowtie2. Samtools was used to filtered for mapping quality > = 25, remove singleton reads, convert to BAM format, remove potential PCR duplicates, index reads, count the number of mapped reads, and subset to normalize for mapped reads after filtering steps. The software that performs these steps as well as all subsequent analyses (fragment analysis, binning analysis) are open source on GitHub (https://github.com/rogerzou/chipseq_pcRNA).

53BP1 and γH2AX enrichment analysis

Custom python code was used to bin read counts every 5 kb, normalized to "reads per million" (RPM) by dividing by the total number of reads in the sequencing sample and multiplying by 1 million.

To calculate proportion change in enrichment for each 5 kb bin between two samples, i.e., from bin A_i in sample A to bin B_i in sample B, is (B_i – A_i) / A_i. Only values A_i greater than or equal to 2 are counted to prevent unstable values caused by a small denominator.

MRE11 enrichment and fragment analysis from paired-end ChIP-seq reads

A fragment is defined by two aligned and correctly oriented paired-end reads. Peak are represented as "fragment pileups," which incorporate the entire inferred DNA fragment, i.e., the middle part of each DNA strand that is not sequenced is counted. For MRE11, enrichment is defined to be the number paired-end reads with both ends in a 5 kb window centered at the cut site, normalized to "reads per million" (RPM) by dividing by the total number of reads in the sequencing sample and multiplying by 1 million.

Mathematical Model A for duration-resolved endpoint editing

Here we will derive a mathematical model to quantify how increased duration of exposure to active enzymes (SpCas9 or AncBE4max) will lead to an increase in effective "conversion" from final unmodified target DNA to final edited target DNA (indels or base edits) at 72 hours after RNP delivery. The goal of this modeling is to allow curve fitting and obtain phenomenological rate constants such that for any new target sequence, the full kinetics curve can be conveniently predicted (Mathematical Model B). We are not attempting to directly model some underlying kinetic processes in cells (i.e., direct conversion from final unmodified to edited target DNA does not biologically occur).

At 72 hours after delivery of SpCas9 or AncBE4max, cells initially exposed to active RNP for various durations of time were harvested. Fraction of genomic DNA that contains either an indel or base edit at the target position was determined by Sanger sequencing-based TIDE analysis (Brinkman et al., 2014) or targeted deep sequencing.

We start by defining the following measurable quantities:

$B(t)$: Fraction of final edited target DNA after t hours of exposure to active RNPs
$A(t)$: Fraction of final unmodified target DNA after t hours of exposure to active RNPs

where $A(t) = 1 - B(t)$.

An important goal of gene editing is to achieve a high level of desired editing at the endpoint. With temporally confined gene editing, it is important to quantify how increasing the duration of exposure to active enzyme translates to a greater proportion of final edited DNA. In other words, what is the effective rate at which $A(t)$ becomes $B(t)$ as t increases? This can be represented conceptually by the process

$$A(t) \overset{k(t)}{\rightarrow} B(t)$$

where $k(t)$ is the rate of change from the final unmodified target DNA to final edited target DNA. $k(t)$ has a dependence on t because the amount of RNP that is able to perform gene editing diminishes over time due to degradation. Therefore, increasing the duration of

Please cite this article in press as: Zou et al., Cas9 deactivation with photocleavable guide RNAs, Molecular Cell (2021), https://doi.org/10.1016/j.molcel.2021.02.007

exposure at later time points should also have diminishing effects on effective $A(t)$ to $B(t)$ conversion. We will therefore represent this conversion rate with

$$k(t) = k_e e^{-k_d \times t}$$

where k_e is the initial "conversion" rate and k_d modulates the rate through an exponential decay function to represent the diminishing conversion effects at later time points.

The practical interpretation of k_e is the rate at which the final unmodified target DNA $A(t)$ changes to final edited target DNA $B(t)$ if the activity duration increases from $t = 0$ to $t = \Delta t$. The practical interpretation of k_d is the rate at which this change is dampened (assuming an exponential decay process) if it occurs at later time points, which can be attributed predominantly to decreasing concentrations of active RNPs over time due to degradation.

We can now define the final model equation for the "conversion" from final unmodified to edited target DNA as a function of t:

$$\frac{dB(t)}{dt} = k(t) \times A(t) = k_e e^{-k_d \times t} \times (1 - B(t)) B(0) = 0$$

A closed-form solution can be obtained from the previous differential equation with initial conditions:

$$B(t) = 1 - e^{\frac{\left(e^{-k_d \times t} - 1\right) \times k_e}{k_d}}$$

However, because only proportion E_f of all cells actually receive active RNP, the actual measured proportions for edited versus unmodified DNA from sequencing is:

$B^*(t) = E_f B(t)$: measured fraction of final edited target DNA
$A^*(t) = 1 - B^*(t)$: measured faction of final unmodified target DNA

E_f is experimentally determined to be 0.97 from immunofluorescence staining with Cas9 antibody 1 hour after electroporation (Figure S3D).

Experimental data are fit to $B^*(t)$ using non-linear least-squares optimization. We used the MATLAB function 'fit' with the default 'Trust-Region' algorithm to perform all fitting.

For SpCas9 indels, k_e was determined for each locus and k_d was determined as a single rate from all loci. The same methodology was used for AncBE4max-mediated base editing and indels.

Mathematical Model B for duration-resolved endpoint editing

For a new target sequence, determining the shortest duration necessary to achieve the desired endpoint gene editing can be tedious. Instead, if one is to solely determine the indel efficiency at 15 hours after electroporation using SpCas9/pcRNA (without deactivation), can the full curve be predicted? This would enable estimation of shortest sufficient duration necessary to achieve a desired level of editing solely using indel efficiencies from a single time-point. We have determined the parameters of the model (Mathematical Model A) using data from 3 target sequences (*ACTB*, *HEK site 4*, *VEGFA site 2* – the *fitting sequences*) (Figure 3B), and the task is to predict the full curve for a fourth target sequence (*MYC* – the *prediction sequence*) only using the SpCas9/pcRNA indel efficiency at 15 hours for this target.

We first define the following known quantities

$B^*(t)$: mathematical model for indel efficiency at 72 hours from deactivating Cas9 at hour t after electroporation (active enzyme pulse of duration t), fit using *ACTB*, *HEK site 4*, and *VEGFA site 2.*
PC_{15h}: indel efficiency with pcRNA at 15 hours after electroporation – this has been previously determined for the *fitting sequences.*

First, there is a strong linear correlation between $B^*(12)$ and PC_{15h} for the *fitting sequences*. Using a linear regression fit, we obtain a slope $\hat{s} = 1.1153$ with $R^2 = 0.93$ (Figure 3D). That is, $B^*(12) = \hat{s} \times PC_{15h} + \varepsilon$ (ε is error term). Assuming $\varepsilon = 0$, we have

$$\hat{s} \times PC_{15h} = E_f \left\{ 1 - e^{\frac{\left(e^{-k_d \times 12} - 1\right) \times k_e}{k_d}} \right\}$$

The degradation rate $\hat{k}_d = 0.036534$ is also estimated from modeling of the *fitting sequences* and assumed to be locus-independent. Therefore, we can solve for $\hat{k}_e$ using known quantities:

$$1 - \frac{\hat{s} \times PC_{15h}}{E_f} = e^{\frac{\left(e^{-\hat{k}_d \times 12} - 1\right) \times k_e}{\hat{k}_d}}$$

Molecular Cell
Technology

CellPress

$$\ln\left(1-\frac{\hat{s}\times \mathrm{PC}_{15h}}{E_f}\right)=\frac{\left(e^{-\hat{k}_d\times 12}-1\right)\times k_e}{\hat{k}_d}$$

$$\hat{k}_e=\ln\left(1-\frac{\hat{s}\times \mathrm{PC}_{15h}}{E_f}\right)\frac{\hat{k}_d}{e^{-\hat{k}_d\times 12}-1}$$

For the *prediction sequence MYC*, we first experimentally obtain PC_{15h}, and use that value to determine $\hat{B}^*(t)$, the predicted indel % at 72 hours after deactivating Cas9/pcRNA at hour t after electroporation.

$$\hat{B}^*(t)=1-e^{\frac{\left(e^{-\hat{k}_d\times t_{-1}}\right)\times \hat{k}_e}{\hat{k}_d}}$$

We obtained the indel timeseries for *MYC* and plotted this data along with the predicted model curve, demonstrating accurate prediction (Figure 3F).

An identical calculation can be performed for the AncBE4max base editor, using $\hat{s}=0.9943$ and $\hat{k}_d=0.43814$ (Figures 3C, 3E, and 3G).

ADDITIONAL RESOURCES

Detailed protocol

A detailed bench protocol is available as Methods S1.

Molecular Cell, Volume *81*

Supplemental information

Cas9 deactivation with photocleavable guide RNAs

Roger S. Zou, Yang Liu, Bin Wu, and Taekjip Ha

Supplemental Information

Cas9 deactivation with photocleavable guide RNAs

Roger S. Zou[1,5], Yang Liu[2,5], Bin Wu[2], Taekjip Ha[1,2,3,4,6,*]
1 Department of Biomedical Engineering, Johns Hopkins University, Baltimore, Maryland, 21205, USA
2 Department of Biophysics and Biophysical Chemistry, Johns Hopkins University, Baltimore, Maryland, 21205, USA
3 Department of Biophysics, Johns Hopkins University, Baltimore, Maryland, 21205, USA
4 Howard Hughes Medical Institute, Baltimore, Maryland, 21205, USA
5 These authors contributed equally
6 Lead contact
* Corresponding Author (tjha@jhu.edu)

Figures S1 to S4

Table S1

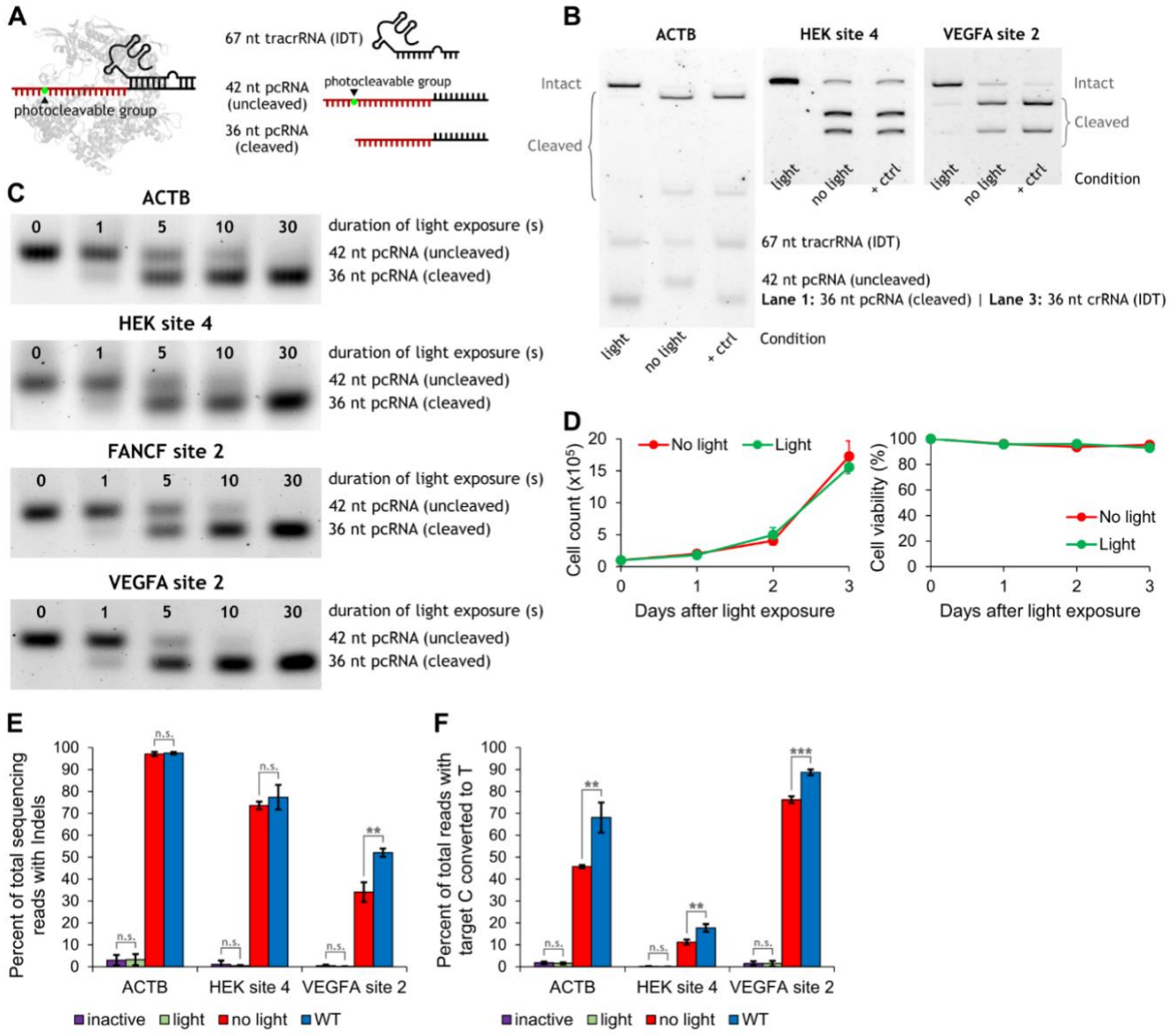
A
67 nt tracrRNA (IDT)
42 nt pcRNA (uncleaved)
36 nt pcRNA (cleaved)
photocleavable group
photocleavable group
B
ACTB
HEK site 4
VEGFA site 2
Intact
Cleaved
light
no light
+ ctrl
Condition
67 nt tracrRNA (IDT)
42 nt pcRNA (uncleaved)
Lane 1: 36 nt pcRNA (cleaved) | Lane 3: 36 nt crRNA (IDT)
C
ACTB
HEK site 4
FANCF site 2
VEGFA site 2
0
1
5
10
30
duration of light exposure (s)
42 nt pcRNA (uncleaved)
36 nt pcRNA (cleaved)
D
No light
Light
Cell count (x10^5)
Days after light exposure
Cell viability (%)
Days after light exposure
E
Percent of total sequencing reads with Indels
ACTB
HEK site 4
VEGFA site 2
inactive
light
no light
WT
F
Percent of total reads with target C converted to T
ACTB
HEK site 4
VEGFA site 2
inactive
light
no light
WT

Figure S1. Validation of Cas9/pcRNA deactivation *in vitro* and in mammalian cells, Related to Figure 1

(A) Schematic of the native and truncated 36 nucleotide (nt) pcRNA, which both hybridize with a 67 nt tracrRNA.
(B) *In vitro* cleavage assay at the *ACTB*, *HEK site 4*, and *VEGFA site 2* target sequences. Light (30 s, 365 nm) catalyzes photocleavage of the chemical group, which renders Cas9 cleavage deficient. The pcRNA band shifts from 42 nt in 'no light' sample to 36 nt in 'light' sample, indicating complete photocleavage with this dose. Positive control ('+ ctrl') uses a cleavage-competent 36 nt crRNA (the 3' end that hybridizes with tracrRNA is truncated by design) hybridized to the same 67 nt tracrRNA. To calculate the cleavage efficiency, the integrated intensity of cleaved bands was divided by that of total DNA as quantified using ImageJ.
(C) Direct test of pcRNA photocleavage by varying duration of light exposure. Cleavage efficiency evaluated by band depletion from 42 nt to 36 nt.
(D) Cell growth and viability assay over time after light exposure (1 min with 365nm LED), measured using automated cell counter with Trypan blue staining (BioRad TC20). No detectable growth arrest or cell death was observed with light exposure, compared to cells with no light exposure.
(E) Indel measurements in cells 72 hours after Cas9 RNP delivery. 'inactive': HEK293T cells electroporated with already-inactivated Cas9/pcRNA (light exposure *in vitro*), 'light': light exposure (deactivation) within 2 min after RNP electroporation, 'no light': no RNP deactivation, 'WT': wild type (unmodified) gRNA as positive control. Error bars represent ±SD across biological replicates (n=3). n.s. indicates not significant; * indicates $p<0.05$, ** indicates $p<0.01$, *** indicates $p<0.001$.
(F) Base editing in cells 72 hours after AncBE4max RNP delivery, with the same conditions as panel E.

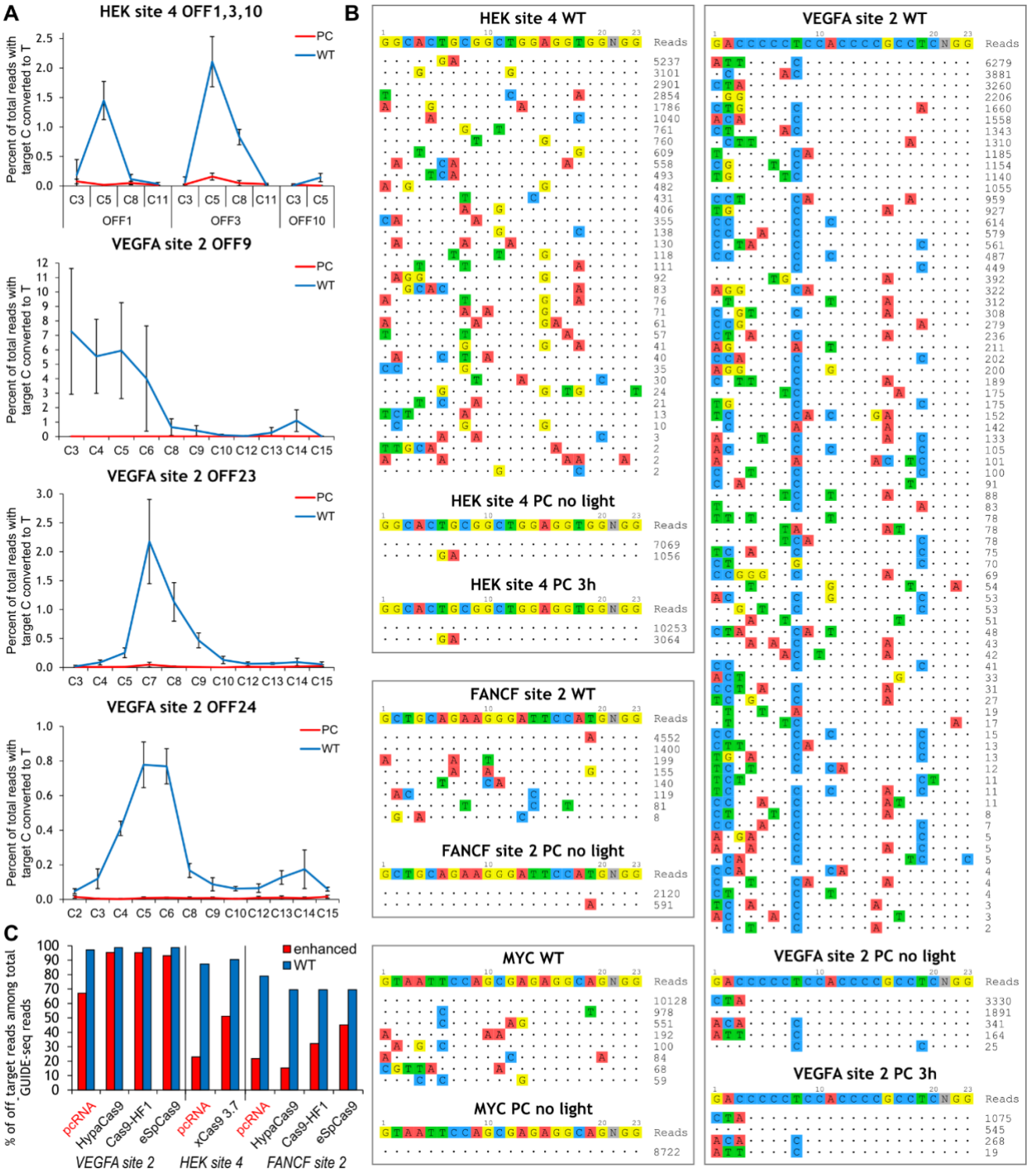
A
HEK site 4 OFF1,3,10
Percent of total reads with target C converted to T
PC
WT
C3 C5 C8 C11 C3 C5 C8 C11 C3 C5
OFF1
OFF3
OFF10
VEGFA site 2 OFF9
C3 C4 C5 C6 C8 C9 C10 C12 C13 C14 C15
VEGFA site 2 OFF23
C3 C4 C5 C7 C8 C9 C10 C12 C13 C14 C15
VEGFA site 2 OFF24
C2 C3 C4 C5 C6 C8 C9 C10 C12 C13 C14 C15
B
HEK site 4 WT
Reads
5237
3101
2901
2854
1786
1040
761
760
609
558
493
482
431
406
355
138
130
118
111
92
83
76
71
61
57
41
40
35
30
24
21
13
10
3
2
2
2
HEK site 4 PC no light
7069
1056
HEK site 4 PC 3h
10253
3064
FANCF site 2 WT
4552
1400
199
155
140
119
81
8
FANCF site 2 PC no light
2120
591
MYC WT
10128
978
551
192
100
84
68
59
MYC PC no light
8722
VEGFA site 2 WT
6279
3881
3260
2206
1660
1558
1343
1310
1185
1154
1140
1055
959
927
614
579
561
487
449
392
322
312
308
279
236
211
202
200
189
175
175
152
142
133
105
101
100
91
88
83
78
78
78
75
70
69
54
53
53
51
48
43
42
41
33
31
27
19
17
15
13
13
12
11
11
11
8
7
5
5
5
4
4
4
3
3
2
VEGFA site 2 PC no light
3330
1891
341
164
25
VEGFA site 2 PC 3h
1075
545
268
19
C
% of off-target reads among total GUIDE-seq reads
enhanced
WT
pcRNA
HypaCas9
Cas9-HF1
eSpCas9
pcRNA
xCas9 3.7
pcRNA
HypaCas9
Cas9-HF1
eSpCas9
VEGFA site 2
HEK site 4
FANCF site 2

Figure S2. pcRNA natively exhibits significantly enhanced specificity, Related to Figure 2

(A) Percent C to T conversion with AncBE4max at every editable C, at select off-target sites of *HEK site 4* (OFF1, OFF3, OFF10) and *VEGFA site 2* (OFF9, OFF23, OFF24). pcRNA (PC) greatly reduces off-target editing at every editable C compared to wild type gRNA (WT). C# indicates the cytosine at base #, counting from the PAM-distal end. Error bars represent ±SD across biological replicates (n=3).
(B) Ordered lists of Cas9 targeting sites from GUIDE-seq 72 hours after Cas9 delivery targeting either *HEK site 4*, *FANCF site 2*, *VEGFA site 2*, or *MYC*, using wild type guide (WT) versus photocleavable guide (PC). For *HEK site 4* and *VEGFA site 2*, RNP deactivation 3h after delivery followed by GUIDE-seq at 72 hours was also performed, yielding 1 fewer detected off-target site for *VEGFA site 2*, and none fewer for *HEK site 4*.
(C) Percent of GUIDE-seq reads attributed to off-target sites between different enhanced specificity Cas9s and wild type ('WT', *i.e.* canonical SpCas9 with gRNA). GUIDE-seq results for pcRNA (red text) were analyzed from panel B. GUIDE-seq results for HypaCas9, Cas9-HF1, eSpCas9, and xCas9 3.7 were obtained from Chen et al., 2017, Kleinstiver et al., 2016, Slaymaker et al., 2016, Hu et al., 2018, respectively. For fair comparison, results are categorized by the same target sequence (*VEGFA site 2*, *HEK site 4*, or *FANCF site 2*).

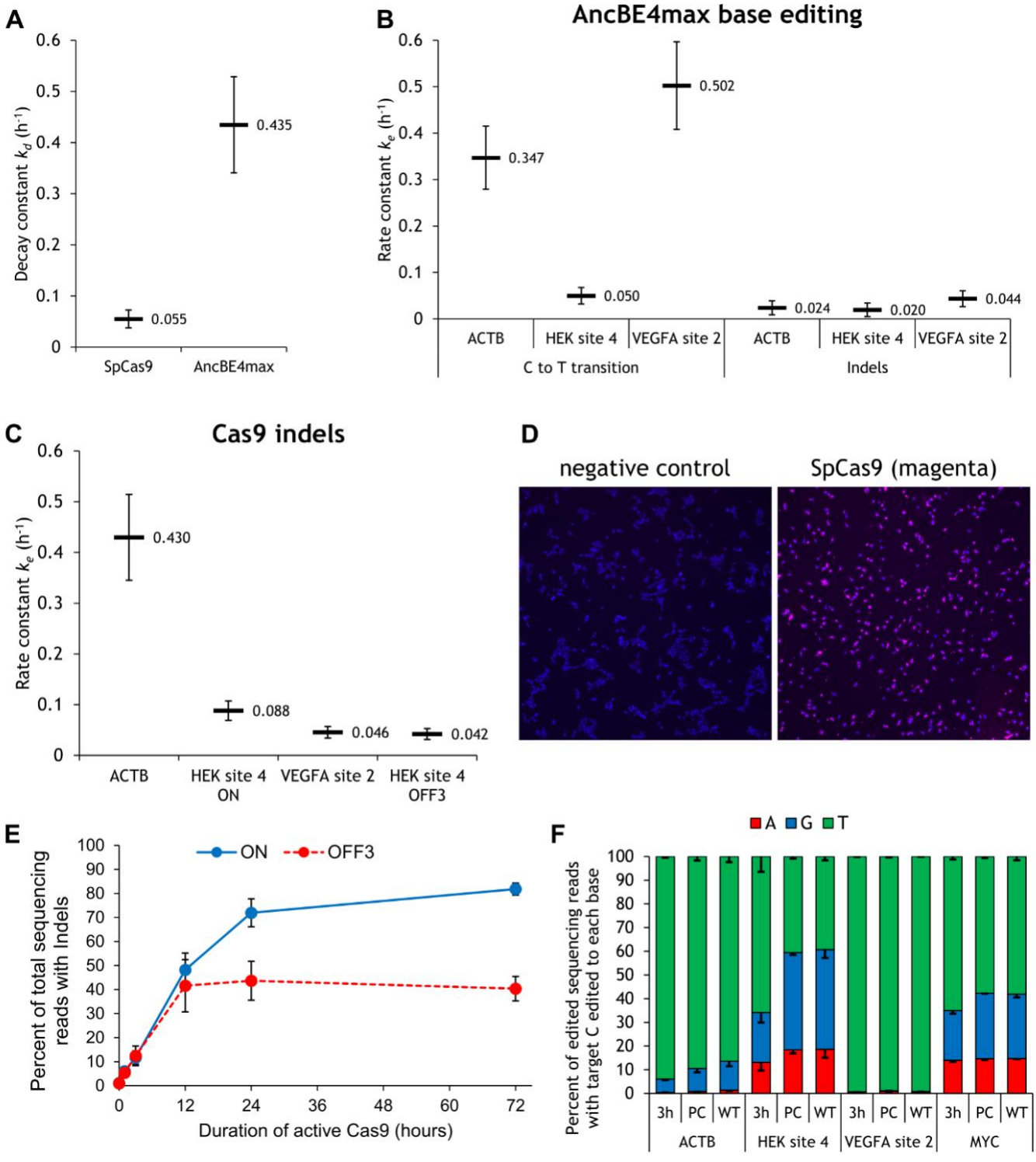
A
Decay constant k_d (h^{-1})
0.6
0.5
0.4
0.3
0.2
0.1
0
0.055
0.435
SpCas9
AncBE4max
B
AncBE4max base editing
Rate constant k_e (h^{-1})
0.347
0.050
0.502
0.024
0.020
0.044
ACTB
HEK site 4
VEGFA site 2
ACTB
HEK site 4
VEGFA site 2
C to T transition
Indels
C
Cas9 indels
Rate constant k_e (h^{-1})
0.430
0.088
0.046
0.042
ACTB
HEK site 4 ON
VEGFA site 2
HEK site 4 OFF3
D
negative control
SpCas9 (magenta)
E
ON
OFF3
Percent of total sequencing reads with Indels
100
90
80
70
60
50
40
30
20
10
0
0
12
24
36
48
60
72
Duration of active Cas9 (hours)
F
A
G
T
Percent of edited sequencing reads with target C edited to each base
100
90
80
70
60
50
40
30
20
10
0
3h
PC
WT
ACTB
HEK site 4
VEGFA site 2
MYC

Figure S3. Dose-minimizing genome editing, Related to Figure 3

(A) k_d for both SpCas9 and AncBE4max.
(B) k_e for both base editing and indels from cytosine base editor AncBE4max.
(C) k_e for indels from SpCas9.
(D) Determination of SpCas9 electroporation efficiency (E_f) from immunofluorescence staining of Cas9 (magenta). Negative control is HEK293T cells without SpCas9 electroporation. E_f was estimated to be 97% from hemocytometer counting of Cas9 positive-cells. This value was used for kinetic modeling in STAR Methods.
(E) SpCas9-mediated indels measured at 72 hours at *HEK site 4* on-target (ON) and off-target 3 (OFF3), as a function of active Cas9 duration (before light-based deactivation) on the x-axis. Each dot therefore corresponds to the time point of Cas9 deactivation. From this kinetic analysis, deactivating Cas9 early actually led to a worse ratio of on- to off-target editing for this off-target site. Error bars represent ±SD across biological replicates (n=3).
(F) Plot of relative fractions of non-cytosine nucleotides at the edited base. All samples were evaluated at 72 hours. '3h' corresponds to Cas9/pcRNA with deactivation at 3 hours, 'PC' corresponds to Cas9/pcRNA with no deactivation, and 'WT' corresponds to Cas9 in complex with wild type gRNA. Base editing purity, defined as the fraction of final thymine divided by the fraction of thymine, adenine, and guanine can be visualized as the fraction that corresponds to thymine in the plot (green – 'T'). Shining light to cells at 3 hours (PC 3hr) improved base editing purity at 72 hours compared to no light (PC) or wild type gRNA (WT).

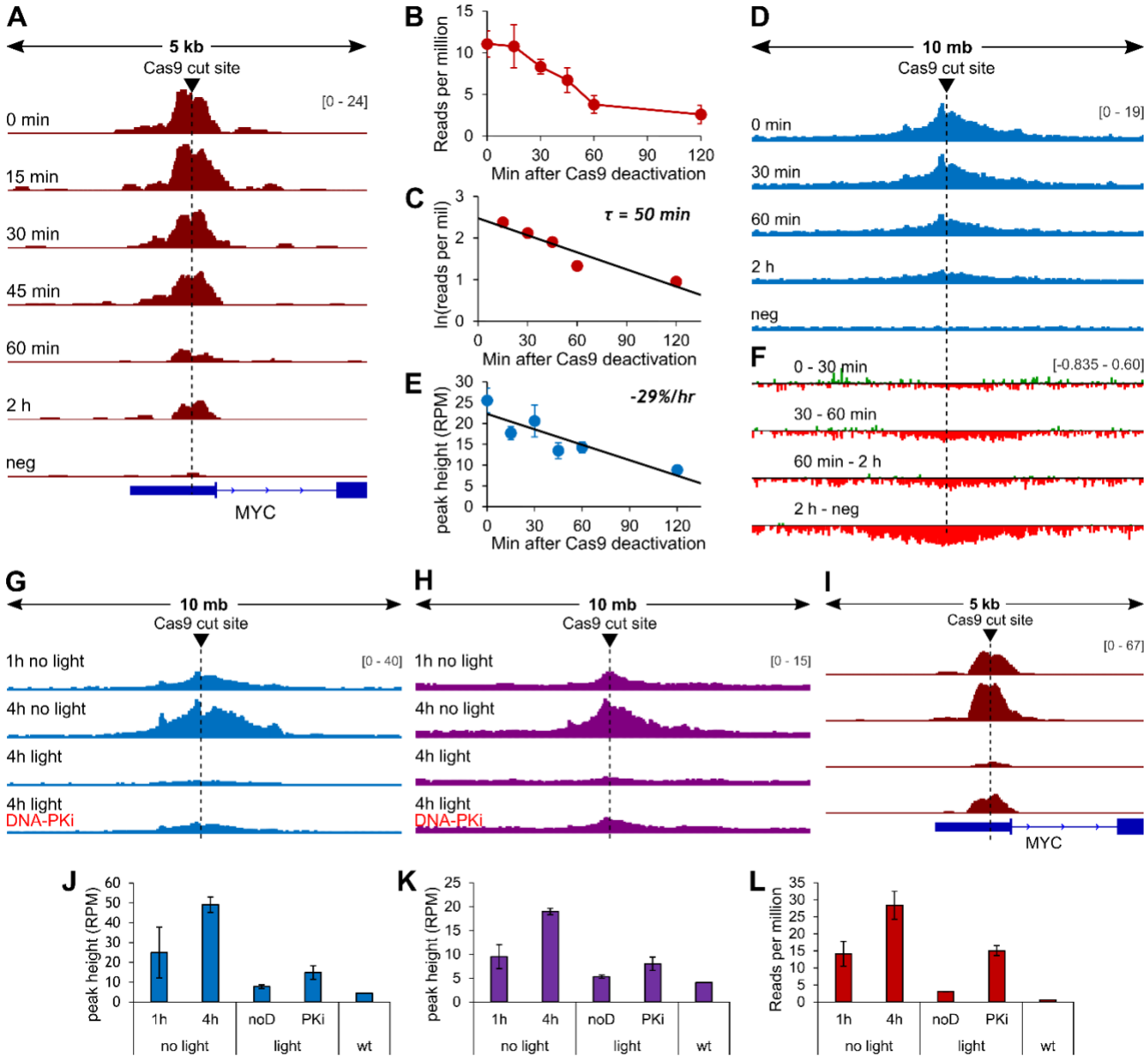

Figure S4. Dynamics of DNA repair factor departure after Cas9 deactivation at *MYC*, Related to Figure 4

(A-L) The same analysis as Figure 4 was performed here for Cas9/pcRNA targeting *MYC* (instead of *ACTB*).

Table S1. Synthetic DNA sequences, Related to STAR Methods

Name	Sequence (5′ to 3′)
tracrRNA	AGCAUAGCAAGUUAAAAUAAGGCUAGUCCGUUAUCAACUUGAAAAAGUGGCACCGAGUCGGUGCUUU
Pcl5_ACTB	GCU AU/iPC-Linker/ CUC GCA GCU CAC CAG UUU UAG AGC UAU GCU GUU UUG
Pcl5_HEKsite4	GGC AC/iPC-Linker/ GCG GCU GGA GGU GGG UUU UAG AGC UAU GCU GUU UUG
Pcl5_VEGFAsite2	GAC CC/iPC-Linker/ CUC CAC CCC GCC UCG UUU UAG AGC UAU GCU GUU UUG
Pcl5_MYC (site 1)	GUA AU/iPC-Linker/ CCA GCG AGA GGC AGG UUU UAG AGC UAU GCU GUU UUG
Pcl5_MYCsite3	CGA GA/iPC-Linker/ GCG GAG GAA CTG CGG UUU UAG AGC UAU GCU
Pcl5_FANCFsite2	GCU GC/iPC-Linker/ GAA GGG AUU CCA UGG UUU UAG AGC UAU GCU GUU UUG
IDT_ACTB	GCU AUU CUC GCA GCU CAC CAG UUU UAG AGC UAU GCU
IDT_HEKsite4	GGC ACU GCG GCU GGA GGU GGG UUU UAG AGC UAU GCU
IDT_VEGFAsite2	GAC CCC CUC CAC CCC GCC UCG UUU UAG AGC UAU GCU
IDT_MYC (site 1)	GUA AUU CCA GCG AGA GGC AGG UUU UAG AGC UAU GCU
IDT_FANCFsite2	GCU GCA GAA GGG AUU CCA UGG UUU UAG AGC UAU GCU
Gib_pET42b_F	CCCAAGAAGAAGAGGAAAGTCTAATAATTG
Gib_pET42b_R	GTGATGGTGATGATGATGACTG
Gib_BEmax_F	gggcagcagtcatcatcatcaccatcacCCAAAGAAGAAGCGGAAAGTC
Gib_BEmax_R	attagactttcctcttcttcttgggCTCGAATTCGCTGCCGTC
ACTB_150nt_fwd	catggacgagctgtacaagggatccGGCGGCCTAAGGACTCGG
ACTB_150nt_rev	ctgaagttagtagctccgctGAAGCCGGCCTTGCACATG
P2A-EGFP_fwd	AGCGGAGCTACTAACTTC
P2A-EGFP_rev	ggtcggcgcgcccacccttggatcctcaCTTGTACAGCTCGTCCATG
ACTB_F	TGGCGGCCTAAGGACTCG
ACTB_R	CTTCAGGGTGAGGATGCCTCTC
HEKs4_F	CCAGTGGTTCAATGGTCATCC
HEKs4_R	GGCCAGTGAAATCACCCTG
VEGFAs2_F	AGAGAAGTCGAGGAAGAGAGAG
VEGFAs2_R	CAGCAGAAAGTTCATGGTTTCG
MYCs1_F	TTGGCGGGAAAAAGAACGG
MYCs1_R	GAGAGCCTTTCAGAGAAGCGG
MYCs3_F	CGTGGTGTTGGGTAGGCG
MYCs3_R	TTTCTTCTTTCTCTCGCCGG
FANCFs2_F	AGTTCGCTAATCCCGGAACT
FANCFs2_R	AGTTGCCCAGAGTCAAGGAA
NGS_ACTB_F	tcgtcggcagcgtcagatgtgtataagagacagTGGCGGCCTAAGGACTCG
NGS_ACTB_R	gtctcgtgggctcggagatgtgtataagagacagGAAGCCGGCCTTGCACATG
NGS_HEKs4_ON_F	tcgtcggcagcgtcagatgtgtataagagacagGGTCCAAAGCAGGATGACAG
NGS_HEKs4_ON_R	gtctcgtgggctcggagatgtgtataagagacagGAGACACACACACAGGCCT
NGS_HEKs4_OFF1_F	tcgtcggcagcgtcagatgtgtataagagacagCACTGCTCTCCAGAGTGGT
NGS_HEKs4_OFF1_R	gtctcgtgggctcggagatgtgtataagagacagGATTCTCCTACTTCCTCCTCGG
NGS_HEKs4_OFF3_F	tcgtcggcagcgtcagatgtgtataagagacagGAGAAAAGCCAACGGGTTCTC
NGS_HEKs4_OFF3_R	gtctcgtgggctcggagatgtgtataagagacagCATTGTCCCAGCTAAGCTCTCA
NGS_HEKs4_OFF10_F	tcgtcggcagcgtcagatgtgtataagagacagCCCTGAGAAGGTAGTAGGAATCC
NGS_HEKs4_OFF10_R	gtctcgtgggctcggagatgtgtataagagacagGTGGTTAAGAGCAGACTCCCT
NGS_VEGFAs2_ON_F	tcgtcggcagcgtcagatgtgtataagagacagCTCCTCCGAAGCGAGAA
NGS_VEGFAs2_ON_R	gtctcgtgggctcggagatgtgtataagagacagGACAGACAGACAGACACCG
NGS_VEGFAs2_OFF9_F	tcgtcggcagcgtcagatgtgtataagagacagGCTCTGACCTTGTTTGTTATTCC
NGS_VEGFAs2_OFF9_R	gtctcgtgggctcggagatgtgtataagagacagGTGACTCCAAGGCTTTTCG
NGS_VEGFAs2_OFF23_F	tcgtcggcagcgtcagatgtgtataagagacagCTCTTGCCTGTCACGCA
NGS_VEGFAs2_OFF23_R	gtctcgtgggctcggagatgtgtataagagacagCCTGGAGTTAAGGGTGTCTC
NGS_VEGFAs2_OFF24_F	tcgtcggcagcgtcagatgtgtataagagacagCATCCTTGTATCAGCTGCCT
NGS_VEGFAs2_OFF24_R	gtctcgtgggctcggagatgtgtataagagacagCCATTCTCAGCCTAAAAGGTAGA
NGS_MYCs1_F	tcgtcggcagcgtcagatgtgtataagagacagGGGATCGCGCTGAGTATAAA
NGS_MYCs1_R	gtctcgtgggctcggagatgtgtataagagacagTGGGCAAAGTTTCGTGGA
NGS_MYCs3_F	tcgtcggcagcgtcagatgtgtataagagacagAAAACCAGGGCGAATCTCCG
NGS_MYCs3_R	gtctcgtgggctcggagatgtgtataagagacagGAGACCCCGCTGCGATAC
NGS_FANCFs2_F	tcgtcggcagcgtcagatgtgtataagagacagAGGTGCTGACGTAGGTAGTG
NGS_FANCFs2_R	gtctcgtgggctcggagatgtgtataagagacagCGTATCATTTCGCGGATGTTC
NGS_Index_F1	AATGATACGGCGACCACCGAGATCTACACCTCTCTATTCGTCGGCAGCGTC
NGS_Index_F2	AATGATACGGCGACCACCGAGATCTACACTATCCTCTTCGTCGGCAGCGTC

NGS_Index_F3	AATGATACGGCGACCACCGAGATCTACACGTAAGGAGTCGTCGGCAGCGTC
NGS_Index_F4	AATGATACGGCGACCACCGAGATCTACACACTGCATATCGTCGGCAGCGTC
NGS_Index_F5	AATGATACGGCGACCACCGAGATCTACACAAGGAGTATCGTCGGCAGCGTC
NGS_Index_F6	AATGATACGGCGACCACCGAGATCTACACCTAAGCCTTCGTCGGCAGCGTC
NGS_Index_F7	AATGATACGGCGACCACCGAGATCTACACCGTCTAATTCGTCGGCAGCGTC
NGS_Index_F8	AATGATACGGCGACCACCGAGATCTACACTCTCTCCGTCGTCGGCAGCGTC
NGS_Index_R1	CAAGCAGAAGACGGCATACGAGATTCGCCTTAGTCTCGTGGGCTCGG
NGS_Index_R2	CAAGCAGAAGACGGCATACGAGATCTAGTACGGTCTCGTGGGCTCGG
NGS_Index_R3	CAAGCAGAAGACGGCATACGAGATTTCTGCCTGTCTCGTGGGCTCGG
NGS_Index_R4	CAAGCAGAAGACGGCATACGAGATGCTCAGGAGTCTCGTGGGCTCGG
NGS_Index_R5	CAAGCAGAAGACGGCATACGAGATAGGAGTCCGTCTCGTGGGCTCGG
NGS_Index_R6	CAAGCAGAAGACGGCATACGAGATCATGCCTAGTCTCGTGGGCTCGG
NGS_Index_R7	CAAGCAGAAGACGGCATACGAGATGTAGAGAGGTCTCGTGGGCTCGG
NGS_Index_R8	CAAGCAGAAGACGGCATACGAGATCAGCCTCGGTCTCGTGGGCTCGG
MNase_F	/5Phos/GATCGGAAGAGCACACGTCT
MNase_R	ACACTCTTTCCCTACACGACGCTCTTCCGATC*T
PE_i5	AATGATACGGCGACCACCGAGATCTACACTCTTTCCCTACACGACGCTCTTCCGATC*T
PE_i701	CAAGCAGAAGACGGCATACGAGAT**CGTGAT**GTGACTGGAGTTCAGACGTGTGCTCTTCCGATC*T
PE_i702	CAAGCAGAAGACGGCATACGAGAT**ACATCG**GTGACTGGAGTTCAGACGTGTGCTCTTCCGATC*T
PE_i703	CAAGCAGAAGACGGCATACGAGAT**GCCTAA**GTGACTGGAGTTCAGACGTGTGCTCTTCCGATC*T
PE_i704	CAAGCAGAAGACGGCATACGAGAT**TGGTCA**GTGACTGGAGTTCAGACGTGTGCTCTTCCGATC*T
PE_i705	CAAGCAGAAGACGGCATACGAGAT**CACTGT**GTGACTGGAGTTCAGACGTGTGCTCTTCCGATC*T
PE_i706	CAAGCAGAAGACGGCATACGAGAT**ATTGGC**GTGACTGGAGTTCAGACGTGTGCTCTTCCGATC*T
PE_i707	CAAGCAGAAGACGGCATACGAGAT**GATCTG**GTGACTGGAGTTCAGACGTGTGCTCTTCCGATC*T
PE_i708	CAAGCAGAAGACGGCATACGAGAT**TCAAGT**GTGACTGGAGTTCAGACGTGTGCTCTTCCGATC*T
PE_i709	CAAGCAGAAGACGGCATACGAGAT**CTGATC**GTGACTGGAGTTCAGACGTGTGCTCTTCCGATC*T
PE_i710	CAAGCAGAAGACGGCATACGAGAT**AAGCTA**GTGACTGGAGTTCAGACGTGTGCTCTTCCGATC*T
PE_i711	CAAGCAGAAGACGGCATACGAGAT**GTAGCC**GTGACTGGAGTTCAGACGTGTGCTCTTCCGATC*T
PE_i712	CAAGCAGAAGACGGCATACGAGAT**TACAAG**GTGACTGGAGTTCAGACGTGTGCTCTTCCGATC*T
PE_i713	CAAGCAGAAGACGGCATACGAGAT**ATCAGT**GTGACTGGAGTTCAGACGTGTGCTCTTCCGATC*T
PE_i714	CAAGCAGAAGACGGCATACGAGAT**AGGAAT**GTGACTGGAGTTCAGACGTGTGCTCTTCCGATC*T
PE_i715	CAAGCAGAAGACGGCATACGAGAT**ATTCCG**GTGACTGGAGTTCAGACGTGTGCTCTTCCGATC*T
PE_i716	CAAGCAGAAGACGGCATACGAGAT**CCACTC**GTGACTGGAGTTCAGACGTGTGCTCTTCCGATC*T
PE_i717	CAAGCAGAAGACGGCATACGAGAT**CGATTA**GTGACTGGAGTTCAGACGTGTGCTCTTCCGATC*T
PE_i718	CAAGCAGAAGACGGCATACGAGAT**CTTCGA**GTGACTGGAGTTCAGACGTGTGCTCTTCCGATC*T
PE_i719	CAAGCAGAAGACGGCATACGAGAT**GAATGA**GTGACTGGAGTTCAGACGTGTGCTCTTCCGATC*T
PE_i720	CAAGCAGAAGACGGCATACGAGAT**GCGGAC**GTGACTGGAGTTCAGACGTGTGCTCTTCCGATC*T
PE_i721	CAAGCAGAAGACGGCATACGAGAT**GGAACT**GTGACTGGAGTTCAGACGTGTGCTCTTCCGATC*T
PE_i722	CAAGCAGAAGACGGCATACGAGAT**TAGTTG**GTGACTGGAGTTCAGACGTGTGCTCTTCCGATC*T
PE_i723	CAAGCAGAAGACGGCATACGAGAT**TCGGGA**GTGACTGGAGTTCAGACGTGTGCTCTTCCGATC*T
PE_i724	CAAGCAGAAGACGGCATACGAGAT**TCTGAG**GTGACTGGAGTTCAGACGTGTGCTCTTCCGATC*T

Methods S1. Protocols for protein purification, light deactivation experiments, and ChIP-seq, Related to STAR Methods

Version 1

Jan 20, 2021

Protocol 1A: Purification of SpCas9

Protocol 1B: Purification of AncBE4max

Protocol 2: In vitro cleavage assays and light deactivation

Protocol 3: Electroporation of Cas9/pcRNA to 800k HEK293T cells, light deactivation, then indel evaluation by Sanger Sequencing 3 days later

Protocol 4: Electroporation of Cas9/pcRNA complex to 32 million HEK293T cells, light deactivation, then harvest cells for ChIP-seq

Protocol 5: ChIP-seq for MRE11, 53BP1, γH2AX at 30 min, 1 hour, 2 hours after deactivation

Protocol 6: Sample preparation for amplicon Illumina sequencing

Protocol 1A: Purification of SpCas9

Reagents

- BL21 CodonPlus (DE3)-RIL cells (Agilent 230245)
- SpCas9 plasmid (https://www.addgene.org/67881/)
- LB Agar Carbenicillin plates (Teknova L1010)
- 100mg/ml Ampicillin
- IPTG (GoldBio I2481C25)
- 2x Laemmli sample buffer (Bio-Rad 1610737)
- Bond-Breaker™ 500mM TCEP Solution, Neutral pH (Thermo Fisher 77720)
- 8-16% miniPROTEAN PAGE gel (Bio-Rad 4561103)
- SimplyBlue™ SafeStain (Thermo Fisher LC6060)
- Ni-NTA Agarose (Qiagen 30210)
- gravity flow chromatography column (G-Biosciences 786-197)
- 5 ml HiTrap Q HP, 5 x 5 ml (Cytiva 17115401)
- 10 kDa SnakeSkin™ dialysis tubing (Thermo Fisher Scientific 68100)
- Millex-GV Syringe Filter Unit, 0.22 µm, PVDF, 33 mm (Millipore Sigma SLGV033RS)
- Amicon Ultra-15 Centrifugal Filter Unit, Ultracel-10 (Millipore Sigma UFC901008)
- cOmplete™ EDTA-free protease inhibitor tablet (Sigma-Aldrich 11836170001)
- Custom buffers

Reagent	**Final concentration**
Lysis buffer (40ml)	20mM Tris-HCl, pH 8.0 250mM KCl 20mM imidazole 10% glycerol 1mM TCEP (fresh right before) 1mM PMSF Add 1 protease inhibitor tablet for 50mL buffer
Wash buffer (40ml)	20mM Tris-HCl, pH 8.0 800mM KCl 20mM imidazole 10% glycerol 1mM TCEP
Elution buffer (7ml x4 for 100, 150, 200, 250mM imidazole)	20mM HEPES pH 8.0 500mM KCl 10% glycerol 100-250mM imidazole
Dialysis buffer (2L)	20mM HEPES pH 7.5 500mM KCl 20% glycerol

Specialized Equipment

- Shaking incubator
- Centrifuge and Ultracentrifuge
- Spectrophotometer to measure absorbance of bacterial culture (OD_{600})
- Sonicator or Microfluidizer to lyse *E. coli*
- 50ml ultracentrifuge round-bottom tubes (Nalgene)
- 500ml centrifuge bottles (Nalgene)
- Electrophoresis chamber and power supply (BioRad)

Day 1

1. [afternoon] Transform Cas9 plasmid into BL21 CodonPlus (DE3)-RIL cells.
2. Plate onto LB Agar Carbenicillin plates.

Day 2

1. [afternoon] Inoculate a colony into 25mL LB media with 25uL of 100mg/mL Ampicillin.
2. Incubate 37C overnight, shaking at 220RPM.
3. Prepare 2L LB media with 0.1% glucose (2g). Autoclave to sterilize.

Day 3

1. [morning] Pour the 25ml of bacterial culture to 2L LB media with 0.1% glucose.
2. Add 2ml of 100mg/ml Ampicillin.
3. Incubate at 37C, shaking at 220RPM.
4. Periodically evaluate bacterial growth the until OD_{600} ~0.5.
5. Once OD_{600} ~0.5, move to ice, incubate 30 min in 4C cold room. Take 1ml of bacterial culture: {A}, store in 4C.
6. Add 0.2mM IPTG (0.4mL) to each 2L culture; incubate 18C overnight, shaking at 220RPM.

Day 4A (very busy day, can split into 2 days – Day 4A and 4B)

1. [morning] Take 1ml of bacterial culture: {B}, store in 4C.
2. Transfer the remainder of bacterial culture to 500ml Nalgene centrifuge bottles. Spin 4500xg for 15 min, pour out supernatant into bleach, store pellet on ice.
3. Run {A} and {B} on protein gel
   a. Take 5ul from sample, mix with 25ul nuclease free water.
   b. Add 30ul of 2x Laemmli sample buffer with 50mM TCEP (1:10 dilution of 500mM TCEP).
   c. Vortex, heat at 100C in heat block for 20min to denature proteins.
   d. Load to 8-16% miniPROTEAN PAGE gel.
   e. Run ~30min at 300V to resolve 150-250kDa
   f. Stain and destain gel with SimplyBlue SafeStain microwave protocol.
4. Determine appearance of new band around 150 kDa only found in {B} and not {A}, which corresponds to IPTG-induced expression of SpCas9.
5. If 150kDa band exists in {B}, start purification (All procedures done on ice or 4C cold room)
6. Resuspend pellets in 40mL Lysis Buffer

- Optional stopping point – flash freeze and store in -80C

Day 4B

1. Lyse cells with sonication (10%, 1.5s ON; 5s OFF, 45min) or Microfluidizer
2. Take 200ul sample for storage in 4C {C}
3. Transfer remainder (~40ml) to 50ml Nalgene ultracentrifuge round-bottom tube
4. Centrifuge at 16000g for 40 min in 4C.
5. Take 200ul of supernatant for storage in 4C {D}. Keep pellet as {E}
6. Filter supernatant with 0.22um PVDF syringe filter unit
7. Use 4mL of Ni-NTA resin solution (for 2L of bacterial culture).
8. Buffer change 4mL of Ni-NTA resin solution to 4mL Lysis Buffer, with two 700g 2min centrifugation and supernatant removal steps)
9. Add 4mL of Lysis Buffer-equilibrated Ni-NTA to ~40ml protein supernatant in Lysis Buffer.
10. Place on rotator in 4C for 1 hour.
11. Transfer all to gravity flow chromatography column. Allow the majority of liquid to flow through, store as {F1}.
12. Wash with 40mL of Wash Buffer: add 10ml at a time, let most flow through column, add another 10ml, repeat until 40ml is used. Keep flowthrough as {F2} to {F4}
13. Elute 4x with 7ml Elution Buffer containing increasing concentrations of imidazole (100, 150, 200, 250mM). Store 200ul volumes as {G1} to {G4}
14. [night] Wash 5mL HiTrap Q HP chromatography column with 20ml of 1M KCl, then 5ml of Elution Buffer containing 250mM imidazole.

15. Flow eluate through HiTrap column
16. Load eluate into 10 kDa SnakeSkin™ dialysis tubing.
17. Place in 1L of Dialysis Buffer, dialyze overnight in 4C

Day 5

1. [morning] Transfer dialysis tubing to another 1L of fresh Dialysis Buffer, dialyze for 3 hours in 4C
2. Take eluate from dialysis tubing
3. [afternoon] Run {A} to {G} on protein gel
    a. Take 5ul from sample, mix with 25ul nuclease free water.
    b. Add 30ul of 2x Laemmli sample buffer with 50mM TCEP (1:10 dilution of 500mM TCEP).
    c. Vortex, heat at 100C in heat block for 20min to denature proteins.
    d. Load to 8-16% miniPROTEAN PAGE gel.
    e. Run ~30min at 300V to resolve 150-250kDa
    f. Stain and destain gel with SimplyBlue SafeStain microwave protocol.
4. Concentrate protein to 10ug/ul with Amicon Ultra-15, Ultracel-10.
5. Split to 10-20ul aliquots, flash-freeze and store at -80C.

Protocol 1B: Purification of AncBE4max

Reagents

- One Shot™ BL21 Star™ (DE3) Chemically Competent E. coli (Thermo Fisher C601003)
- AncBE4max plasmid (https://www.addgene.org/165157/)
- LB Agar Kanamycin plates (Teknova L1027)
- 100mg/ml Kanamycin
- IPTG (GoldBio I2481C25)
- 2x Laemmli sample buffer (Bio-Rad 1610737)
- Bond-Breaker™ 500mM TCEP Solution, Neutral pH (Thermo Fisher 77720)
- 8-16% miniPROTEAN PAGE gel (Bio-Rad 4561103)
- SimplyBlue™ SafeStain (Thermo Fisher LC6060)
- HisPur™ Ni-NTA Resin (Thermo Fisher 88222)
- gravity flow chromatography column (G-Biosciences 786-197)
- 5 ml HiTrap Q HP, 5 x 5 ml (Cytiva 17115401)
- 20k MWCO Slide-A-Lyzer™ G2 Dialysis Cassette (Thermo Fisher 87736)
- Millex-GV Syringe Filter Unit, 0.22 µm, PVDF, 33 mm (Millipore Sigma SLGV033RS)
- Amicon Ultra-15 Centrifugal Filter Unit, Ultracel-10 (Millipore Sigma UFC901008)
- cOmplete™ EDTA-free protease inhibitor tablet (Sigma-Aldrich 11836170001)
- Custom buffers

Reagent	**Final concentration**
Lysis buffer (40ml)	100mM Tris-HCl, pH 8.0 1M NaCl 20% glycerol 5mM TCEP (fresh right before) 0.4mM PMSF Add 1 protease inhibitor tablet for 50mL buffer
Wash buffer (40ml)	100mM Tris-HCl, pH 8.0 1M NaCl 20% glycerol 5mM TCEP
Elution buffer (7ml x4 for 100, 150, 200, 250mM imidazole)	100mM Tris-HCl, pH 8.0 0.5M NaCl 20% glycerol 5mM TCEP 100-250mM imidazole
Dialysis buffer (2L)	20 mM HEPES pH 7.5 500mM KCl 20% glycerol

Specialized Equipment

- Shaking incubator
- Centrifuge and Ultracentrifuge
- Spectrophotometer to measure absorbance of bacterial culture (OD_{600})
- Sonicator or Microfluidizer to lyse *E. coli*
- 50ml ultracentrifuge round-bottom tubes (Nalgene)
- 500ml centrifuge bottles (Nalgene)
- Electrophoresis chamber and power supply (BioRad)

Day 1

1. [afternoon] Transform AncBE4max plasmid into One Shot™ BL21 Star™ (DE3) cells.
2. Plate onto LB Agar Kanamycin plates.

Day 2

1. [afternoon] Inoculate a colony into 25mL LB media with 25uL of 100mg/mL Kanamycin.
2. Incubate 37C overnight, shaking at 220RPM.
3. Prepare 2L LB media with 0.1% glucose (2g). Autoclave to sterilize.

Day 3

1. [morning] Pour the 25ml of bacterial culture to 2L LB media with 0.1% glucose.
2. Add 2ml of 100mg/ml Kanamycin.
3. Incubate at 37C, shaking at 220RPM.
4. Periodically evaluate bacterial growth the until OD_{600} ~0.7-0.75.
5. Once OD_{600} ~0.7-0.75, move to ice, incubate 30 min in 4C cold room. Take 1ml of bacterial culture: {A}, store in 4C.
6. Add 0.5mM IPTG (1mL) to 2L culture; incubate 18C overnight, shaking at 220RPM.

Day 4 (very busy day, can split into 2 days)

1. [morning] Take 1ml of bacterial culture: {B}, store in 4C.
2. Transfer the remainder of bacterial culture to 500ml Nalgene centrifuge bottles. Spin 4500xg for 30 min, pour out supernatant into bleach, store pellet on ice.
3. Run {A} and {B} on protein gel
   a. Take 5ul from sample, mix with 25ul nuclease free water.
   b. Add 30ul of 2x Laemmli sample buffer with 50mM TCEP (1:10 dilution of 500mM TCEP).
   c. Vortex, heat at 100C in heat block for 20min to denature proteins.
   d. Load to 8-16% miniPROTEAN PAGE gel.
   e. Run ~30min at 300V to resolve 150-250kDa
   f. Stain and destain gel with SimplyBlue SafeStain microwave protocol.
4. Determine appearance of new band around 200 kDa only found in {B} and not {A}, which corresponds to IPTG-induced expression of AncBE4max.
5. If 200kDa band exists in {B}, start purification (All procedures done on ice or 4C cold room)
6. Resuspend pellets in 40mL Lysis Buffer

- Optional stopping point – flash freeze and store in -80C

Day 4B

1. Lyse cells with sonication (10%, 1.5s ON; 5s OFF, 45min) or Microfluidizer
2. Take 200ul sample for storage in 4C {C}
3. Transfer remainder (~40ml) to 50ml Nalgene ultracentrifuge round-bottom tube
4. Centrifuge at 16000g for 40 min in 4C.
5. Take 200ul of supernatant for storage in 4C {D}. Keep pellet as {E}
6. Filter supernatant with 0.22um PVDF syringe filter unit
7. Use 4mL of Ni-NTA resin solution (for 2L of bacterial culture).
8. Buffer change 4mL of Ni-NTA resin solution to 4mL Lysis Buffer, with two 700g 2min centrifugation and supernatant removal steps)
9. Add 4mL of Lysis Buffer-equilibrated Ni-NTA to ~40ml protein supernatant in Lysis Buffer.
10. Place on rotator in 4C for 1 hour.
11. Transfer all to gravity flow chromatography column. Allow the majority of liquid to flow through, store as {F1}.
12. Wash with 40mL of Wash Buffer: add 10ml at a time, let most flow through column, add another 10ml, repeat until 40ml is used. Keep flowthrough as {F2} to {F4}
13. Elute 4x with 7ml Elution Buffer containing increasing concentrations of imidazole (100, 150, 200, 250mM). Store 200ul volumes as {G1} to {G4}
14. [night] Wash 5mL HiTrap Q HP chromatography column with 20ml of 1M KCl, then 5ml of Elution Buffer containing 250mM imidazole.

15. Flow eluate through HiTrap column
16. Load eluate to 20k MWCO Slide-A-Lyzer™ G2 Dialysis Cassette following manufacturer instructions (using a 18-21-gauge beveled needle).
17. Place in 1L of Elution Buffer, dialyze overnight in 4C

Day 5

1. [morning] Transfer dialysis cassette to 1L of fresh Elution Buffer, dialyze for 3 hours in 4C
2. Take eluate from dialysis cassette.
3. [afternoon] Run {A} to {G} on protein gel
    a. Take 5ul from sample, mix with 25ul nuclease free water.
    b. Add 30ul of 2x Laemmli sample buffer with 50mM TCEP (1:10 dilution of 500mM TCEP).
    c. Vortex, heat at 100C in heat block for 20min to denature proteins.
    d. Load to 8-16% miniPROTEAN PAGE gel.
    e. Run ~30min at 300V to resolve 150-250kDa
    f. Stain and destain gel with SimplyBlue SafeStain microwave protocol.
4. Concentrate protein to 10ug/ul with Amicon Ultra-15, Ultracel-10.
5. Split to 10-20ul aliquots, flash-freeze and store at -80C.

Protocol 2: In vitro cleavage assays and light deactivation

Reagents

- Purified Cas9 (10mg/ml) from Protocol 1A
- Photocleavable crRNA, tracrRNA (Integrated DNA Technologies, sequences in Table S1)
- HEK293T cells (ATCC)
- DNeasy Blood & Tissue Kit (Qiagen 69504)
- Q5® High-Fidelity 2X Master Mix (New England BioLabs M0492)
- NEBuffer 3.1 (New England BioLabs)
- Proteinase K, Molecular Biology Grade (New England BioLabs P8107S)
- *ACTB* Fwd/Rev primer set (Integrated DNA Technologies, sequences in Table S1)
- QIAquick PCR Purification Kit (Qiagen 28104)
- Nuclease-Free Duplex Buffer (Integrated DNA Technologies 11-01-03-01)
- Dialysis Buffer from Protocol 1
- Agarose gels
- (Optional) E-Gel Precast Agarose Electrophoresis System (Thermo Fisher)

Specialized Equipment

- Thermocycler
- JAXMAN 365nm LED flashlight (Amazon https://www.amazon.com/JAXMAN-Ultraviolet-365nm-Detector-Flashlight/dp/B06XW7S1CS/)
- Gel electrophoresis

Obtain target DNA at *ACTB* for *in vitro* cleavage

1. Purify genomic DNA (gDNA) from HEK293T cells using DNeasy Blood & Tissue Kit. Elute in 200ul AE. Store gDNA in -20C.
2. Mix for PCR reaction

Component	**Volume**
Nuclease Free Water (NFW)	3 uL
Genomic DNA	1 uL
ACTB_F/ACTB_R mixture (10uM)	1 uL
Q5® High-Fidelity 2X Master Mix	5 uL
Total	**10 uL**

3. Start thermocycling protocol

Step	**Temp**	**Time**
Initial Denaturation	98C	30 sec
35 cycles	98C	10 sec
	71C (*ACTB*)	10 sec
	72C	20 sec
Final extension	72C	2 min
Hold	4C	Inf

4. Extract PCR-amplified target DNA with QIAquick PCR Purification Kit, elute in 30 uL EB supplied with kit.

* For other target sites, use the following annealing temperatures:
68C (HEK site 4 – HEKs4_F/HEKs4_R)
65C (VEGFA site 2 – VEGFAs2_F/VEGFAs2_R)
67C (MYC site 1 – MYCs1_F/MYCs1_R)
67C (MYC site 3 – MYCs3_F/MYCs3_R)
67C (FANCF site 2 – FANCFs2_F/FANCFs2_R)

Prepare 10uM Cas9 and annealed cr/trRNA

1. Dilute crRNA and tracrRNA purchased from IDT to 100uM with Duplex Buffer
2. Mix 2ul of 100uM photocleavable crRNA with 2ul of 100uM tracrRNA in PCR tube
3. Heat at 95C for 5 min in thermocycler with heated lid
4. Cool on benchtop for 5 min
5. Mix in 16ul of Duplex Buffer to make 20ul of 10uM annealed cr/trRNA

- Dilute 3ul of 10mg/ml Cas9 with 15ul of Dialysis Buffer to make 18ul of 10uM SpCas9

***In vitro* cleavage of target DNA with Cas9/pcRNA**

1. Mix the following components together in order. Thoroughly mix NFW and NEBuffer 3.1 before adding cr/trRNA and Cas9. Prepare two identical volumes {A} and {B}, both in PCR tubes.

Component	**Volume**
Nuclease Free Water (NFW)	8.1 uL
NEBuffer 3.1	1 uL
10uM cr/trRNA targeting *ACTB*	0.5 uL
10uM Cas9	0.4 uL
Total	**10ul**

2. Leave on benchtop (room temperature) for 30 minutes to form RNP complex
3. Move both tubes to thermocycler set to 37C, leave for 1 minute with tube caps (and thermocycler lid) open
4. Within arm's reach, leave a pipette holding 2ul of PCR-amplified *ACTB* target DNA in its tip.
5. Hold 365 nm LED flashlight 2 cm above {A} for 30 seconds to deactivate Cas9/pcRNA
6. Immediately transfer the 2ul of *ACTB* target DNA into {A}, mix thoroughly
7. Get 2ul more of *ACTB* target DNA, transfer into {B}, mix thoroughly
8. Close tube caps, close thermocycler lid, incubate for 1 hour at 37C
9. Add 0.5ul of Proteinase K, incubate at 55C for 15 minutes
10. Run on ~2% agarose gel or E-Gel system (Thermo Fisher), visualize with gel imager

Expected Result

- Visualization of cleaved target DNA bands only in sample {B}, which is not deactivated. Sample {A} only has original target DNA band.

Protocol 3: Electroporation of Cas9/pcRNA to 800k HEK293T cells, light deactivation, then indel evaluation by Sanger Sequencing 3 days later

Reagents

- SF Cell Line 4D-Nucleofector™ X Kit S (Lonza V4XC-2032)
- Purified Cas9 (10mg/ml) from Protocol 1
- Photocleavable crRNA, tracrRNA (Integrated DNA Technologies, sequences in Table S1)
- HEK293T cells (ATCC)
- PBS
- Trypsin-EDTA (0.05%), phenol red (Thermo Fisher 25300062)
- Corning™ DMEM with L-Glutamine, Glucose, Sodium Pyruvate (Fisher Scientific MT10013CV)
- Corning™ Regular Fetal Bovine Serum (Fisher Scientific MT35011CV)
- Penicillin-Streptomycin (Thermo Fisher 15070063)
- Nalgene™ Rapid-Flow™ Sterile Single Use Vacuum Filter Units (Fisher Scientific 09-741-02)
- Alt-R® Cas9 Electroporation Enhancer, 10 nmol (Integrated DNA Technologies 1075916)
- Collagen I, rat tail (Thermo Fisher A1048301)
- DNeasy Blood & Tissue Kit (Qiagen 69504)
- Q5® High-Fidelity 2X Master Mix (New England BioLabs M0492)
- Fwd/Rev primer sets (Integrated DNA Technologies, sequences in Table S1)
- QIAquick PCR Purification Kit (Qiagen 28104)

Specialized Equipment

- 4D-Nucleofector™ Core Unit and 4D-Nucleofector™ X Unit (Lonza AAF-1002B & AAF-1002X)
- Thermocycler
- Hemocytometer
- JAXMAN 365nm LED flashlight (Amazon https://www.amazon.com/JAXMAN-Ultraviolet-365nm-Detector-Flashlight/dp/B06XW7S1CS/)

Small volume electroporation (800k cells, Lonza SF Kit S)

"DMEM complete" media for cell culture

1. Mix 450ml of DMEM with 50ml fetal bovine serum and 5ml of penicillin-streptomycin
2. Filter with Nalgene vacuum filter, store in 4C, optionally aliquot

Anneal cr/tr (cover with aluminum foil whenever possible)

1. Add 1.2ul crRNA with 1.2ul tracrRNA (100uM) in PCR tube to form 2.4uL of 50uM cr/trRNA
2. Heat at 95C in thermocycler for 3min -> cool on benchtop (room temperature) for 5min

Formation of RNP complex

1. Add Cas9 to cr/trRNA, mix, add PBS, mix again (cover with aluminum foil)

Component	**Volume**
cr/trRNA (50uM)	2.4 uL
Cas9 (10mg/ml)	1.7 uL
PBS	0.9 uL
Total	**5 uL**

2. In a separate tube, mix 16.4ul of SF nucleofection reagent and 3.6ul of Supplement 1 for each reaction to form 20ul mixed nucleofection reagent.
3. Proceed to prepare cells for electroporation, leaving the RNP complex at benchtop (room temperature)

Prepare 800k HEK293T cells for electroporation

** Leave the RNP complex aside, covered with aluminum foil*

1. First, add enough PBS with 1:100 collagen to cover six wells of a 48-well plate. Make sure the wells are very spaced apart. Incubate in 37C incubator. **CRITICAL** (collagen-coated plates allow for rapid cell adherence after electroporation).
2. Aspirate medium of cell culture; Wash cells with prewarmed PBS.
3. Add enough pre-warmed 0.05% Trypsin-EDTA into the culture flask to completely cover cells.
4. Incubate for 5 min in a CO2 incubator. **CRITICAL** (Efficient transfection requires single cell suspension).
5. Add equal volumes of "DMEM complete", gently mix and collect the cell suspension into a 15 mL centrifuge tube.
6. Count the number of cells using hemocytometer.
7. 800k cells are required for each reaction. Add the volume of cell suspension that contain 800k cells into a separate 15ml tube, centrifuge at 200g for 3 min.
8. Carefully aspirate the supernatant. Resuspend with 2ml PBS. **CRITICAL** ("DMEM complete" contains serum, which could degrade guide RNA)
9. Centrifuge at 200g for 3 min. Remove as much supernatant as possible without disturbing the pellet.
10. During centrifugation, take the 48-well plate from incubator and remove the collagen solution, let it dry in the cell culture hood.
11. Add the 20ul mixed nucleofection reagent into the cell pellet to form ~25ul cell suspension. Mix well.
12. Make sure that the cell culture hood lights are turned OFF. Move RNP mixture into hood, and remove aluminum foil covering.
13. Transfer ~25ul cell suspension to the 5ul RNP mixture; add 1ul Cas9 EP enhancer; transfer all (~30ul) to one unused well of the 16-well electroporation cuvette.
14. Electroporate with 4D-Nucleofector. For HEK293T cells, use "Cell Line SF", code CA-189.

** If there is some white precipitate that only shows up after electroporation, do not worry. If anything, it is a visual cue that the electroporation worked.*

15. After electroporation, go back to culture hood with lights OFF, add 50ul of PBS into cuvette, transfer all to 250ul PBS in an Eppendorf tube for ~330ul total.
16. Split 50ul each to six wells of 48-well plate (A, B, C, D, E, F).
17. Add 300ul "DMEM complete" media to wells B-F.

Light-mediated deactivation of Cas9/pcRNA in cells

<u>Deactivation right after electroporation</u>

1. Turn on 365nm LED flashlight, hold it 2 cm above well A for 1 minute. Cells in well A are now deactivated.
2. Add 300ul "DMEM complete" media to well A. Cover plate with aluminum foil, move back to incubator.

<u>Deactivation at least 30 min after electroporation</u>

1. By 30 min after electroporation, the cells should be adherent if collagen is coated properly.
2. To deactivate, first remove most of media, turn on and hold 365nm LED flashlight 2 cm above well for 1 minute. **CRITICAL** ("DMEM complete" can partially block the light, which greatly reduces deactivation efficiency)
3. Add back 300ul fresh "DMEM complete" media. Cover plate with aluminum foil, move back to incubator.

Sanger sequencing to evaluate genome editing

1. 3 days after electroporation, wash cells off 48-well plates with 200ul PBS, using pipette or cell scraper.
2. From cells suspended in 200ul PBS, purify genomic DNA (gDNA) using DNeasy Blood & Tissue Kit. Elute in 200ul AE supplied with kit. Store gDNA in -20C.

3. Mix for PCR reaction

Component	Volume
Nuclease Free Water (NFW)	3 uL
Genomic DNA	1 uL
Fwd/Rev primer set (10uM)	1 uL
Q5® High-Fidelity 2X Master Mix	5 uL
Total	**10 uL**

* Primer set sequences are found in Table S1.
ACTB – ACTB_F/ACTB_R
HEK site 4 – HEKs4_F/HEKs4_R
VEGFA site 2 – VEGFAs2_F/VEGFAs2_R
MYC site 1 – MYCs1_F/MYCs1_R
MYC site 3 – MYCs3_F/MYCs3_R
FANCF site 2 – FANCFs2_F/FANCFs2_R

4. Start thermocycling protocol

Step	Temp	Time
Initial Denaturation	98C	30 sec
35 cycles **X**=71C (*ACTB*), 68C (*HEK site 4*), 65C (*VEGFA site 2*), 67C (*MYC site 1*, *MYC site 3*, *FANCF site 2*)	98C	10 sec
	X	10 sec
	72C	20 sec
Final extension	72C	2 min
Hold	4C	Inf

5. Extract PCR-amplified target DNA with QIAquick PCR Purification Kit, elute in 30 uL EB supplied with kit.
6. Submit 10uL for Sanger Sequencing, using the Fwd and/or Rev PCR primer as the sequencing primer. We use GeneWiz or a core facility at our institution.
7. Also sequence wild type HEK293T cells for a “negative control” sample with no genome editing.
8. Use TIDE to estimate % of indels (http://shinyapps.datacurators.nl/tide/)

Protocol 4: Electroporation of Cas9/pcRNA complex to 32 million HEK293T cells, light deactivation, then harvest cells for ChIP-seq

Reagents

- SF Cell Line 4D-NucleofectorTM X Kit L (Lonza V4XC-2012)
- Purified Cas9 (10mg/ml) from Protocol 1
- Photocleavable crRNA, tracrRNA (Integrated DNA Technologies, sequences in Table S1)
- HEK293T cells (ATCC)
- Dialysis Buffer from Protocol 1
- PBS
- Trypsin-EDTA (0.05%), phenol red (Thermo Fisher 25300062)
- Corning™ DMEM with L-Glutamine, Glucose, Sodium Pyruvate (Fisher Scientific MT10013CV)
- Corning™ Regular Fetal Bovine Serum (Fisher Scientific MT35011CV)
- Penicillin-Streptomycin (Thermo Fisher 15070063)
- Nalgene™ Rapid-Flow™ Sterile Single Use Vacuum Filter Units (Fisher Scientific 09-741-02)
- Alt-R® Cas9 Electroporation Enhancer, 10 nmol (Integrated DNA Technologies 1075916)
- Collagen I, rat tail (Thermo Fisher A1048301)

Specialized Equipment

- 4D-Nucleofector™ Core Unit and 4D-Nucleofector™ X Unit (Lonza AAF-1002B & AAF-1002X)
- Hemocytometer
- JAXMAN 365nm LED flashlights (Amazon https://www.amazon.com/JAXMAN-Ultraviolet-365nm-Detector-Flashlight/dp/B06XW7S1CS/)
- (Optional) 3D printer design for LED flashlight holder (https://github.com/rogerzou/chipseq_pcRNA/blob/master/Jaxman_LED_flashlight_holder_design/files/8zeFECPViSo.stl)
- (Optional) MakerBot Replicator+ 3D printer

Two large volume electroporations (32 mil cells total, 16 mil cells each, Lonza SF Kit L)

"DMEM complete" media for cell culture

1. Mix 450ml of DMEM with 50ml fetal bovine serum and 5ml of penicillin-streptomycin
2. Filter with Nalgene vacuum filter, store in 4C, optionally aliquot

Anneal cr/tr (cover with aluminum foil whenever possible)

1. Add 4ul crRNA with 4ul tracrRNA (100uM) in PCR tube to form 8uL of 50uM cr/trRNA
2. Heat at 95C in thermocycler for 3min -> cool on benchtop (room temperature) for 5min

Formation of RNP complex

1. Add Cas9 to cr/trRNA, mix, add Dialysis Buffer, mix again (cover with aluminum foil)

Component	**Volume**
cr/trRNA (50uM)	8 uL
Cas9 (10mg/ml)	6 uL
Dialysis Buffer	16 uL
Total	**30 uL**

2. In a separate tube, mix 147.6ul of SF nucleofection reagent and 32.4ul of Supplement 1 to form 180ul of mixed nucleofection reagent.
3. Proceed to prepare cells for electroporation, leaving the RNP complex at benchtop (room temperature)

Prepare 32mil HEK293T cells for electroporation

** Leave the RNP complex aside, covered with aluminum foil*

1. First, add enough PBS with 1:100 collagen to cover 6 wells (wells colored light green in 12-well representation), each in four 12-well plates (A, B, C, D). Incubate in 37C incubator. **CRITICAL** (collagen-coated plates allow for rapid cell adherence after electroporation).

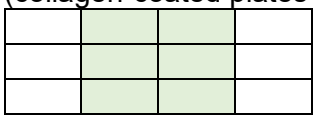

2. Aspirate medium of cell culture; Wash cells with prewarmed PBS.
3. Add enough pre-warmed 0.05% Trypsin-EDTA into the culture flask to completely cover cells.
4. Incubate for 5 min in a CO2 incubator. **CRITICAL** (Efficient transfection requires completely single cell suspension).
5. Add equal volumes of "DMEM complete", gently mix and collect the cell suspension into a 15 mL or 50mL centrifuge tube.
6. Count the number of cells using hemocytometer.
7. 32 mil cells are required. Add the two volumes of cell suspension that each contain 16 mil cells into separate 15ml tubes, centrifuge at 200g for 3 min.
8. Carefully aspirate the supernatant. Resuspend with 2ml PBS. **CRITICAL** ("DMEM complete" contains serum, which could degrade guide RNA)
9. Centrifuge at 200g for 3 min. Remove as much supernatant as possible w/o disturbing pellet.
10. During centrifugation, take the four 12-well plates from incubator and remove the collagen solution, let it dry in the cell culture hood.
11. Add all 180ul of mixed nucleofection reagent into the cell pellet of one 15ml tube. Mix well. Transfer all to other 15ml tube, mix well. Now, all 32 mil cells are suspended in 180ul of nucleofection reagent.
12. Make sure that the cell culture hood lights are turned OFF. Move RNP mixture into hood, and remove aluminum foil covering.
13. Transfer all (~220ul) to the 30ul RNP mixture; add 4ul Cas9 EP enhancer; Split the total volume (~250ul) to two 100ul electroporation cuvettes.
14. Electroporate with 4D-Nucleofector. For HEK293T cells, use "Cell Line SF", code CA-189.

** If there is some white precipitate that only shows up after electroporation, do not worry. If anything, it is a visual cue that the electroporation worked.*

15. After electroporation, go back to culture hood with lights OFF, add 200ul of "DMEM complete" into cuvette, transfer all to 24ml of "DMEM complete" in a 50ml falcon tube.
16. Aliquot 1ml of electroporated cells in "DMEM complete" to each well of 12-well plates with collagen coating (24 wells total).
17. Cover all 12-well plates with aluminum foil.

Light-mediated deactivation of Cas9/pcRNA in cells

Deactivation at 1 hour after electroporation

1. By 1 hour after electroporation, the cells should be adherent if collagen is coated properly.
2. Deactivate 12-well plates B, C, and D. Plate A corresponds to no-light control.
3. To deactivate, first remove most of media, turn on and hold 365nm LED flashlight 2 cm above well for 1 minute. **CRITICAL** ("DMEM complete" can partially block the light, which greatly reduces deactivation efficiency)
4. For multiplexed deactivation, use the 3D printed flashlight holder design, which is designed for use with 12-well plates and can support up to 6 flashlights at once.
5. Add back 1ml fresh "DMEM complete" media. Move back to incubator. Proceed with Protocol 5.

Protocol 5: ChIP-seq for MRE11, 53BP1, γH2AX at 30 min, 1 hour, 2 hours after deactivation

Reagents

- All oligo sequences are in Table S1 (MNase_F, Mnase_R, PE_i5, PE_i7XX for XX in {01-24})
- Pierce™ 16% Formaldehyde (w/v), Methanol-free (Thermo Fisher 28908)
- Dynabeads™ Protein A for Immunoprecipitation (Thermo Fisher 10002D)
- Halt™ Protease Inhibitor Cocktail (100X) (Thermo Fisher 78438)
- MRE11 antibody (Novus NB100-142)
- γH2AX antibody (Abcam ab81299)
- 53BP1 antibody (Novus NB100-305)
- IDTE pH 8.0 (Integrated DNA Technologies 11-05-01-09)
- AMPure XP for PCR Purification (Beckman Coulter A63881)
- NEBNext® Ultra™ II End Repair/dA-Tailing Module (New England BioLabs E7546S)
- T4 DNA Ligase (New England BioLabs M0202S)
- Phusion® High-Fidelity PCR Master Mix with HF Buffer (New England BioLabs M0531S)

General stock buffers (store all in 4C)		
Reagent	**Final concentration**	**Volume**
5M NaCl solution (50ml)	5M NaCl	58.44g/mol * 5mol/L * 0.05L = 14.61g NaCl
5M LiCl solution (50ml)	5M LiCl	42.39g/mol * 5mol/L * 0.05L = 10.60g LiCl
10% Triton X-100 solution (50ml)	10% Triton X-100	5ml of 100% Triton X-100 in 45ml NFW
10% Igepal CA-630 (50ml)	10% Igepal CA-630	5ml of 100% Igepal CA-630 in 45ml NFW
10% Na-Deoxycholate (50ml) Protect from light	10% Na-Deoxycholate	5g Na-Deoxycholate in 45ml NFW
2M glycine in PBS (50ml)	2M glycine in PBS	75.07g/mol * 2mol/L * 0.05L = 7.507g glycine Up to 50ml with PBS
0.5% BSA in PBS (50ml)	0.5% BSA in PBS	2.5ml of 10% BSA in 47.5ml PBS
PEG/NaCl solution for SPRI cleanup (10ml)	2.5M NaCl 20% PEG8000 In nuclease free water	2.5mol/L * 58.44g/mol * 0.01L = **1.461g NaCl** 20% PEG8000 = **2g PEG8000** Fill with water to 10ml. it is viscous and slow to dissolve, so place on rotator overnight. 2000xg centrifugation removed bubbles. Invert to mix, store in 4C

ChIP-seq buffers (store all in 4C except LB3 and ChIP-EB) *LB3 and ChIP-EB can precipitate due to ionic detergents if stored in 4C. Leave in room temp.*		
Reagent	**Final concentration**	**Volume**
LB1 (500ml) Non-ionic detergents to lyse only the cell membrane	50mM HEPES 140mM NaCl 1mM EDTA 10% glycerol 0.5% Igepal CA-630 0.25% Triton X-100 KOH pH to 7.5 1% of 100x PI right before	238.3g/mol * 0.05mol/L * 0.5L = 5.96g HEPES powder 58.44g/mol * 0.14mol/L * 0.5L = 4.1g NaCl pellets 1ml of 0.5M EDTA 50ml of 100% glycerol 2.5ml of Igepal CA-630 1.25ml of 100% Triton X-100 2M KOH to pH 7.5 (starts around pH 5.5) 1% of 100x PI right before
LB2 (500ml) Wash step to remove free cytoplasmic components, but keeping nuclei intact	10mM Tris-HCl pH 8 200mM NaCl 1mM EDTA 0.5mM EGTA HCl pH to 8.0 1% of 100x PI right before	5ml of 1M Tris-HCl pH 8.0 58.44g/mol * 0.2mol/L * 0.5L = 5.844g NaCl pellets 1ml of 0.5M EDTA 568ul of 0.44M EGTA 1N HCl to pH 8.0 (starts around pH 8.25) 1% of 100x PI right before

LB3 (500ml) Ionic detergents to lyse nuclear membrane	10mM Tris-HCl pH 8 100mM NaCl 1mM EDTA 0.5mM EGTA 0.1% Na-Deoxycholate 0.5% N-lauroylsarcosine HCl pH to 8.0 1% of 100x PI right before	5ml of 1M Tris-HCl pH 8.0 58.44g/mol * 0.1mol/L * 0.5L = 2.922g NaCl pellets 1ml of 0.5M EDTA 568ul of 0.44M EGTA 500mg Na-Deoxycholate powder 2.5g of N-lauroylsarcosine powder 1N HCl to pH 8.0 (starts around pH 8.25) 1% of 100x PI right before
RIPA WB1 (500ml)	50mM HEPES 500mM LiCl 1mM EDTA 1% Igepal CA-630 0.7% Na-Deoxycholate KOH pH to 7.5	238.3g/mol * 0.05mol/L * 0.5L = 5.96g HEPES powder 42.39g/mol * 0.5mol/L * 0.5L = 10.6g LiCl powder 1ml of 0.5M EDTA 5ml of Igepal CA-630 3.5g of Na-Deoxycholate powder 2M KOH to pH 7.5 (starts around pH 6.5)
TBS WB2 (50ml)	20mM Tris-HCl pH 7.5 150mM NaCl	1ml of 1M Tris-HCl pH 7.5 3.75ml of 2M NaCl
ChIP-EB (50ml)	50mM Tris-HCl pH 8.0 10mM EDTA 1% SDS	2.5ml of 1M Tris-HCl pH 8.0 1ml of 0.5M EDTA 2.5ml of 20% SDS

Specialized Equipment

- Argos Technologies™ RotoFlex™ Tube Rotator (Fisher Scientific 22-505-001)
- Q125 sonicator (Qsonica Q125-110)
- Some magnetic rack to manipulate magnetic beads. We use the items listed below as Optional
- (Optional) 96 well Magnet Plate (Alpaqua A001322)
- (Optional) 3D printed magnetic rack (https://www.thingiverse.com/thing:319772 or https://www.thingiverse.com/thing:79424)
- (Optional) MakerBot Replicator+ 3D printer
- (Optional) Whole Housewares 4" Square Glass Vase, Candle Holder, 6 Pack Clear Cube Centerpiece (Amazon https://www.amazon.com/Whole-Housewares-Square-Candle-Centerpiece/dp/B07MT8TDJ8/)
- (Optional) 3D printed tube holder for sonication (https://github.com/rogerzou/chipseq_pcRNA/blob/master/2mL_tube_holder_for_sonication/files/k77AEoSKdcg.stl)

**Magnetic Beads Wash Protocol: add liquid, close cap, invert tubes while in magnetic rack twice, set down, lift tube away from magnetic rack, turn tube clockwise 180 degrees in the air, set down on magnetic rack – magnetic beads should flow from one side of tube to other side – repeat this with another 180 degree rotation after lifting tube away from rack, decant)*

Day 0 (day of electroporation)

Harvest cells

1. Harvest cells without light exposure at 1 hour after electroporation from Protocol 4, corresponding to 12-well plate A. This corresponds to 0 min after Cas9 deactivation.
2. Harvest cells at 30 min, 1 hour, and 2 hours after Cas9 deactivation from Protocol 4 (*i.e.* 1.5 hours, 2 hours, 3 hours after electroporation since Cas9 deactivation occurred at 1h after electroporation), corresponding to 12-well plates B, C, and D.
3. Remove media from cells, wash cells off with 10ml DMEM (no FBS or Penn-Strep) in room temperature. Use of cell scraper can help.
4. Add 721ul of 16% formaldehyde to final 1.077% concentration; incubate RT 15min on rotator
5. Add 750ul of 2M glycine in PBS to 130mM final concentration to quench; 3min RT on rotator
6. Spin 1200xg 3min 4C, decant by pouring

7. Wash cells twice with 10ml ice cold PBS -> same spin protocol each time
8. decant by pouring (decant remainder with pipette next time)
9. (Optional) Snap freeze and store pellets in -80C, which is stable for a few months

Day 1 of ChIP

Prebind antibody to magnetic beads [morning] – 3 different antibodies

- For each ChIP sample, use 50ul of Protein A with 3 ul of antibody
- There are four samples (00m, 30m, 1h, 2h), each with 3 antibodies = 600ul total of Protein A.

1. Add 600ul of Protein A to 2ml tube, add 1ml 0.5% BSA in PBS
2. Collect beads on magnetic rack, remove supernatant
3. Wash with 1ml 0.5% BSA in PBS two times, following *Magnetic Beads Wash Protocol*.
4. Resuspend Protein A beads in 1.2ml 0.5% BSA in PBS (100ul for each antibody)
5. Split 400ul of Protein A beads to three 2ml tubes. In each tube, add 12ul of either γH2AX, MRE11, or 53BP1 antibody.
6. Incubate 1-2h on rotating platform at room temperature. Immediately move on to cell lysis during incubation.

Cell Lysis [morning] – four cell samples

- For each cell sample, use 4ml LB1, 4ml LB2, and 1.5ml LB3

1. For 4 samples: prepare 16ml LB1 (add 160ul of 100x proteinase inhibitor), 16ml LB2 (add 160ul of 100x proteinase inhibitor), and 6ml LB3 (add 60ul of 100x proteinase inhibitor)
2. For each cell sample, resuspend pellet of crosslinked cells in 4ml of LB1 (w/ 1x protease inhibitor). Use a 1ml pipette to gently break up the cell pellet, then place on rotator in 4C for 10min.
3. Pellet nuclei at 2000xg 3min 4C -> decant by pouring
4. For each cell sample, resuspend pellet in 4ml of LB2 (w/ 1x protease inhibitor). Use a 1ml pipette to gently break up the cell pellet, then place on rotator in 4C for 5min.
5. Pellet nuclei at 2000xg 3min 4C -> decant by pouring, remove residual liquid with pipette.
6. Resuspend pellet in 1.5ml LB3 (w/ 1x protease inhibitor), use 1ml pipette to thoroughly mix, transfer to 2ml Eppendorf tube.

Sonication [noon] for each sample, done in 4C cold room (~15 min each, four samples total)

1. Prepare glass vase with 3D-printed custom Eppendorf tube holder, filled with ice water
2. Sonication protocol: 30s ON, 30s OFF, 12 min total time, 55% amplitude
3. Spin mixture at 20,000xg 10min 4C to pellet debris; transfer 1.2ml supernatant to new 5ml tube

** There may be a small dark pellet after centrifugation. This is normal and the amount should look similar for all samples. A sample without a dark pellet may indicate insufficient sonication.*

ChIP antibody binding [afternoon]

1. For each sonicated sample, add an additional 1.5ml LB3 (no protease inhibitor)
2. Add 300ul 10% Triton X-100 for ~3ml total per sample
3. Take 15ul of final 3ml mixture, add 40ul of ChIP-EB, transfer all (~55ul) to PCR tube and incubate at 65C overnight. These are the **QC samples**.
4. Split each ~3ml sample to three 1ml samples in 2ml Eppendorf tubes (for 12 tubes total)
5. Take the three antibody/magnetic bead tubes currently rotating at room temperature, move to magnetic racks.
6. Wash beads 3x in 1ml 0.5% BSA in PBS, following *Magnetic Beads Wash Protocol*.
7. Resuspend each in 200ul 0.5% BSA in PBS (50ul per IP, four IPs per antibody).
8. Add 50ul of antibody/bead to 1ml sonicated cell lysates, for all 12 combinations (00m, 30m, 1h, 2h are the 4 cell samples; MRE11, γH2AX, 53BP1 are the 3 antibodies)

00m MRE11	00m γH2AX	00m 53BP1	30m MRE11	30m γH2AX	30m 53BP1
1h MRE11	1h γH2AX	1h 53BP1	2h MRE11	2h γH2AX	2h 53BP1

9. Mix on rotator 4C for 7h or overnight

Day 2 of ChIP

ChIP wash [early morning] for all 12 ChIP samples

1. Move all 12 tubes to magnetic stand, let sit, remove S/N
2. For each tube, add 1ml RIPA WB, wash following *Magnetic Beads Wash Protocol*. Repeat 5 more times.
3. Wash once with 1ml TBS, following *Magnetic Beads Wash Protocol*.
4. Add 50ul ChIP-EB to suspend the 12 decanted bead-antibody-chromatin samples
5. Transfer liquid to PCR tubes -> Incubate 65C for over 7 hours. These are the **ChIP samples**.

ChIP extraction [late afternoon]

- Applies to all 12 ChIP samples and 4 QC samples
  1. Add 40ul IDTE to each tube, mix, add 2ul RNase A, mix, incubate 37C 15min
  2. Add 4ul Proteinase K, mix, incubate 55C for 30min
  3. For samples still containing magnetic beads (the 12 ChIP samples), use magnetic rack to separate supernatant from magnetic beads. Use supernatant for next steps, discard beads.
  4. Spin column cleanup all 16 samples with Qiagen MinElute, elute in 41ul EB supplied with kit. Store in -20C.
  5. Load 10ul of QC samples on 2% agarose gel to verify appropriately sheared DNA between 300-700bp.

Day 3

Sequencing library preparation

1. MNase-seq adapter annealing and dilution (adapter sequence in Table S1)

a. MNase_F and MNase_R stock are in 100uM TE buffer.

b. Mix 5ul MNase_F, 5ul MNase_R, and 40ul duplex buffer (IDT)

c. Incubate 95C for 5 min, lower temperature 1C/min to 4C. Store in -20C.

2. End Repair/A-tailing (12 samples total)

a. Use 16.67ul from each ChIP sample

b. Mix in PCR tubes

Reagent	**Volume**
ChIPed DNA	16.67ul
NEBNext Ultra II End Prep Reaction Buffer	2.33ul
NEBNext Ultra II End Prep Enzyme Mix	1ul
Total	**20ul**

c. Cycle 20C 30min -> 65C 30min -> 4C hold in thermocycler

d. Clean up reaction with AMPure beads, 1.2x (24ul) volume. Elute in 16.5ul nuclease free water with beads still in solution.

3. Adapter ligation

a. Mix in PCR tubes

Reagent	**Volume**
DNA in water mixed with beads	16.5ul
MNase-seq adapter (10uM)	0.5ul
T4 DNA ligase buffer	2ul
T4 DNA ligase	1ul
Total	**20ul**

b. Cycle 16C 30min -> 22C 30min -> 4C hold in thermocycler

c. Add 24ul of PEG/NaCl solution to reaction which already contains AMPure beads, essentially resulting in a 1.2x SPRI cleanup with reused beads; elute in 20ul IDTE.

4. PCR

a. Mix (primer sequences in Table S1)

Reagent	Volume
DNA	9.5ul
10uM Primer mix (PE_i5/PE_i7XX)	0.5ul
Phusion 2x master mix	10ul
Total	**20ul**

b. Cycle 98C for 3 min -> **X** cycles of {10s at 98C -> 30s at 68C -> 30s at 72C} -> 4C hold
c. **X**=10 for γH2AX, 13 for 53BP1 and MRE11
d. Clean up reaction with AMPure beads, 1x (20ul) volume. Elute in 40ul IDTE.
5. Run on 2% agarose gel to verify correct library size (~300bp-1kb)
6. Can run qPCR for quality control. Submit to core facility for 2x36bp Illumina sequencing, with at least 10 million reads per sample.

Protocol 6: Sample preparation for amplicon Illumina sequencing

Reagents

- All oligo sequences are in Table S1 (NGS_*)
- DNeasy Blood & Tissue Kit (Qiagen 69504)
- Q5® High-Fidelity 2X Master Mix (New England BioLabs M0492)
- AMPure XP for PCR Purification (Beckman Coulter A63881)
- Agarose gels
- (Optional) E-Gel Precast Agarose Electrophoresis System (Thermo Fisher)
- Qubit™ dsDNA HS Assay Kit (Thermo Fisher Q32851)

Specialized Equipment

- Thermocycler (Bio-Rad)
- Qubit 4 Fluorometer (Thermo Fisher)

Genomic PCR

1. Purify genomic DNA (gDNA) from HEK293T cells using DNeasy Blood & Tissue Kit. Elute in 200ul AE supplied with kit. Store gDNA in -20C.
2. Mix for PCR reaction (options for Fwd/Rev primer sets listed under step 3)

Component	**Volume**
Nuclease Free Water (NFW)	3 uL
Genomic DNA	1 uL
F/R primer set (10uM)	1 uL
Q5® High-Fidelity 2X Master Mix	5 uL
Total	**10 uL**

3. Start thermocycling protocol (options for # cycles and annealing temps listed under step 3)

Step	**Temp**	**Time**	
Initial Denaturation	98C	30 sec	
A cycles (touchdown PCR)	98C	10 sec	
	Ax	10 sec	(-1C/cycle)
	72C	20 sec	
B cycles	98C	10 sec	
	Bx	10 sec	
	72C	20 sec	
Final extension	72C	2 min	
Hold	4C	Inf	

* Options for Fwd/Rev primer sets, # cycles, and annealing temperatures

NGS_ACTB_F/NGS_ACTB_R [**A=0, B=28, Bx=71C]**
NGS_HEKs4_ON_F/NGS_HEKs4_ON_R [**A=6, B=26, Ax=72-67C, Bx=67C]**
NGS_HEKs4_OFF1_F/NGS_HEKs4_OFF1_R [**A=6, B=26, Ax=72-67C, Bx=67C]**
NGS_HEKs4_OFF3_F/NGS_HEKs4_OFF3_R [**A=6, B=29, Ax=72-67C, Bx=67C]**
NGS_HEKs4_OFF10_F/NGS_HEKs4_OFF10_R [**A=6, B=26, Ax=72-67C, Bx=67C]**
NGS_VEGFAs2_ON_F/NGS_VEGFAs2_ON_R [**A=8, B=22, Ax=72-65C, Bx=65C]**
NGS_VEGFAs2_OFF9_F/NGS_VEGFAs2_OFF9_R [**A=8, B=22, Ax=72-65C, Bx=65C]**
NGS_VEGFAs2_OFF23_F/NGS_VEGFAs2_OFF23_R [**A=8, B=22, Ax=72-65C, Bx=65C]**
NGS_VEGFAs2_OFF24_F/NGS_VEGFAs2_OFF24_R [**A=8, B=22, Ax=72-65C, Bx=65C]**
NGS_MYCs1_F/NGS_MYCs1_R [**A=8, B=24, Ax=72-65C, Bx=65C]**
NGS_MYCs3_F/NGS_MYCs3_R [**A=6, B=26, Ax=72-67C, Bx=67C]**
NGS_FANCFs2_F/NGS_FANCFs2_R [**A=8, B=24, Ax=72-65C, Bx=65C]**

4. Clean up reaction with AMPure beads, 1.6x (16ul) volume. Elute in 50uL of nuclease free water.
5. Optionally run a few uL of DNA on an agarose gel to verify specific product amplification.

Index PCR

1. Mix for PCR reaction. Select different combinations of Fwd and Rev primer sets (sequences found in Table S1)

Component	**Volume**
Nuclease Free Water	3 uL
Purified genomic PCR amplicon	1 uL
NGS_Index_F* (10uM)	0.5 uL
NGS_Index_R* (10uM)	0.5 uL
KAPA HiFi HotStart 2x ReadyMix	5 uL
Total	**10 uL**

2. Start thermocycling protocol

Step	**Temp**	**Time**
Initial Denaturation	95C	3 min
10 cycles	95C	30 sec
	55C	30 sec
	72C	30 sec
Final extension	72C	5 min
Hold	4C	Inf

3. Clean up reaction with AMPure beads, 1x (10ul) volume. Elute in 30uL of nuclease free water.
4. Optionally run a few uL of DNA on an agarose gel to verify specific product amplification.
5. Measure concentration using QuBit HS assay. Pool samples for approximately equal quantity of DNA. Run 2x150bp on MiSeq, aiming for 20k reads per sample.